NASA CONTRACTOR REPORT 166518

Large Deployable Reflector (LDR) Feasibility Study Update

W. H. Alff
L. W. Banderman

CONTRACT NAS2--11358
August 1983

NASA

NASA CONTRACTOR REPORT 166518

Large Deployable Reflector (LDR) Feasibility Study Update

W. H. Alff
L. W. Banderman
Lockheed Missiles and Space Company
Palo Alto Research Laboratory
Palo Alto, CA 94304

Prepared for
Ames Research Center
Under NASA Contract NAS2-11358

National Aeronautics and
Space Administration

Ames Research Center
Moffett Field, California 94035

June 20, 1983

FOREWORD

This report was prepared by Lockheed Missiles and Space Company, Inc., Palo Alto Research Laboratory, under contract NAS2-11358 for NASA Ames Research Center. The report consists of the annotated VU-graphs of the final briefing presented to Ames by LMSC on June 13, 1983 and covers all work carried out under this contract.

Effective Date of Contract: Oct. 15, 1982
Contract Expiration Date: June 20, 1983
Program Manager: W. H. Alff
415-493-4411 Ext. 45624
Principal Investigator: L. W. Bandermann
415-493-4411 Ext. 45559
Ames Technical Monitor: B. Pittman
415-965-5692

In addition to the authors, the following persons contributed to the technical work during the contract: R. Engdahl, D. Trites, K. Marks, and C. Klug.

The view and conclusions contained in this report are those of the authors and should not be interpreted as necessarily representing the official policies or views of NASA.

L. Bandermann, Principal Investigator
J. Aubrun
K. Lorell
B. Sridhar

CONTENTS

LDR FEASIBILITY STUDY UPDATE

FINAL REVIEW

13 JUNE 1983

NASA AMES RESEARCH CENTER

CONTRACT NAS2-11358

Electro-Optics Laboratory
LOCKHEED MISSILES & SPACE COMPANY, INC.
Palo Alto, California 94304

AGENDA

▷ INTRODUCTION AND SUMMARY	W. ALFF
MIRROR SEGMENTS	L. BANDERMANN
SUNSHADE	L. BANDERMANN
STRUCTURE MODEL (INTRODUCTION)	L. BANDERMANN
STRUCTURE AND CONTROL OVERVIEW	J. AUBRÜN
SECONDARY MIRROR CHOPPING	K. LORELL
CONTROL SYSTEM PERFORMANCE	B. SRIDHAR

The Large Deployable Reflector (LDR) is a NASA concept of an earth-orbiting astronomical telescope for infrared to submillimeter observations. The telescope is diffraction limited at 30 microns, and the nominal primary mirror diameter is 20 meters. The primary mirror is not actively cooled and to have a temperature of 200 K or less. Other performance and systems specifications, which are tentative at this time, are listed in Appendix A. They are the basis for the present study.

An initial feasibility study of LDR was carried out by Lockheed Palo Alto Research Laboratory for NASA/Ames in 1979/80 under contract NAS2-10427. A number of critical technology issues were then identified, and in 1981/82 the Perkin Elmer Corporation conducted a detailed study of one of these. namely lightweight mirror segments (contract NAS2-1104). The LDR concept, relevant technology issues and science goals as well as performance requirements were outlined in a workshop at Asilomar, Calif., in the summer of 1982.

LDR FEASIBILITY UPDATE

- PURPOSE
  - REEVALUATE FEASIBILITY ISSUES IN CRITICAL AREAS
- BACKGROUND
  - LMSC STUDY (1979/80)
  - P-E STUDY (1981/82)
  - ASILOMAR WORKSHOP (1982)

The purpose of this study was to re-evaluate certain feasibility issues in the light of technology developments and LDR studies carried out since the initial LDR study by Lockheed. The issues lie in the areas

- o Mirror Configuration
- o Thermal Behavior
- o Structural Definition
- o Dynamical Control

of the LDR.

Within the confinement of the contract, LMSC addressed selected issues in these areas to shed further light on LDR feasibility and thereby facilitate the concept selection and technology definition of LDR by NASA. The issues are listed in this Vu-graph.

CRITICAL AREAS

- SEGMENTS (SIZE, MATERIAL, DESIGN, SHAPE)
- TEMPERATURE (AND GRADIENT) CONTROL
- STRUCTURAL DEFINITION
- DYNAMICAL CONTROL

This foil summarizes the main results of the study. In agreement with Perkin Elmer, lightweight, low-expansion glass segments are preferred over either metal or composite structures. The segment shape is not a critical issue (hexes or trapezoids) but the size deserves further consideration because of a possible significant impact on segment phasing and sensing control requirements.

A substantial sunshade (i.e. a thermal enclosure preventing direct sunlight or earthshine on the primary mirror) is required for various reasons including low ambient temperature, and lateral and vertical temperature gradients and variations with time. The preferred sunshade concept is a cylinder with a flared front (frustrum), but it involves a substantial weight penalty (about 2000 kg).

A structural model of the LDR dish and secondary support was generated which uses Graphite-Magnesium material because of the superior physical properties (thermal inertia and stiffness/weight ratio). The packaging of LDR in the shuttle was briefly considered in terms of the required volume, and a serious problem of using only one shuttle load seems to exist.

Based on the structural model of the LDR, a strawman control model was derived and when applied showed that it can satisfy most of the requirements on slewing, chopping and nodding the LDR. It was found that disturbances by mechanical focal plane coolers can introduce signiciant disturbances and require further attention downstream.

RESULTS

- SEGMENTS
  - LIGHTWEIGHT FUSED SILICA
  - 1- TO 2-m DIAMETER PREFERRED, BUT SIZE ISSUE STILL TO BE RESOLVED RE: CONTROL COMPLEXITY

- SUNSHADE
  - REQUIRED; PREFERRED CONCEPT FLARED CYLINDER
  - MIRROR TEMPERATURE BELOW 200 K ACHIEVABLE PASSIVELY
  - LARGE WEIGHT PENALTY

- STRUCTURE
  - Gr/METAL TRUSS PREFERRED; TRUSS + MIRROR WEIGHT ~ 12,000 kg
  - LOWEST MODE ~ 6 Hz
  - PACKAGING PROBLEMATIC; MAY REQUIRE SEVERAL SHUTTLE LOADS

- STRUCTURE CONTROL
  - SIMPLE CONTROL SYSTEM CAN MEET MOST LDR REQUIREMENTS
  - ACCURATE STAR TRACKER REQUIRED
  - CRYO-COOLER DISTURBANCES CAN BE LARGE

In addition to the recommendations listed in this foil, LMSC urges that a closer look be taken at these issues:

- How passive should the LDR be in terms of thermal and mechanical control? Some thermal control (semi-active cooling such as phase change methods) can relieve the substantial sunshade requirements, and perhaps very modest segment figure control (say, focus only) may relieve some of the segment design requirements and widen the choice of materials and segment designs.

- An extensive study of the probable mission profile of the LDR may lead to a more certain definition of the orbit, slewing and nodding requirements, the instrument package and its impact on the system design. One should avoid "boxing in" the LDR concept and requirements too soon and thereby establish unnecessary and costly system drivers.

RECOMMENDATIONS

- STUDY SEGMENT SIZE ISSUE FURTHER (→ STRUCTURE AND CONTROL IMPACTS)
- PACKAGING PROBLEM NEEDS URGENT ATTENTION
- CONDUCT TRADE STUDY: LESS CUMBERSOME SHADE VERSUS SOME (SEMI-) ACTIVE TEMPERATURE CONTROL
- LOOK AT BENEFITS OF MODERATE SEGMENT FIGURE CONTROL
- EXTEND STRUCTURE/DYNAMICS MODEL TO INCLUDE SUNSHADE, CRYO-COOLER EFFECTS, etc.
- CONDUCT EXHAUSTIVE STUDY OF LDR MISSION PROFILE TO BETTER DEFINE SYSTEM REQUIREMENTS

AGENDA

INTRODUCTION AND SUMMARY	W. ALFF
▷ MIRROR SEGMENTS	L. BANDERMANN
SUNSHADE	L. BANDERMANN
STRUCTURE MODEL (INTRODUCTION)	L. BANDERMANN
STRUCTURE AND CONTROL OVERVIEW	J. AUBRUN
SECONDARY MIRROR CHOPPING	K. LORELL
CONTROL SYSTEM PERFORMANCE	B. SRIDHAR

In the technical area of the LDR primary mirror configuration, we reconsidered the issue of the materials and designs of the segments, particularly in the light of the recent Perkin Elmer study. Our earlier views concerning materials and segment design have not changed and agree with PE. The segment shape is a minor issue which probably cannot be resolved without considering a number of other problems such as fabrication methods and the LDR figure sensing scheme, but trapezoids appear to have a slight edge over hexes: they give a naturally smooth mirror boundary and require fewer different segments.

The size issue is rather complex and is addressed further on p. 27. We originally chose 4 m (diameter) since this is about the largest segment to fit the shuttle bay and requiring fewest (tilt/piston) actuators. But they are risky in fabrication and handling .

LDR MIRROR SEGMENTS

	1979 LMSC STUDY RECOMMENDED	1981 P-E STUDY RECOMMENDED
• SIZE	4 m	≤2 m
• SHAPE	HEXAGONAL	TRAPEZOID
• MATERIAL	LOW EXPANSION GLASS	SAME
• DESIGN	LIGHTWEIGHT	SAME

Two important merit parameters for mirror as well as structural materials are: the resistance to thermal deformation, namely κ/α , where κ is the thermal conductivity and α the linear thermal expansion coefficient; and E/ρ^3, or E/ρ, where E is Young's modulus and ρ the specific density. (The lowest vibrational mode of a plate is proportional $\sqrt{\text{to } E/\rho^3}$). This foil shows candidate mirror (segment) and structure materials at room temperature: It is seen that ULE is outstanding mirror material.

LDR MATERIALS AT ROOM TEMPERATURE

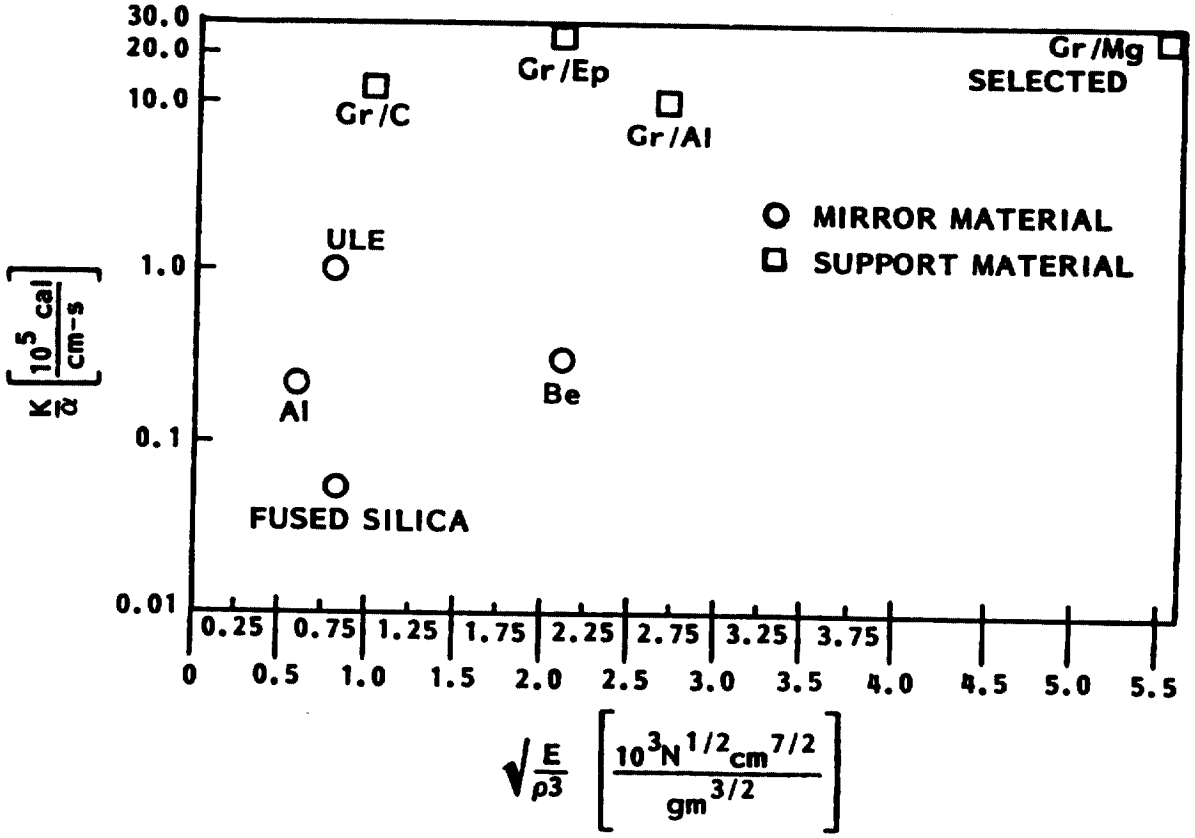

ORIGINAL PAGE IS
OF POOR QUALITY

This foil shows the same materials (as the previous foil) but the mirror materials are now at the presumed LDR ambient operating temperature of 175 K: The situation has changed: ULE has slipped in terms of these merit in favor of fused silica which seems no better than aluminum, whereas beryllium is now outstanding. The question arises: why not choose Al or Be? The next foil lists some answers.

LDR MATERIALS AT OPERATIONAL TEMPERATURES

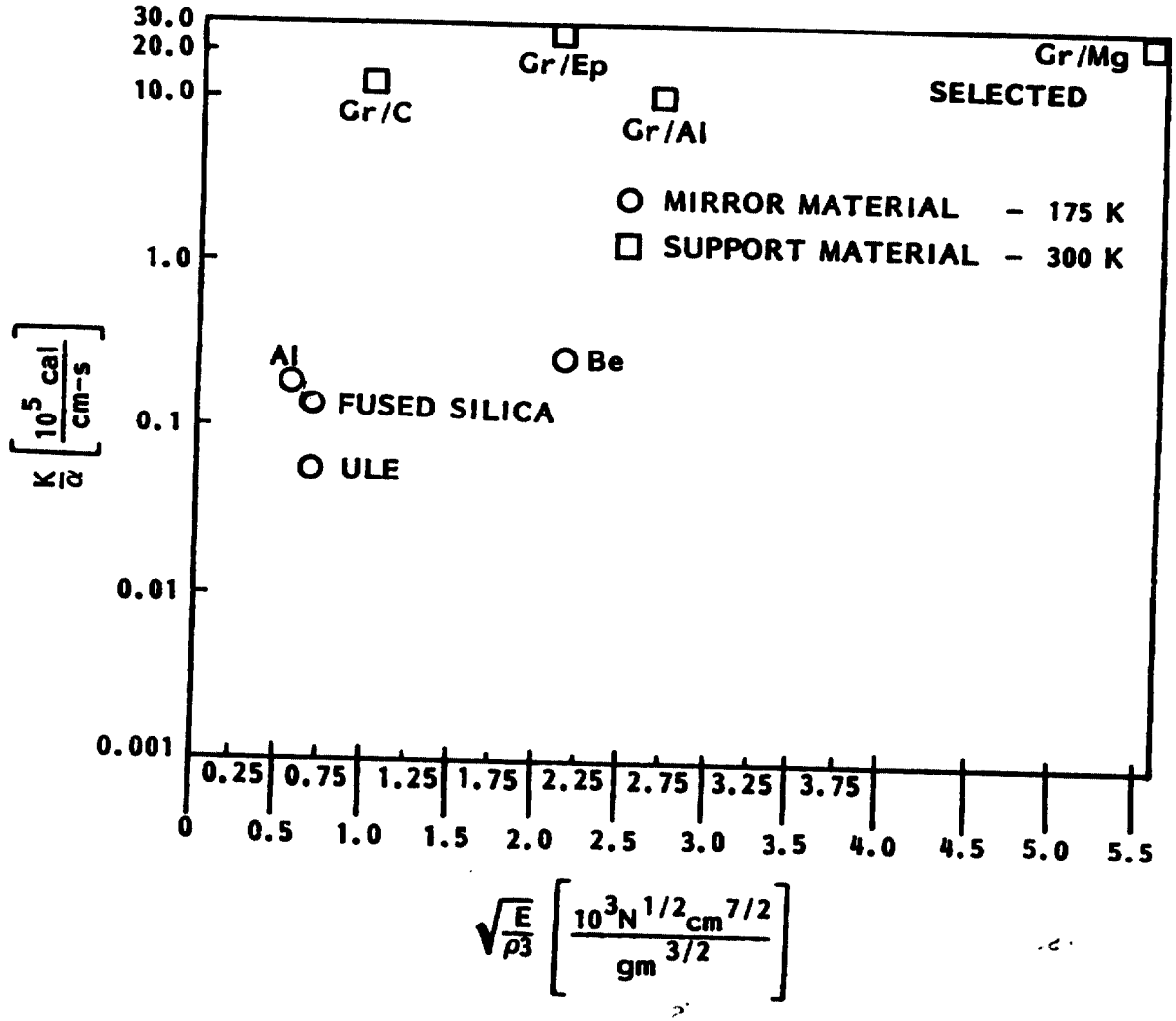

ORIGINAL PAGE IS
OF POOR QUALITY

It may very well be argued that the initial raw material cost of LDR materials should not be of great concern since the total design and fabrication cost of the system is very much larger: Therefore only the best material, in terms of the physical and optical properties, should be considered in a final selection. This foil gives some reasons why it seems likely that only the low expansion glasses are viable candidates for mirror materials. (It should be remembered that operation of the LDR at 2 microns diffraction limited - could be come a goal although not a requirement).

WHY NOT ALUMINUM OR BERYLLIUM?

- Be EXPENSIVE (MATERIAL/FABRICATION)
- Al MATERIAL CHEAP, BUT FAB COST TO STRESS – RELIEVE SEGMENTS HIGH – NO SIGNIFICANT COST ADVANTAGE OVER L. E. GLASS EXPECTED
- NO DEVELOPMENT PROGRAMS (e.g., DOD) FOR LARGE Al OR Be ULTRALIGHTWEIGHT MIRRORS (NASA WOULD HAVE TO FUND THEM)
- DIMENSIONAL STABILITY POOR – THERMAL CYCLING CHANGES FIGURE SIGNIFICANTLY
- POTENTIAL FOR USE IN NEAR-IR POOR

Although Be is outstanding segment material for the LDR in terms of the merit paramters: resistance to thermal deformation and specific stiffness, it is less well suited to provided an optically perfect surface at the short wavelenght end of the LDR operating range.

SCATTERING BRDF MEASUREMENTS (AT 10.6 μm) OF SELECTED MIRROR SURFACES

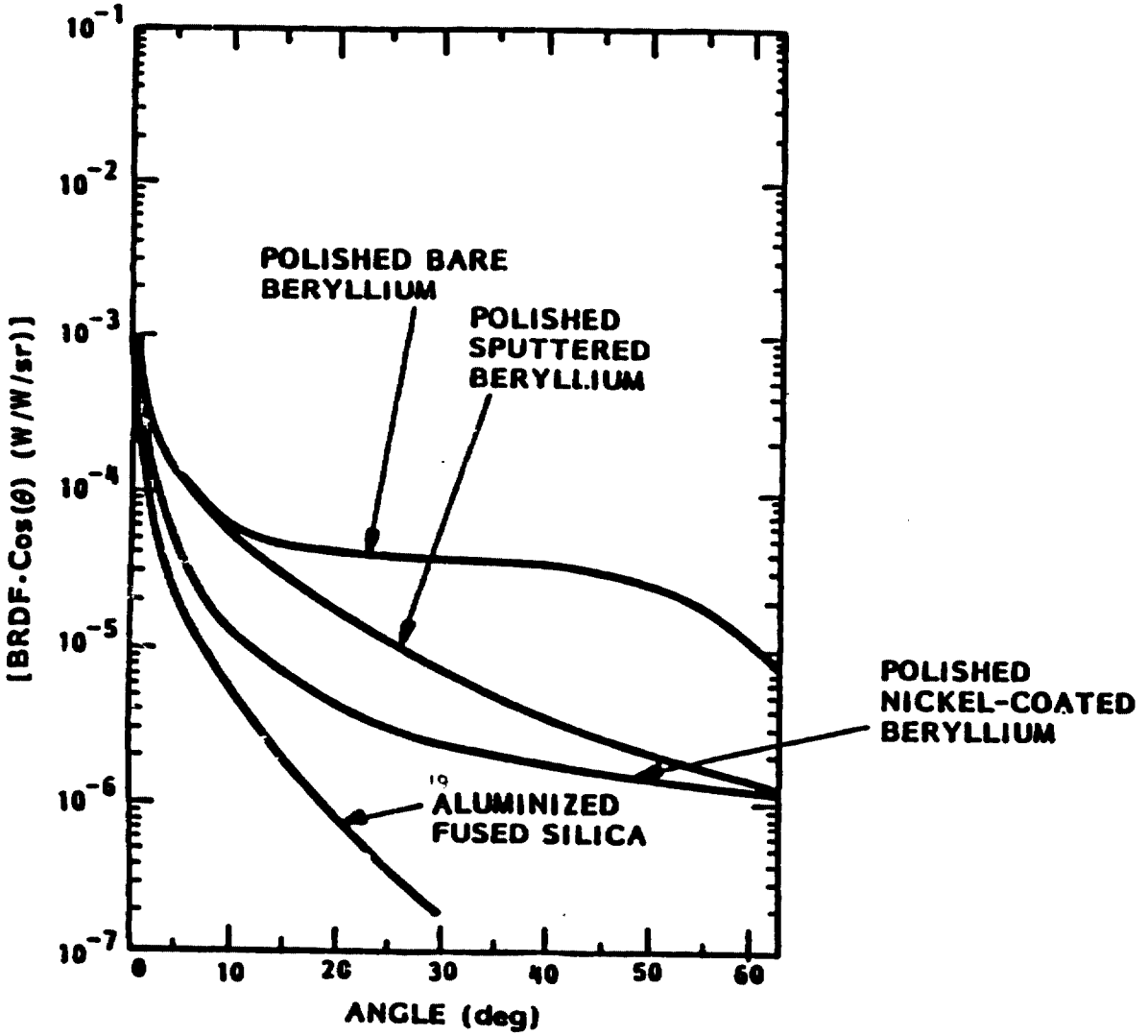

Having settled on fused silica as the choice of LDR segment material we consider further the operating temperature of the LDR primary mirror: This foil shows how the linear expansion coefficient of the fused silica systems varies with temperature and with the amount of TiO_2: If the LDR temperature is -100 ^{o}C (about 175 K), then 3% doping would provide the lowest value of α and highest resistance to thermal deformation brought about by temperature changes of the segments. If the thermal enclosure design results in a different operating temperature, the doping could be chosen to fit that temperature as well.

THERMAL EXPANSION OF SiO_2 - TiO_2 SYSTEMS

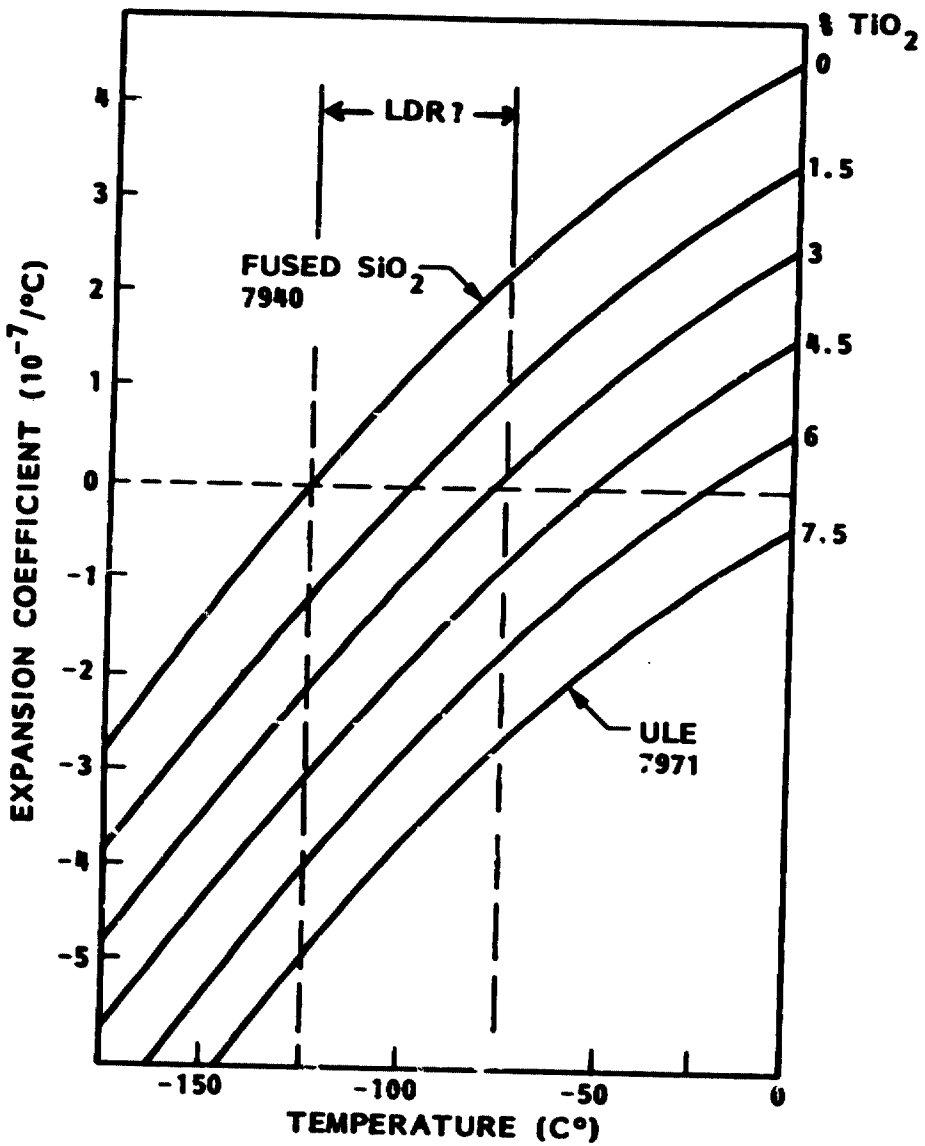

This foil summarizes arguments pro and con the preferred segment diameter. They can be divided into two categories: (i) manufacturing , handling and deplomentconsiderations i.e. practicality, and (ii) performance. PE strongly favors small segments (1-2 m), whereas we preferred (in the 1979 study) large segments, to reduce operational complexity. We feel that the issue requires further study.

SEGMENT SIZE 4 m VERSUS < 2 M DIAMETER

- MANUFACTURE + HANDLING EASIER WITH SMALL SEGMENTS (INCLUDING COATING)
- SMALL SEGMENTS STIFFER FOR SAME M/A
- SMALL SEGMENTS DEFORM LESS UNDER THERMAL LOAD CHANGES
- SMALL SEGMENTS LESS EDGE CURL
- LOSS OF SEGMENT OPERATION LESS CATASTROPHIC FOR SMALL SEGMENTS
- MORE ACTUATORS AND SENSORS REQUIRED FOR SMALL SEGMENTS (BUT LESS DYNAMIC RANGE/ACTUATOR). SUPPORT STRUCTURE MORE COMPLEX

SMALL SEGMENTS PREFERRED BUT STRUCTURE AND CONTROLS IMPACT TO BE STUDIED FURTHER

Some of the more important issues of segment design are addressed here. The thermal study (see: SUNSHADE) shows that the main heat flow through the LDR primary mirror, which determines the thermal stress of the segments, is from the back to the front. In that flow, radiation transfer within the segment core (by silvering the walls and blackening the top and bottom surfaces) can be important. The rear face plate (in a closed core design) is thus not the primary barrier in the heat flow aided by conduction, but the core web. There is no thermal advantage then in leaving off the rear plate, which would provide greater stiffness as well as other advantages listed in this foil.

SEGMENT DESIGN: OPEN VERSUS CLOSED CORE (GLASS)

- HEAT TRANSFER: BACK TO FRONT
- HEAT TRANSFER: RADIATIVE DOMINANT; FOR CONDUCTION, CORE WEB IS PROBLEM, NOT REAR FACEPLATE
- NO ADVANTAGE, THERMALLY, IN OPEN CORE
- CLOSED CORE
  - STIFFER FOR SAME M/A
  - BETTER SURFACE TO ATTACH THERMAL BLANKET
  - EASIER HANDLING
  - EASIER ACTUATION CAPABILITY

Trapezoidal segments provide a naturally smooth mirror boundary: Hexagonal segments, which require more different segments (for the same segment diameter and primary diameter) in any case, would require additional partial segments to provide that boundary. However, each hex segment is referenced to six neighbors, if edge referencing is used in the segment alignment (mirror figure sensing) such as capacitive sensing used in the UC Berkeley 10-m optical telescope. Arguments were made by LMSC in the 1979 study, that because of disadvantages in this sensing scheme - such as error propagation which would be particularly severe for small LDR segments - another alignment scheme will be used (perhaps in addition to edge alignment) such as Optical Position Sensing (OPS) or other schemes now under development in various space mirror programs.

SEGMENT SHAPE: HEXAGONAL VERSUS TRAPEZOID

- FEWER DIFFERENT TRAPEZOID SEGMENTS
- LESS OBSCURED AREA WITH TRAPEZOIDS
- MORE SEGMENT-SEGMENT REFERENCING (ASSUME CAPACITIVE EDGE SENSING USED) WITH HEXES

OPEN QUESTION

A second issue addressed in the study was the need and the preferred design of a thermal enclosure of the LDR (loosely called sunshade) providing low mirror temperature and gradients.

AGENDA

INTRODUCTION AND SUMMARY	W. ALFF
MIRROR SEGMENTS	L. BANDERMANN
▷ SUNSHADE	L. BANDERMANN
STRUCTURE MODEL (INTRODUCTION)	L. BANDERMANN
STRUCTURE AND CONTROL OVERVIEW	J. AUBRUN
SECONDARY MIRROR CHOPPING	K. LORELL
CONTROL SYSTEM PERFORMANCE	B. SRIDHAR

LDR is presently visualized as a passive system in that the primary mirror is ambient and there is no segment figure control. The operating temperature is to be less than 200 K. Can this be achieved without an extensive thermal enclosure, and can the thermal gradients be held within required bounds?

LDR SHIELDING CONSIDERATIONS

- GLOBAL SURFACE TEMPERATURE
- RADIAL GRADIENTS
- AXIAL GRADIENTS

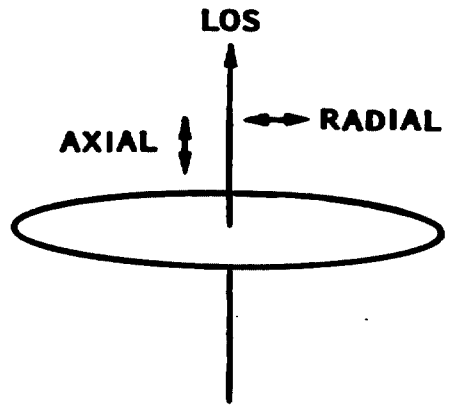

If the axial (across-the-mirror) temperature variations are large, scanning the field of view by secondary mirror oscillation (chopping; cf. section on CHOPPING) introduces a false signal as the effective primary mirror area shifts back and forth. If there is no sunshade, the temperature at opposite sides of the mirror (one side having grazing incidence sun, the other the sun almost 30^{0} from the segment vertical) varies by as much as 45 ^{0}C. This difference occurs because the thermal relaxation time through the segments is large and the front of the unshielded LDR mirror heats up without the backside following suit rapidly enough.

The value of 45 ^{0}C is based on the (simplified) assumption that the solar load is absorbed totally in the front facesheet of the segments; that the absorptivity is 5%, and the facesheed is 2.5 mm thick (as in the PE "optimal" segment design). Then

$$\Delta T = \frac{q\ t}{\tau\ \rho\ c}$$

where q the absorbed heat (per unit area), t the time, τ the facesheet thickness, ρ the specific density, and c the thermal heat capacity per unit mass of the facesheet.

LDR RADIAL TEMPERATURE GRADIENT

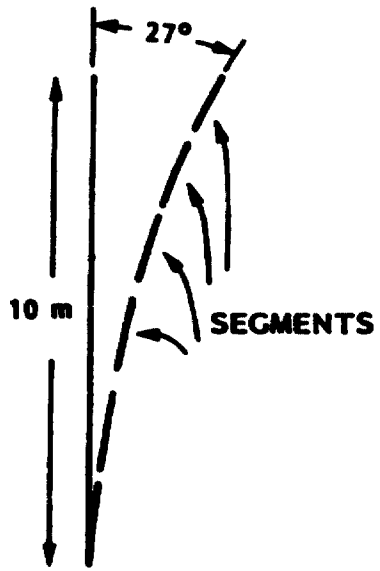

- 20-m DIAMETER, f/0.5 PRIMARY
- α = 5% ASSUMED
- SOLAR HEAT LOAD VARIATION: q = 0 TO 60 W/m^2
- CONDUCTIVE HEAT TRANSFER FRONT-BACK TIME CONSTANT ~ 2 h (P-E "OPTIMAL" SEGMENT)
- q x t = 4000 J/M^2 FOR 1°C FACEPLATE TEMPERATURE CHANGE
- ABSORBED HEAT 1/2 ORBIT ~ 60 x 3000 J/M^2
- TEMPERATURE DIFFERENTIAL ~ 45°C TOO LARGE (SCANNING NOISE!)

SUNSHADE REQUIRED

We define the acceptable scanning noise as ΔP, where $\Delta P \cong NEP$, the noise power of the primary at the temperature T and emissivity ε. We find

$$\Delta P/NEP \cong \frac{\pi}{4}\sqrt{2\varepsilon \ \frac{c}{\lambda}\frac{1}{f}\frac{\Delta\lambda}{\lambda}\exp(-hc/\lambda kT)} \ \frac{hc}{\lambda kT} \ \frac{\Delta T}{T}$$

where λ=30 microns, c the speed of light, k Boltzmann's constant, h Planck's constant, f the scanning f requency. The mirror area shifts by $\delta x \cong \delta A/D$, D the mirror diameter. Approximately $\delta x = 3.2\sqrt{D/F}.\Delta\alpha$, F the primary focal length and $\Delta\alpha$ the FOV shift. For the values, $\Delta\lambda/\lambda$=0.1, f=2 Hz, T=175 K, D=20 m, F=0.5, ε=3% and $\Delta\alpha$=1 arcmin, we find $T_L - T_R < 1$ K , for the temperature difference between the two shaded areas in the sketch in this foil. This value is much less than the 45 ^{o}C determined previously; however, it must be remembered that the extreme temperature difference is somewhat larger than $T_L - T_R$, and that a 3% total emissivity is perhaps a little optimistic. Nevertheless, the scanning noise appears to be too large without a sunshade.

ACCEPTABLE ΔT (RADIAL) FROM SCANNING NOISE

- SCANNING SECONDARY SHIFT EFFECTIVE PRIMARY MIRROR AREA

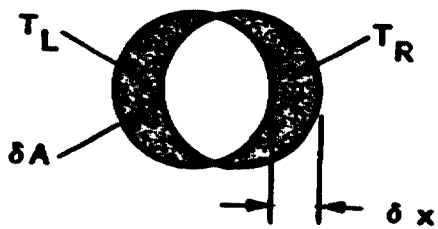

- $\Delta P/NEP_{\substack{MIRROR \\ AT\ T}} \propto \frac{\Delta T}{T}$ WHERE $\Delta T \sim (T_L - T_R)\ \frac{\delta A}{\pi D^{2/4}}$, $T \sim 175$ K

- $\Delta P/NEP\big|_{SHORT\ \ell} < 1$ REQUIRES $T_L - T_R < 1$ K

LDR SUNSHADE CONCEPTS

- CONSIDERATIONS
  - EFFECTIVENESS
  - WEIGHT
  - DEPLOYMENT } COMPLEXITY
  - OPERATION } COMPLEXITY
- CANDIDATES
  - "SUGAR SCOOP"
  - BARREL (CYLINDER)
  - BARREL + CONE OR SCOOP
  - INFLATABLES (SEMISPHERICAL)
  - FREE-FLYER
  - UMBRELLA

One may divide sunshade into symmetrical and non-symmetrical ones. The latter require reorientation with retargeting of the LDR, and some, the balloon, umbrella and scoop do not provide shading from the earth. On a conceptual level then, the symmetrical shades are prefereable.

SUNSHADE CONCEPTS

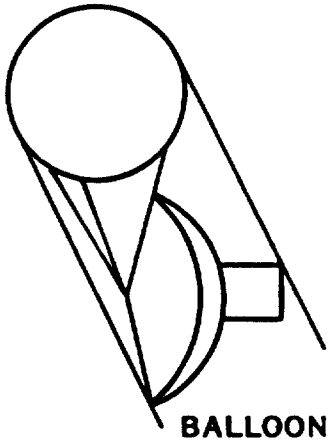

BALLOON

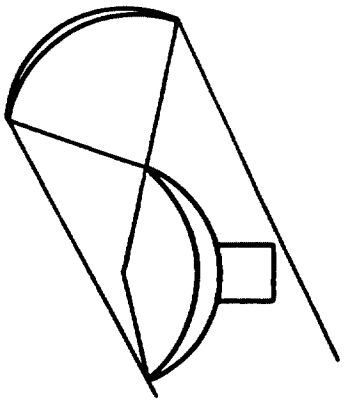

UMBRELLA

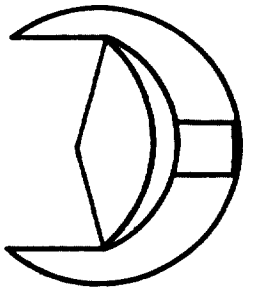

SPHERICAL ENCLOSURE

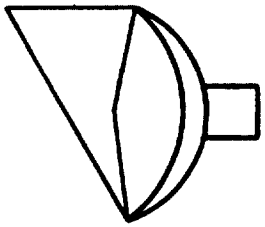

SCOOP

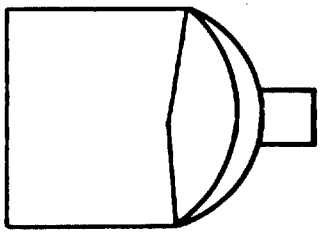

BARREL

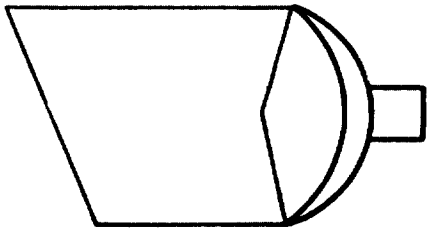

BARREL & SCOOP

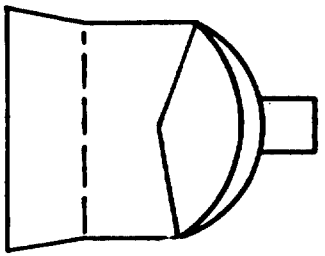

FLARED BARREL

A quasi-spherical LDR enclosure was briefly considered, made of inflated 1-ft diameter tubes. The attractive features are light weight and easy storage and deployment, if no further support structure is required. It disadvantage is that heat flow to the exterior from the LDR primary through the shade is slow, e.g. compared with the preferred cylindrical sunshade discussed later on.

QUASI-SPHERICAL ENCLOSURE

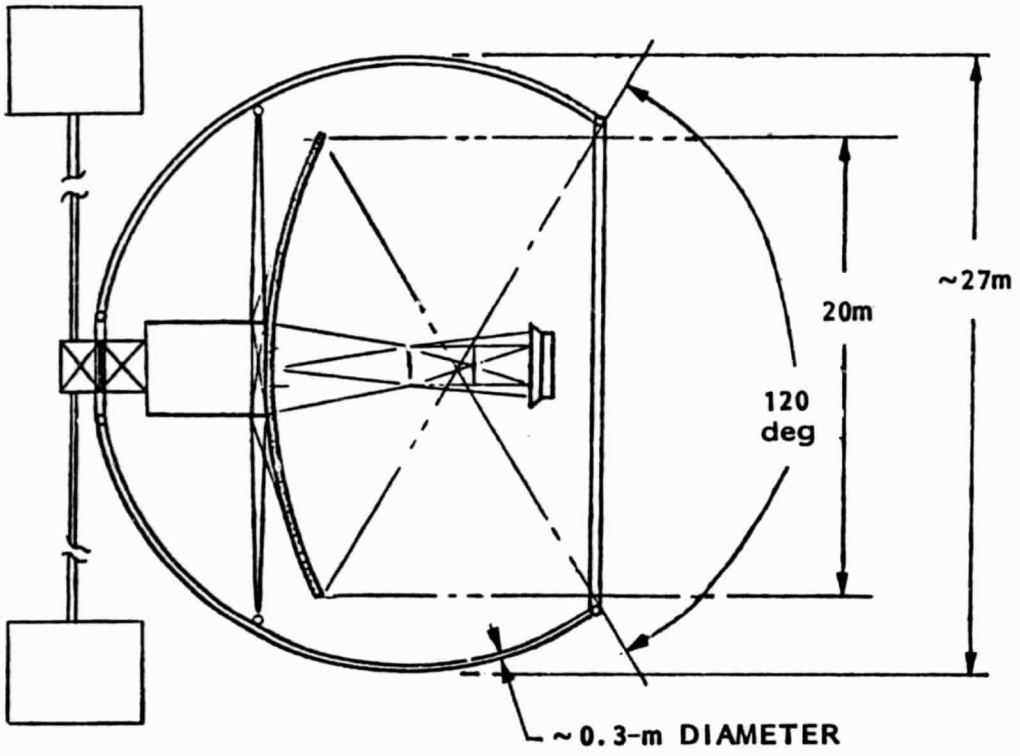

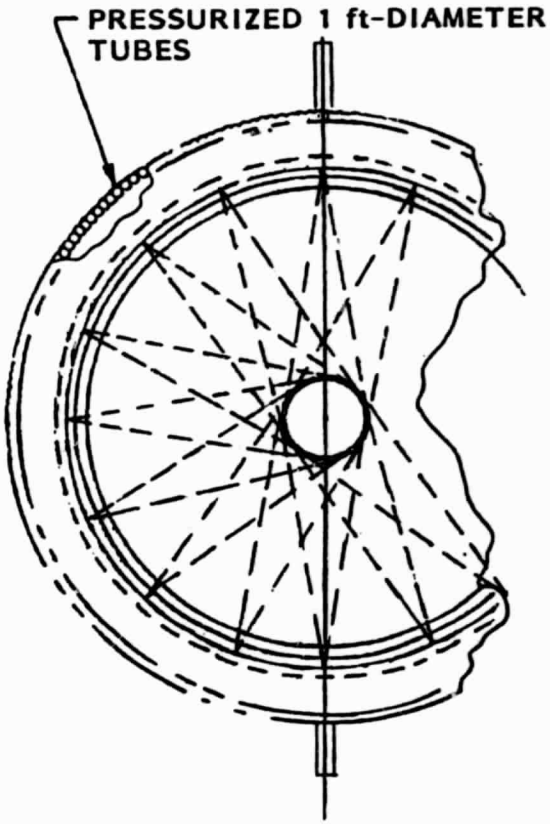

This foil summarizes the conceptual assessment of the various sunshade designs depicted earlier. In storage and deployment, support structure must be considered. Concerning operation (divided into simple and complex), the symmetrical designs were preferred (simple) since they require no re-orientation. However, the impact on dynamic control of the LDR by the sunshade is a complex issue which was not studied and may be of greater importance than the reorientation issue.

SUNSHADE SUITABILITIES

	EFFICIENCY	WEIGHT	STORAGE/ DEPLOYMENT	OPERATION
SCOOP	POOR	LOW	SIMPLE	COMPLEX
BARREL	GOOD	HIGH	COMPLEX	SIMPLE
BARREL & SCOOP	BEST	HIGHER	COMPLEX	COMPLEX
BARREL & CONE	BEST	HIGHEST	COMPLEX	SIMPLE
UMBRELLA	POOR	MEDIUM	SIMPLE	COMPLEX
BALLOON	POOR	LOW	SIMPLE	COMPLEX
INFLATABLES	POOR	?	?	SIMPLE

Two versions of a 25 m long cylindrical thermal enclosure were considered - the straight design shown here and a design with a flared mouth. Both have a conical section enclosing the back of the LDR but not including the equipment section (spacecraft). The spacecraft radiates toward the conical enclosure, and heat is transferred, by conduction, toward the back of the LDR mirror.

CYLINDRICAL SUNSHADE

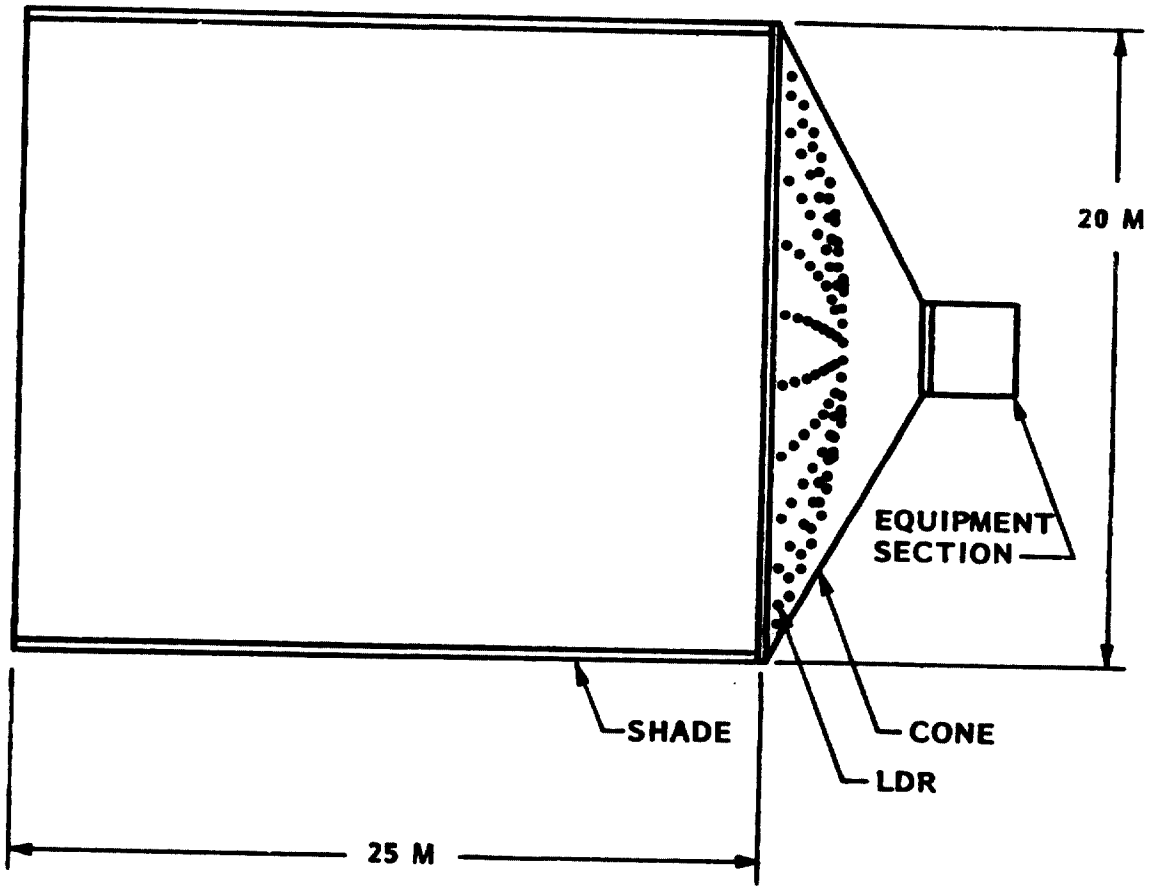

A flared cylinder has the advantage of providing better rejection of the incident radiation as well as better view angle to space for radiation of internal heat away from the mirror. This advantage is paid for in terms of greater weight and moment of inertia, impacting depoyment and operation of the LDR.

FLARED CYLINDRICAL SUNSHADE

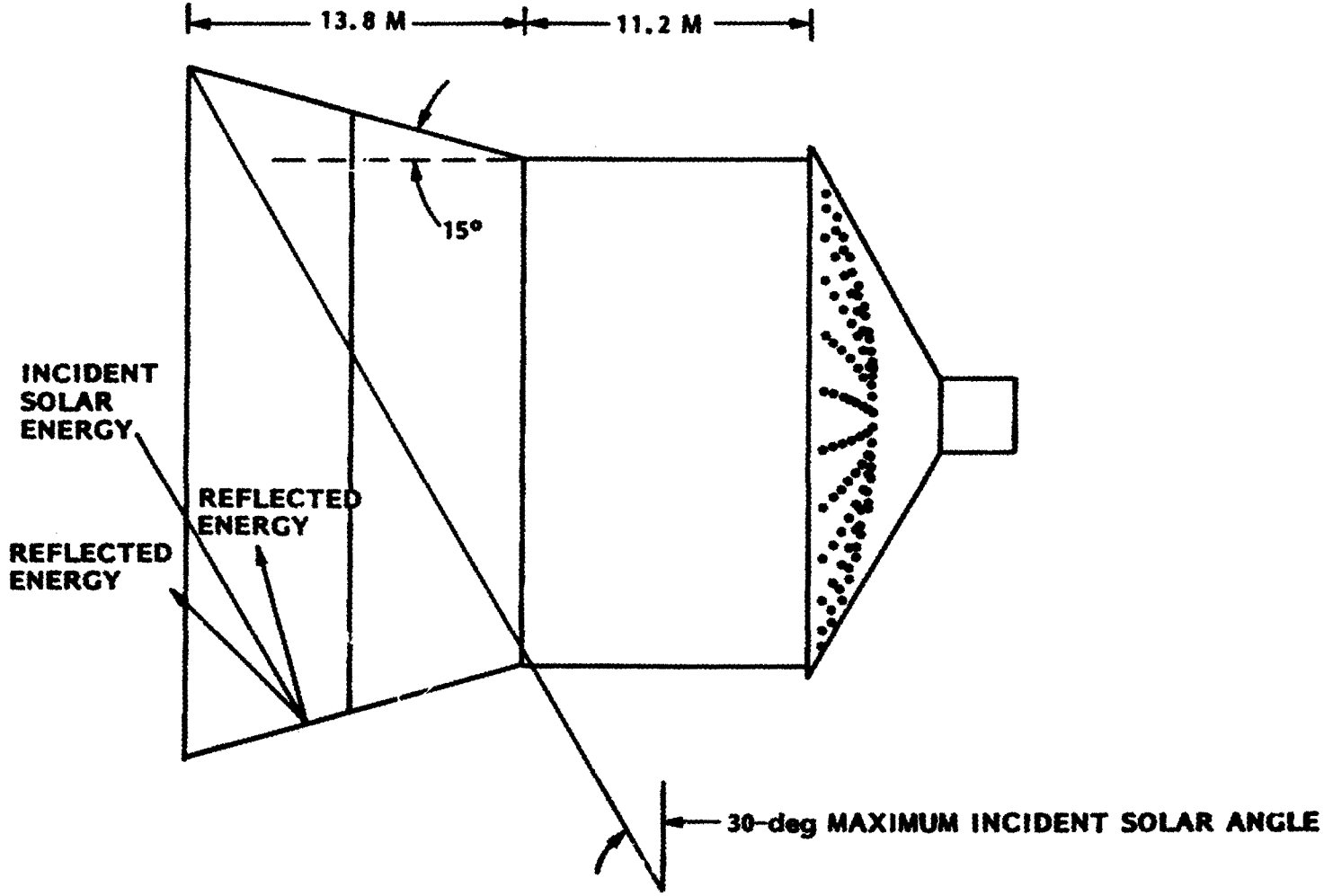

This foil lists the physical properties of the cylindrical LDR sunshades, including the absorptivity/emissivity ratio of the enclosure material (silverized Flexible Optical Solar Reflector, FOSR), and of the thermal blanket covering the rear of the LDR primary mirror. The thermal behavior was modeled using numerous thermal nodes and standard modeling programs.

FOSR is a space-proven effective reflective material, consisting of aluminized or silverized (first or second surface) Teflon, 1-5 mils thick. It was found that for LDR, Ag is required rather than Al coating. The second surface silvering provides better α than first-surface coating. However, degrades (in reflectivity) more rapidly.

LDR – SUNSHADE THERMAL PARAMETERS

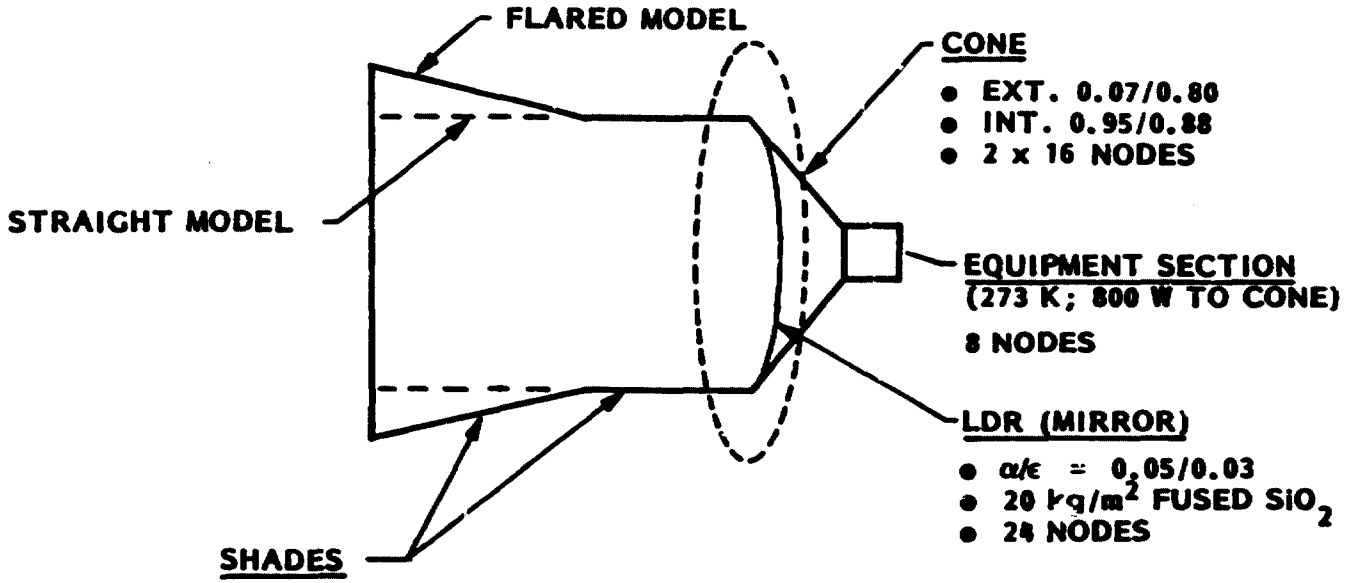

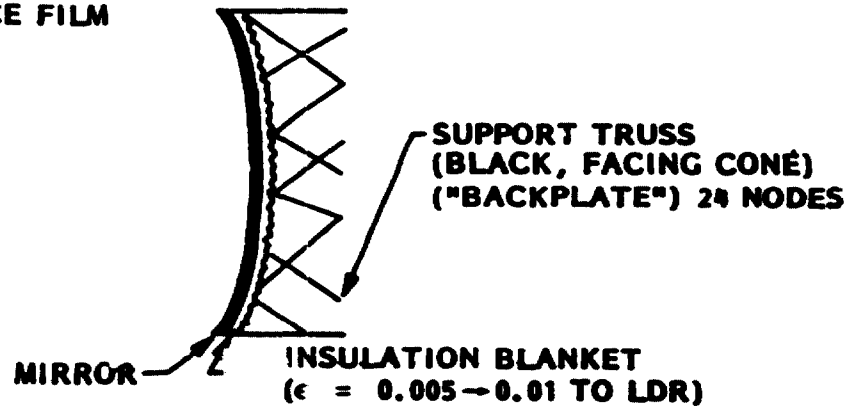

The performance of the straight and flared sunshades was evaluated using the nominal LDR orbit and an orientation of the spacecraft such as to obtain a realistic assessment of the LDR average mirror temperature: This involved the specified 60^{o} sun angle but an earth limb avoidance angle of 60^{o} instead of 45^{o}, kept constant over the orbit - in contrast with the actual situation in which the telescope is pointed at a fixed point in space during an astronomical observation and is reoriented only to see another target. The specified three 120 degree slews (see Appendix A) of the LDR is simulated by the continuous reorientation used here. The procedure used overestimates the lateral (across-the-mirror) temperature gradient (4 ^{o}C was obtained; it is estimated that a value of less than 1 ^{o}C is more realistic).

SUNSHADE STUDY: ORBITAL MODEL

- **INCLINATION:** 28.5 deg
- **ALTITUDE:** 700 km
- **SUN ANGLE:** 60 deg
- **EARTH LIMB ANGLE:** 60 deg
  - WAS KEPT CONSTANT TO SIMULATE OVER-ALL MISSION THERMAL CONDITIONS; RESULTING IN REALISTIC ASSESSMENT OF LDR SURFACE GLOBAL TEMPERATURE
  - OVER ESTIMATES RADIAL GRADIENT

The net heat flow is from the rear of the spacecraft through the LDR primary to the outside. The foil shows the heat budget. A heat input to the sunshade of 60 W by the secondar mirror drive was assumed. The heat input to the rear sunshade cone was assessed at 800 W. Inputs to LDR by the segment position actuators was not modeled but could be included in the head budget by increasing the emissivity of the thermal blanket in rear of the mirror appropriately (for modeling purposes). The value is probablye less than a few 100 W (average value!), corresponding to a change in ε from 0.005 to 0.01.

The average LDR temperature goal of 200 K or less can be achieved, as these calculations show, without active cooling.

SUNSHADE STUDY RESULTS

- HEAT BUDGET

SOURCE	AVERAGE INPUT TO MIRROR (W)
SOLAR, EARTH	+ 10
SPACE	- 60
SUNSHADE	- 176 (60 W INPUT TO SHADE INSIDE BY SECONDARY DRIVE)
BACK OF LDR	+ 226

- TEMPERATURE OF LDR (K)

	FLARED SHADE	STRAIGHT SHADE
BLANKET ϵ = 0.005	165	203
BLANKET ϵ = 0.010	179	207

The next four foils show examples of the variation with time (in orbit) of various points on the sunshade (the cylinder) and the mirror itself. It is seen that (i) although the temperature of the enlosure at some points may vary strongly with time, the mirror temperature stays practically constant, and (ii) the flared sunshade is in every case more efficient than the straight cylinder, and (iii), the cylinder temperature at the base i.e. near the LDR perimeter is lower than the mirror temperature.

SHADE TEMPERATURES: STRAIGHT SHADE

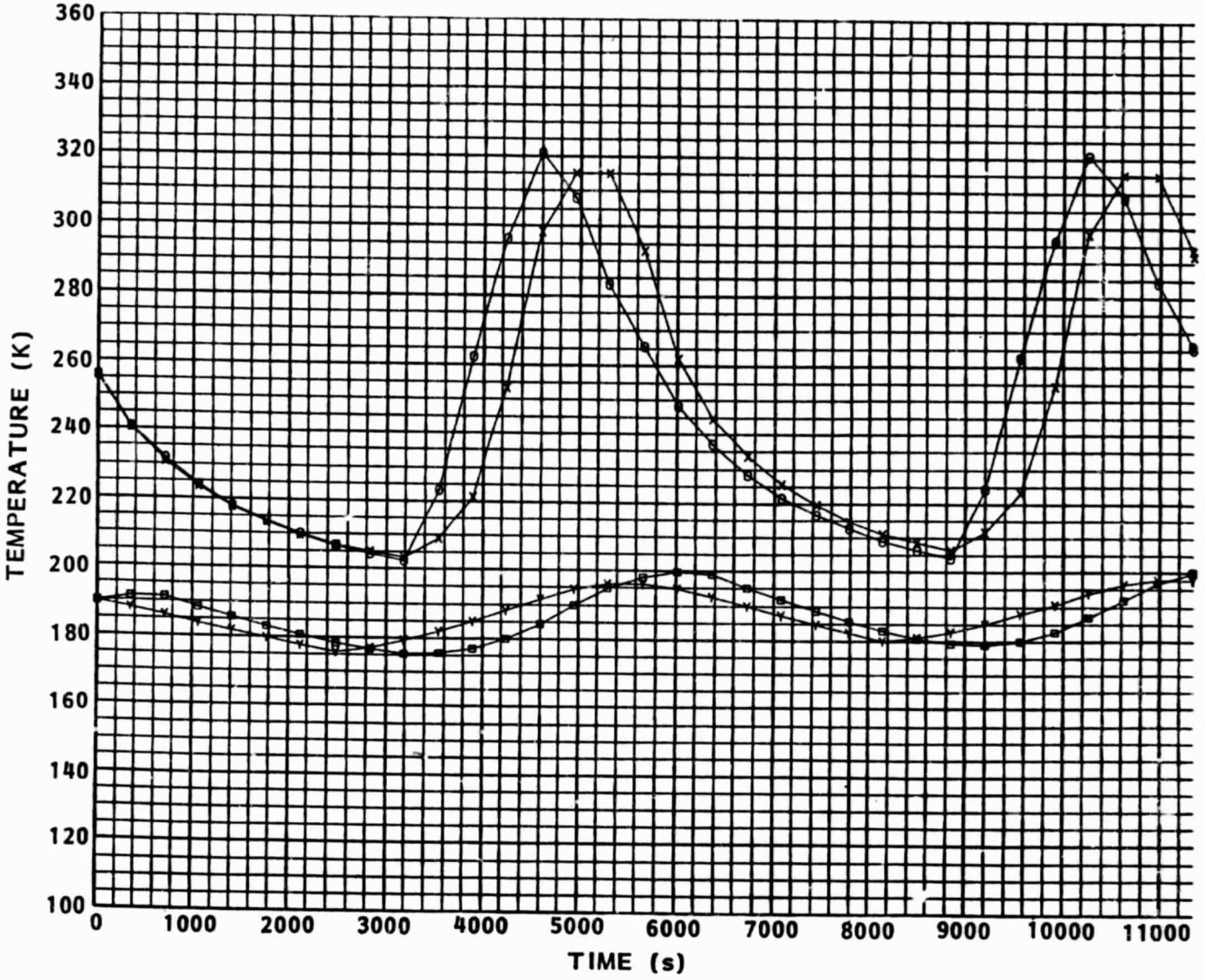

SHADE TEMPERATURE: FLARED SHADE

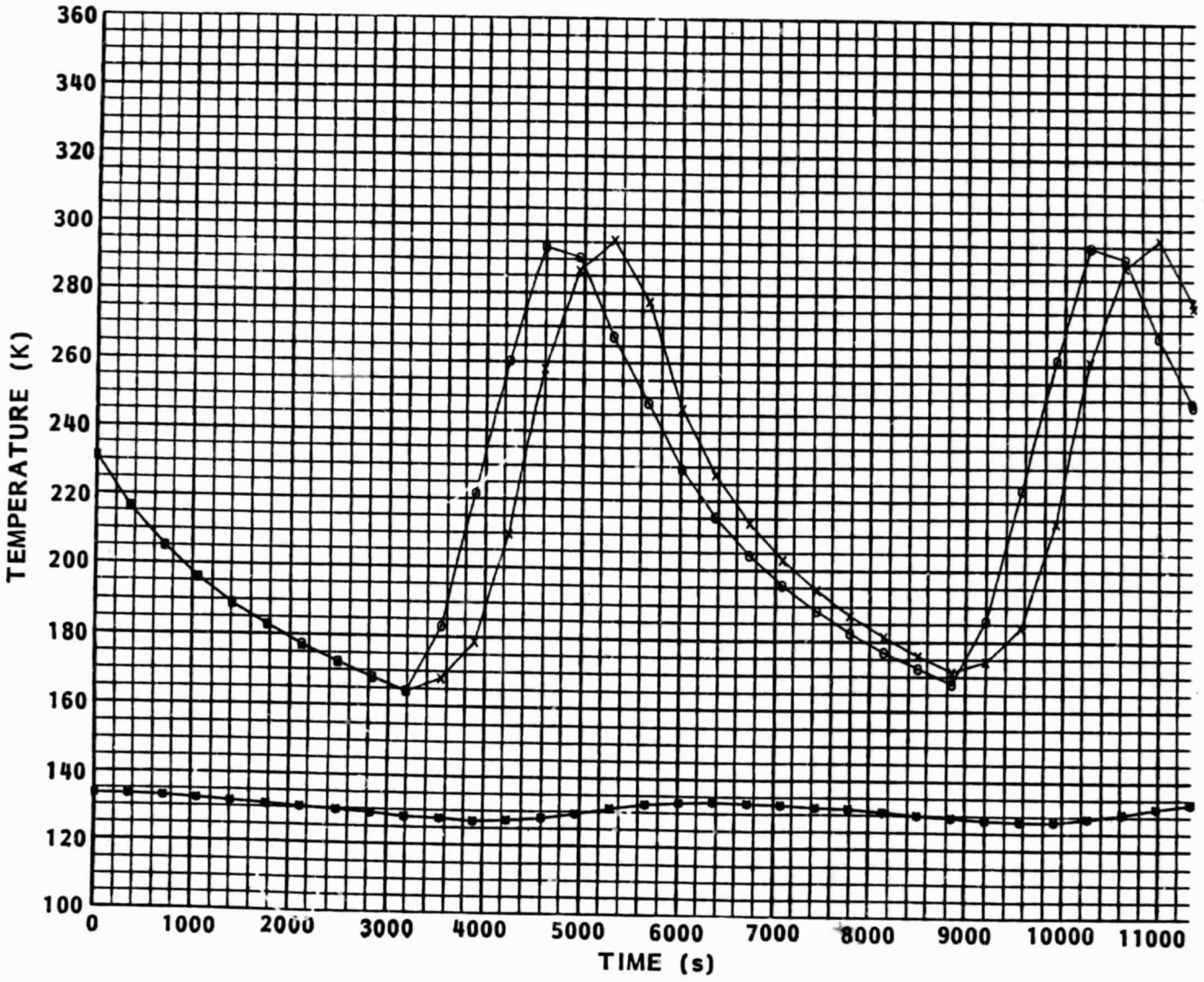

MIRROR TEMPERATURES: STRAIGHT SHADE

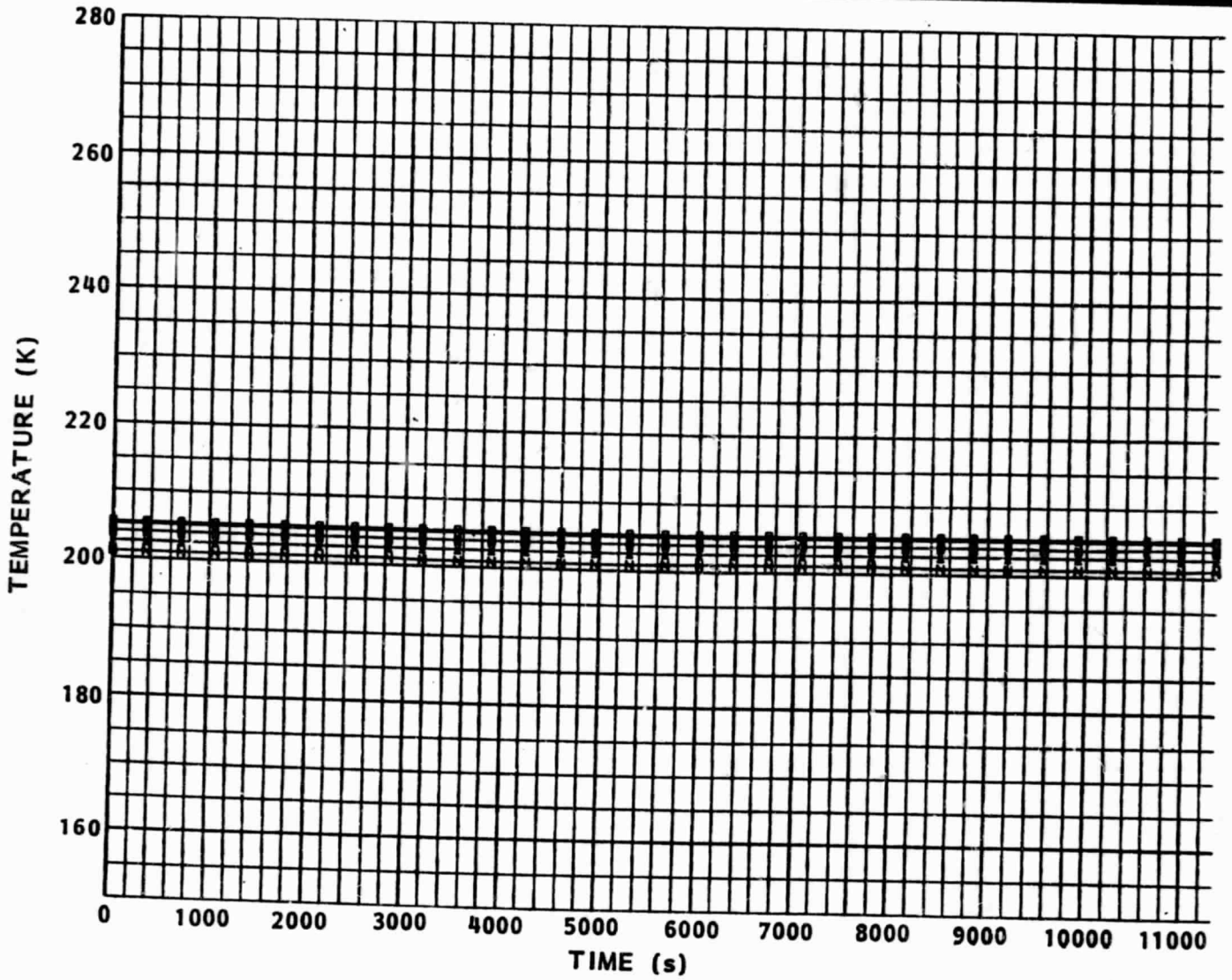

MIRROR TEMPERATURE: FLARED SHADE

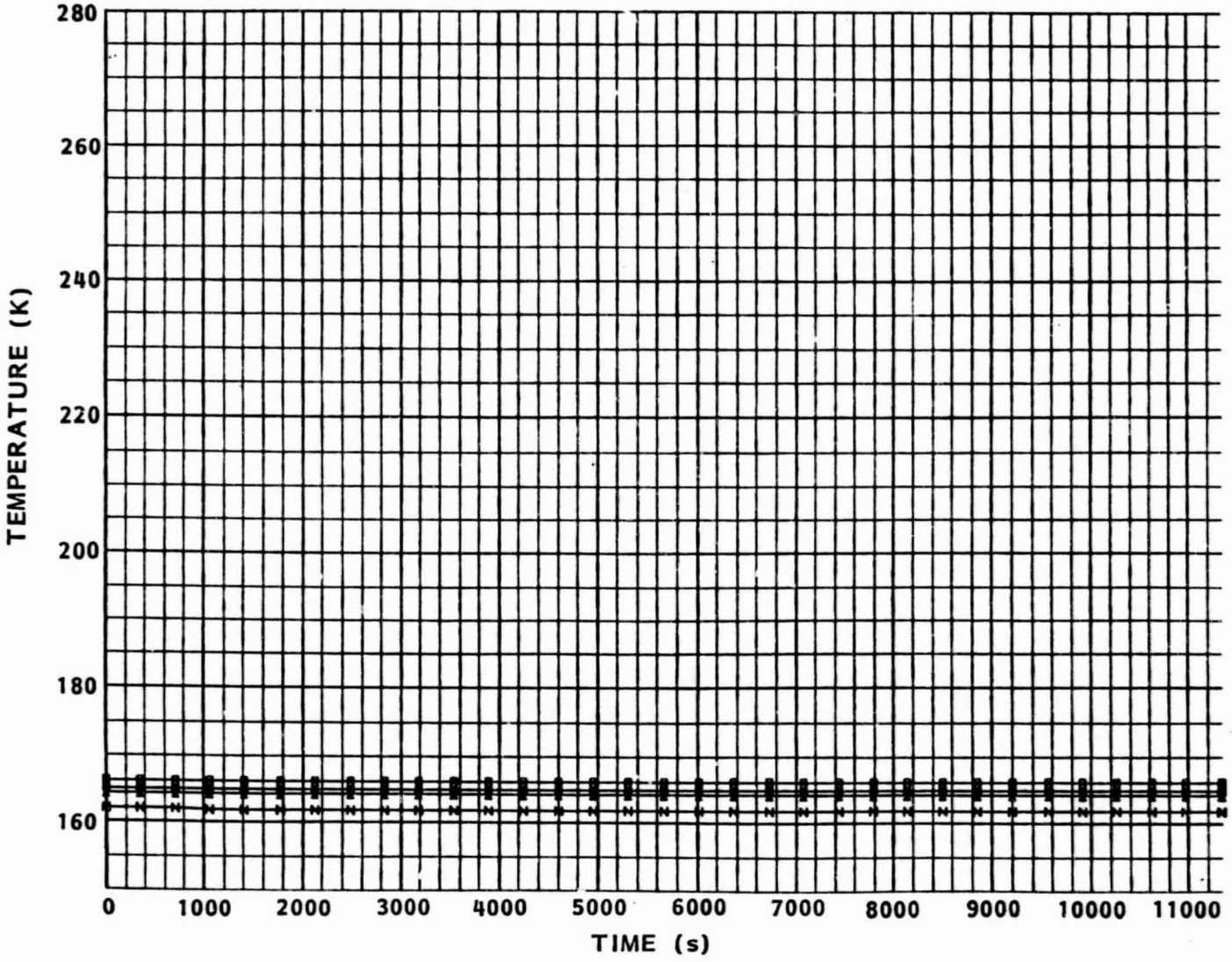

The net heat transport through the mirror is maintained by a temperature difference between front and back, ΔT_a. Considering only conduction through the mirror, for the moment, we find that for the "optimal" PE segment, with a segment thickness h=5 cm, and segment dimensions as shown in the figure (left bottom), core cross-section A_c (segment area A), $\Delta T_a \approx 1\ ^{o}C$. As a result of the temperature difference, the segment bends and has a maximum sag of σ= 0.5 microns. This is near the required maximum value allowed by the total figure error budget of the LDR. (The thermal expansion coefficient assumed here, $10^{-7}/^{o}C$ may be considered pessimistic; with "fine tuning" of the value for an anticipated LDR temperature, this tuning being accomplished for example by properly choosing the amount of TiO_2 doping, the value of α could be lowered somewhat.

AXIAL TEMPERATURE GRADIENT

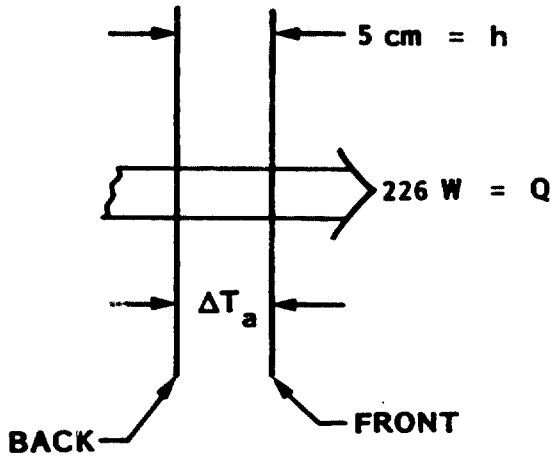

- RATE OF CONDUCTIVE HEAT TRANSFER: $q = 0.72\ W/m^2$
- $\Delta T_a = \frac{qh}{K_{eff}} = \frac{qh}{K} \cdot \frac{A}{A_c} \sim 1°C$

$[A/A_c \sim 38;\ K \sim 1.1\ W/m.°C]$

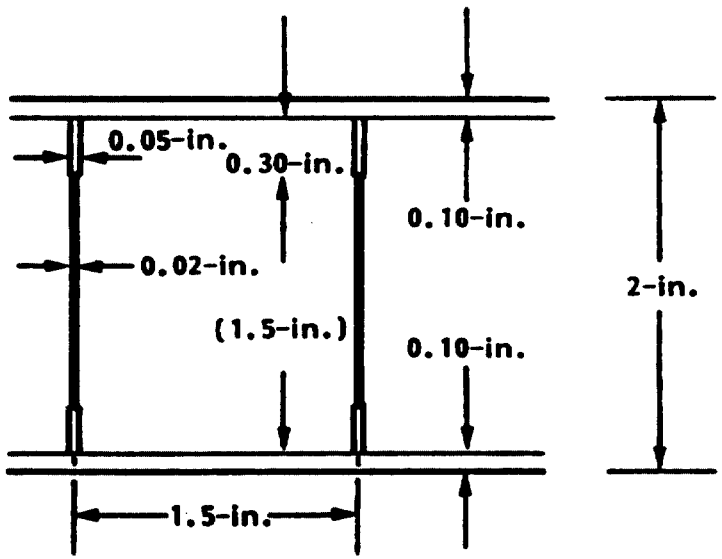

$\alpha = 10^{-7}/°C$; $d^2 = 2\ m^2$ GIVES

- SEGMENT SAG

$$\sigma = \frac{\alpha}{8} \frac{d^2}{h} \Delta T_a \sim 0.5\,\mu m\ (= \lambda/60\ AT\ 30\,\mu m)$$

- WHAT ABOUT – RADIATIVE HEAT TRANSFER?

ORIGINAL PAGE IS
OF POOR QUALITY

If the walls of the cells of the segment core are silverized and the top and bottom made highly emissive, radiation transfer through the core aids in reducing the thermal gradient, ΔT_a, as shown in this foil.

EFFECT OF RADIATION TRANSFER

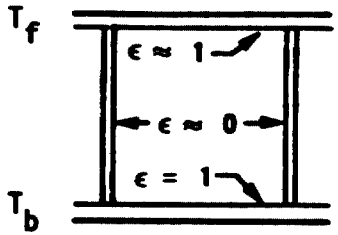

MIRROR CELL

- $q_{rad} \approx \sigma \Delta \left(T_{f-b}^4 \right)$
- $0.72 \ \frac{W}{m^2} \approx \sigma \ 4 \ \bar{T}^3 \ \Delta T_a$; $\bar{T} \sim 170$ K
- $\Delta T_a \sim 0.6°C$
- CONCLUSION: RADIATION TRANSFER HELPS REDUCE ΔT_a TO ABOUT 1/2°C

$\sigma \sim \lambda/120$

To obtain a more detailed picture of the LDR temperature distribution and variation with time, an accurate, detailed model of the LDR mission profile must be available. This model includes slew rates, orbit, heat inputs by the instrument package, etc. The results obtained with the numerical calculations here are encouraging concerning the passively obtained LDR temperature and are in agreement with PE's estimates.

The penalty of passivity lies in a heavy, perhaps difficult to deploy, sunshade which will also have some impact on the dynamical control of the LDR. It should also be reiterated that the quality of the thermal enclosure may decrease with time due to the degradation of the FOSR.

LDR TEMPERATURES: COMMENTARY

- MISSION PROFILE NEEDS TO BE MORE ACCURATELY DEFINED
- THEN: MORE EXTENSIVE MODELING REQUIRED TO PIN DOWN TEMPERATURES AND THEIR VARIATIONS (SPATIAL, TEMPORAL)
- $T \lesssim 200$ K POSSIBLE WITHOUT COMPLEX THERMAL CONTROL (SEMIACTIVE AND ACTIVE METHODS)

A top-level estimate of the shunshad weight was made assuming 5-mil FOSR and a Gr/epoxy sunshade structure on which the FOSR is attached. It is seen that the main contribution to the weight derives from the structure, and that the total weight is about 2000 kg.

SUNSHADE WEIGHT ESTIMATE (kg)

- SUPPORT STRUCTURE Gr/Ep TUBING 4-in. o.d., 3.5-in. i.d.

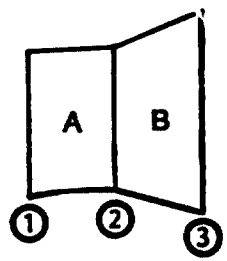

W_A ~ 380

W_B ~ 480

W_1, W_2 ~ 225

W_3 ~ 320

~ 1630 kg

- FABRIC (FOSR; 5-mil THICK)

W_A ~ 135

W_B ~ 220

~ 355

- TOTAL: 1985 kg + MECHANISMS

The emphasis of this study lay on the structure and dynamical control of the LDR. The main issues are discussed in the remainder of this presentation.

AGENDA

INTRODUCTION AND SUMMARY	W. ALFF
MIRROR SEGMENTS	L. BANDERMANN
SUNSHADE	L. BANDERMANN
▷ STRUCTURE MODEL (INTRODUCTION)	L. BANDERMANN
STRUCTURE AND CONTROL OVERVIEW	J. AUBRUN
SECONDARY MIRROR CHOPPING	K. LORELL
CONTROL SYSTEM PERFORMANCE	B. SRIDHAR

A detailed structure of the LDR dish and secondary mirror truss was generated. The model is outlined further later on. The mirror diameter is 20 m, f No. 0.5; the structural members are Graphite/Magnesium cylindrical tubes of various diameters, as required to provide a nigh stiffness to weight ratio. The lowest normal frequency (bending mode) is about 6 Hz. The total mass is about 12,000 kg, which is within the allowed weight budget of the LDR

LDR STRUCTURAL MODEL

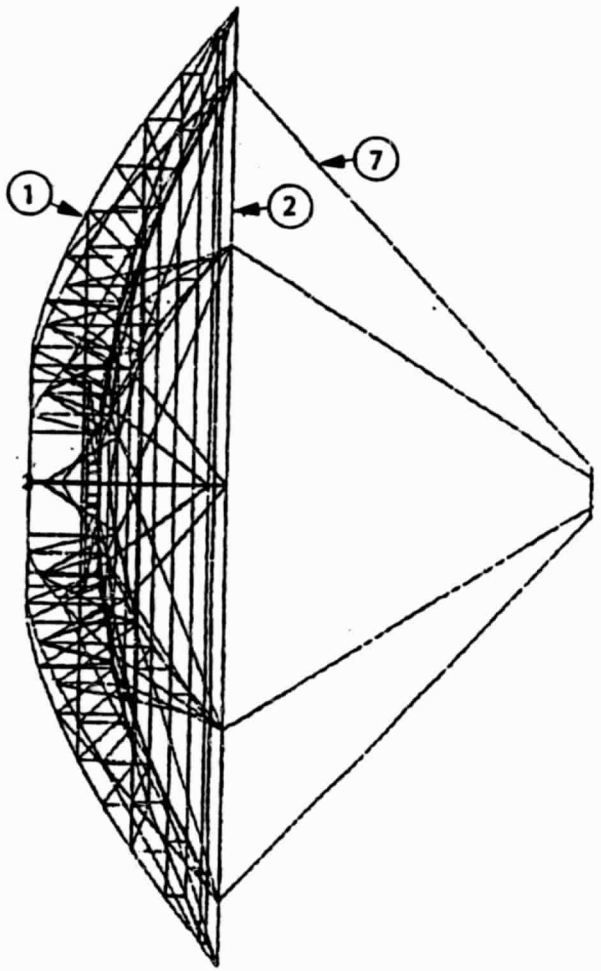

- 20 m, f/0.5
- Gr/Mg STRUCTURE
- 20 kg/m^2 MIRROR
- LOWEST fn ~ 6 Hz
- 12,000-kg WEIGHT

TYPE	RADIUS (cm)	
	INNER	OUTER
1	6.25	7.25
2	3.00	3.25
3	2.50	3.00
4	3.15	4.00
5	2.60	3.00
6	4.00	5.00
7	19.60	20.00

The next 3 foils discuss reasons why Gr/Mg was chosen as structural material. As in the case of the LDR segment material we argue that only the best material (resulting in minimum active control of the LDR) should be considered since the basic material cost -as compared with the total system cost- is negligible. (An estimate of the materials cost of the LDR structure is less than 0.5%)

WHY GR/METAL?

- SUPERIOR MATERIAL PROPERTIES
- DEVELOPMENT STRONGLY ADVANCING
- EXPECTED COST DECREASE
- RAW MATERIAL COST NEGLIGIBLE

This foil documents the superiority of Gr/Mg in terms of two important merit parameters: specific stiffness and thermal deformation resistance.

FIGURE OF MERIT

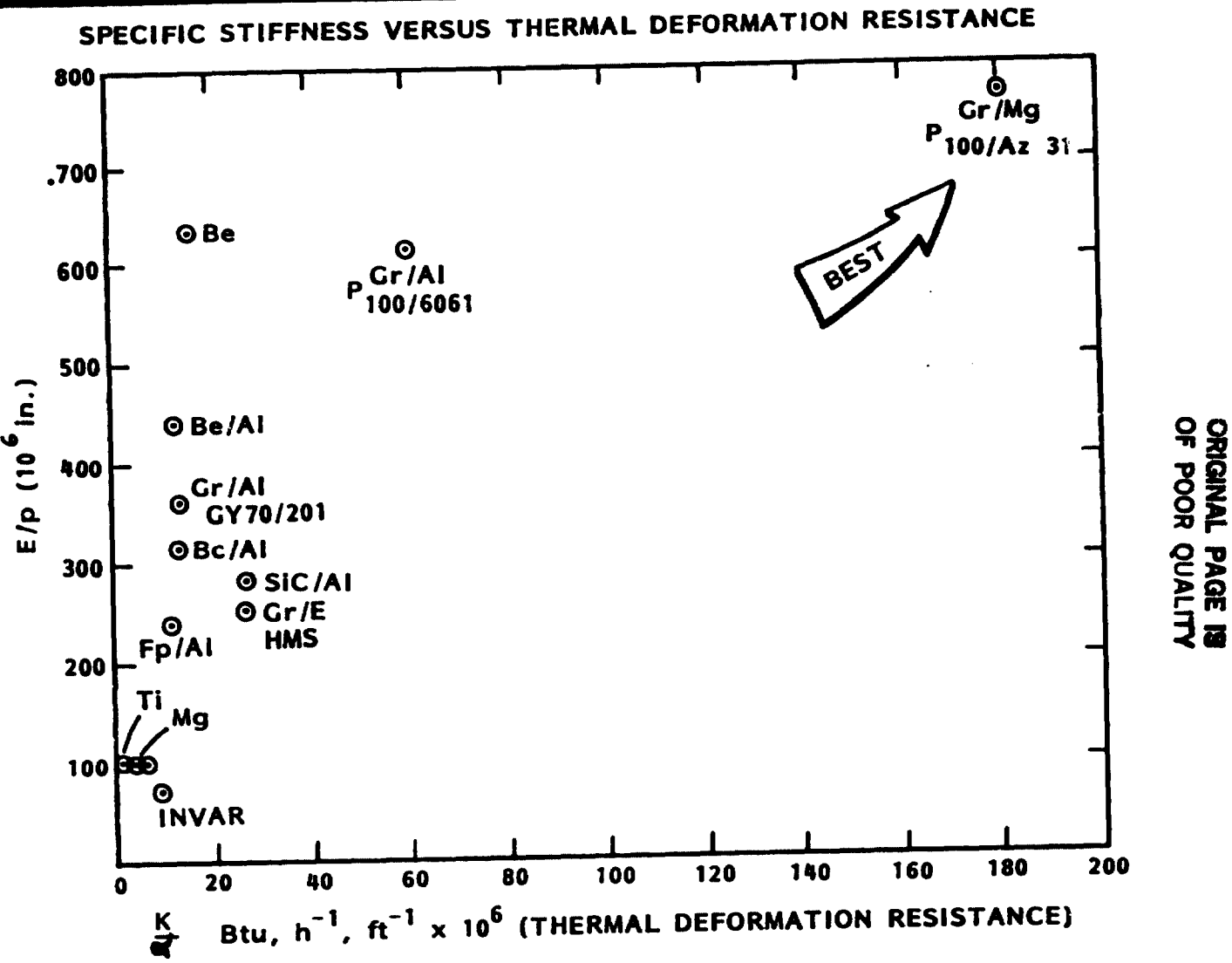

The cost of the main ingredient of the metal matrix materials, the precursor wires, is steadily decreasing with time.

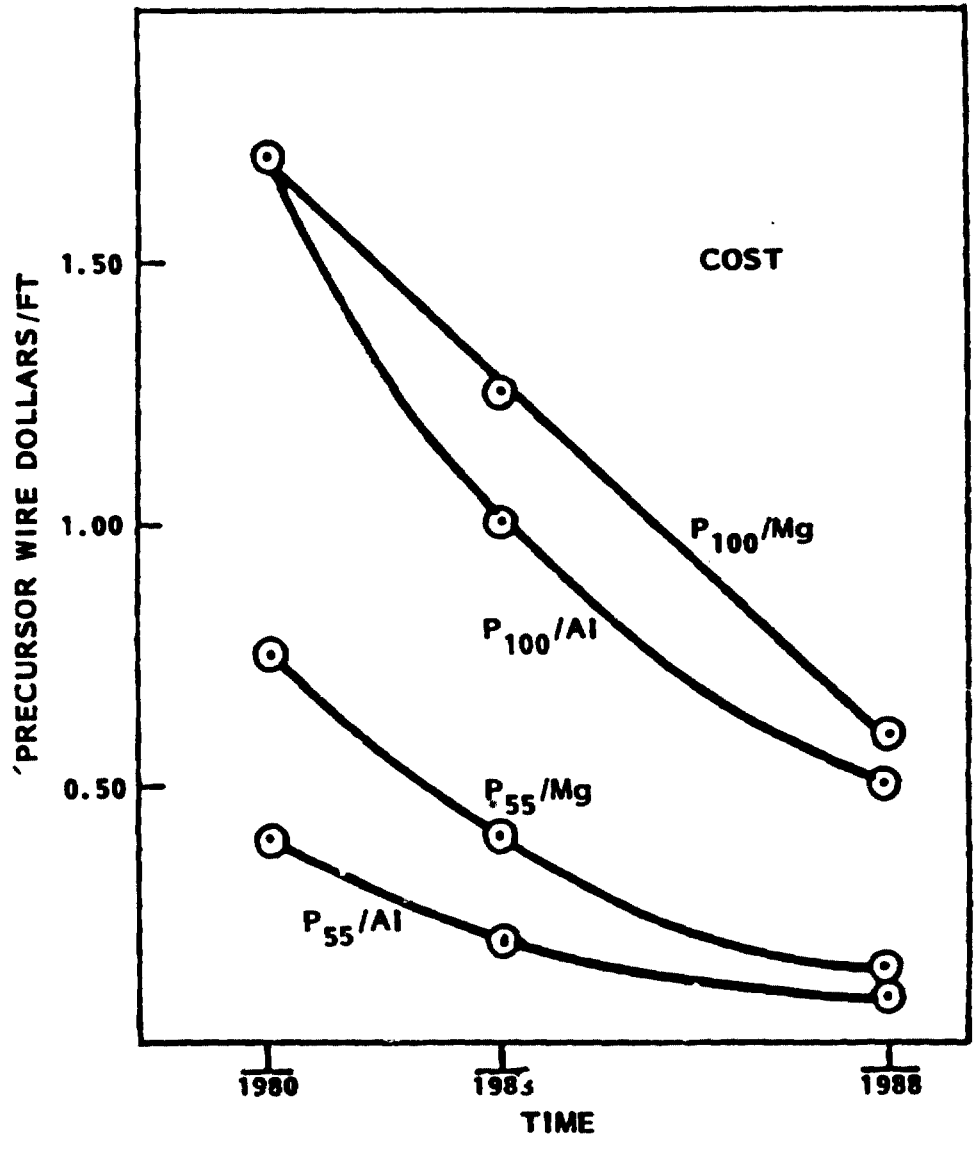

A potential critical systems issue (as well as cost issue) is the packaging and depoyment of the LDR in the shuttle. Earlier studies showed that volume, not weight, may be the limiting factor in packaging the LDR. The next two foils show a simple assessment of the packaging volume of the LDR dish alone. The volume enclosed by the dish is about 2/3 of the shuttle payload bay volume.

STRUCTURAL VOLUME OF DISH

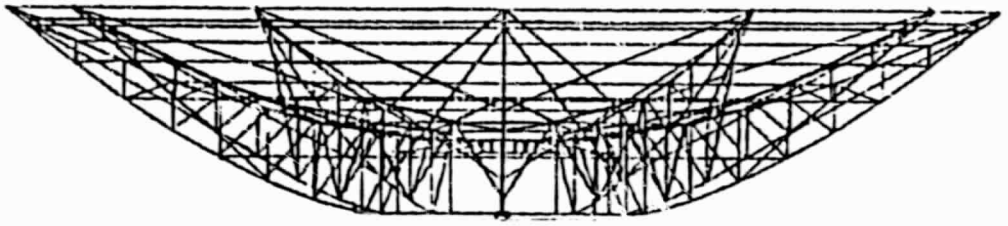

APPROXIMATE DISH TO TWO SPHERICAL SEGMENTS

V_1 = 662 cu m V_2 = 401 cu m

STRUCTURAL VOLUME OF DISH

$V_1 - V_2$ = 662 - 401 = 261 cu m

SPACE SHUTTLE PAYLOAD BAY ≈ 5 m x 20 m

∴ VOLUME ≈ 393 cu m

If the LDR dish is sectioned into 16 sections and two are packaged together as shown in this foil, the total volume the packed dish requires is about 2 shuttle loads. To this must be added the volume required by the rest of the system: spacecraft, sunshade, solar arrays and antennas, etc. We conclude that a highly sophisticated packaging scheme needs to be devised to pack LDR into one shuttle. Such a packaging scheme could require a highly sophisticated deployment mechanism and perhaps extensive manual assistances including EVA by the shuttle crew.

Clearly, packaging and deployment of the LDR is one of the foremost issues to be addressed in further systems or feasibility studies.

POSSIBLE PACKAGING CONCEPT

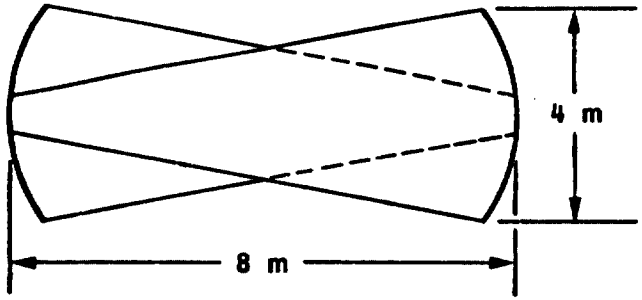

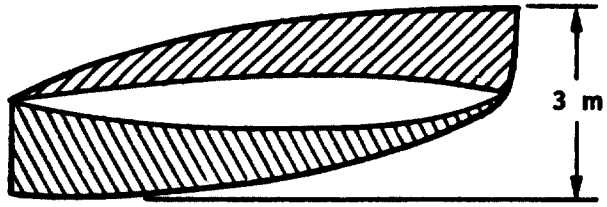

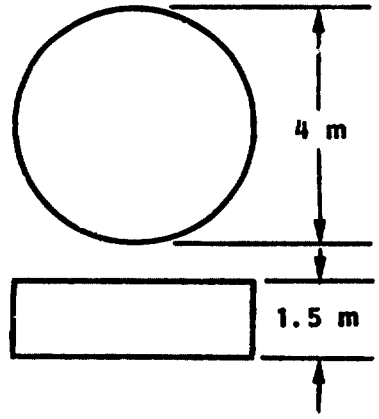

2 SEGMENTS 3 x 4 x 8 = 96 cu m

8 PACKAGES/DISH = 8 x 96 = 768 cu m
(16 SEGMENTS)

HUB VOLUME = 19 cu m

TOTAL PACKAGED VOLUME
OF DISH = 787 cu m

PLUS SPACECRAFT
SUNSHADE } ?

SHUTTLE PAYLOAD BAY VOLUME 393 cu m

AGENDA

INTRODUCTION AND SUMMARY	W. ALFF
MIRROR SEGMENTS	L. BANDERMANN
SUNSHADE	L. BANDERMANN
STRUCTURE MODEL (INTRODUCTION)	L. BANDERMANN
▷ STRUCTURE AND CONTROL OVERVIEW	J. AUBRUN
SECONDARY MIRROR CHOPPING	K. LORELL
CONTROL SYSTEM PERFORMANCE	B. SRIDHAR

POINTING AND VIBRATION CONTROL STUDIES

AGENDA

OVERVIEW — **J. N. AUBRUN**

- CONTROL ISSUES
- DISTURBANCE SOURCES
- STRAWMAN MODEL
- CONTROL METHOLODOLOGY

SECONDARY MIRROR CHOPPING — **K. R. LORELL**

CONTROL SYSTEM/PERFORMANCE STUDY — **B. SRIDHAR**

- REQUIREMENTS
- CONTROL SYSTEM CONCEPTS
- SIMULATION MODEL
- SIMULATION RESULTS:
  - NODDING
  - POINTING
  - SLEWING
  - VIBRATION PROPAGATION
- CONCLUSION AND RECOMMENDATIONS

This foil list important issues concerning the pointing and vibration control of the LDR which will be addressed.

POINTING AND VIBRATION CONTROL STUDIES
CONTROL ISSUES

- LARGE FLEXIBLE STRUCTURE
- HIGH POINTING PERFORMANCE
- SURFACE FIGURE ERROR
- VEHICLE MANEUVERING (SLEW, NODDING)
- SPACE CHOPPING
- ONBOARD VIBRATION SOURCES

Of the various disturbance sources affecting LDR pointing performance, thermal, gravity gradient and solar loads are slowly varying and relatively easy to handle with the low bandwidth alignment and figure control system (tilt/piston control of the segments). The other disturbances involve dynamic effects which have to be addressed specifically by the strawman control system discussed later on.

POINTING AND VIBRATION CONTROL STUDIES
DISTURBANCE SOURCES

- EXTERNAL
  - THERMAL
  - GRAVITY GRADIENT
  - SOLAR
- INTERNAL
  - CMG NOISE
  - SECONDARY MIRROR CHOPPING
  - CRYO-COOLER VIBRATIONS
- INDUCED
  - SLEW AND NODDING MANEUVERS

This foil explains the criteria in the selction of a strawman control model for the study of the performance of the LDR. In addition, the model selection is influenced by the amount of effort required to develop such a model.

POINTING AND VIBRATION CONTROL STUDIES

STRAWMAN MODEL

(1) MUST BE ABLE TO FAIRLY REPRESENT:

- OVERALL GEOMETRY ⇒ OPTICAL PERFORMANCE
- MASS/INERTIA PROPERTIES ⇒ ACTUATOR SIZING
- FLEXIBILITY EFFECTS ⇒ PERFORMANCE EVALUATION

(2) CAN BE USED TO GENERATE A WORKABLE MATHEMATICAL MODEL

- MODEL FREQUENCIES
- MODE SHAPES

The characteristics and limitations of the finite element model used to develop the strawman control model are shown in the next two Vu-foils. It is a complex model, represented by a large amount of data.

LDR STRUCTURAL MODEL (1 OF 2)

- LDR FINITE ELEMENT MODEL WAS DEVELOPED USING A MODIFIED VERSION OF SPAR COMPUTER PROGRAM
- HIGHLIGHTS OF THE MODEL
  - 20-m, F/0.5 REFLECTOR
  - 720 BEAM ELEMENTS
  - 168 PLATE ELEMENTS
  - 500 JOINTS
- NO ATTEMPT WAS MADE TO INTEGRATE THE MIRROR SEGMENTS IN DETAIL
- THE STRUCTURAL MODEL DOES NOT INCLUDE THE SUNSHADE

Although the sunshade was not modeled, it will not pose a critical problem for the attitude control system when included because of the type of controller used will always account for flexibility effects. However, the sunshade will likely reduce the spacecraft maneuverability.

LDR STRUCTURAL MODEL (2 OF 2)

- SINCE THE SUNSHADE IS A NONSTRUCTURAL COMPONENT OF THE LDR, THERE IS A GREAT LATITUDE AVAILABLE IN ITS DESIGN
- EFFECT OF THE SUNSHADE ON POINTING STABILITY CAN BE GREATLY REDUCED BY A DESIGN WHICH ISOLATES THE SUNSHADE FROM THE REFLECTOR
- SOME POSSIBILITIES ARE
  - SHOCK MOUNT
  - ACTIVE DAMPING
  - ACTIVE ISOLATION

The first normal mode of vibration of the LDR is a bending mode at about 6 Hz.

STRAWMAN STRUCTURAL MODEL

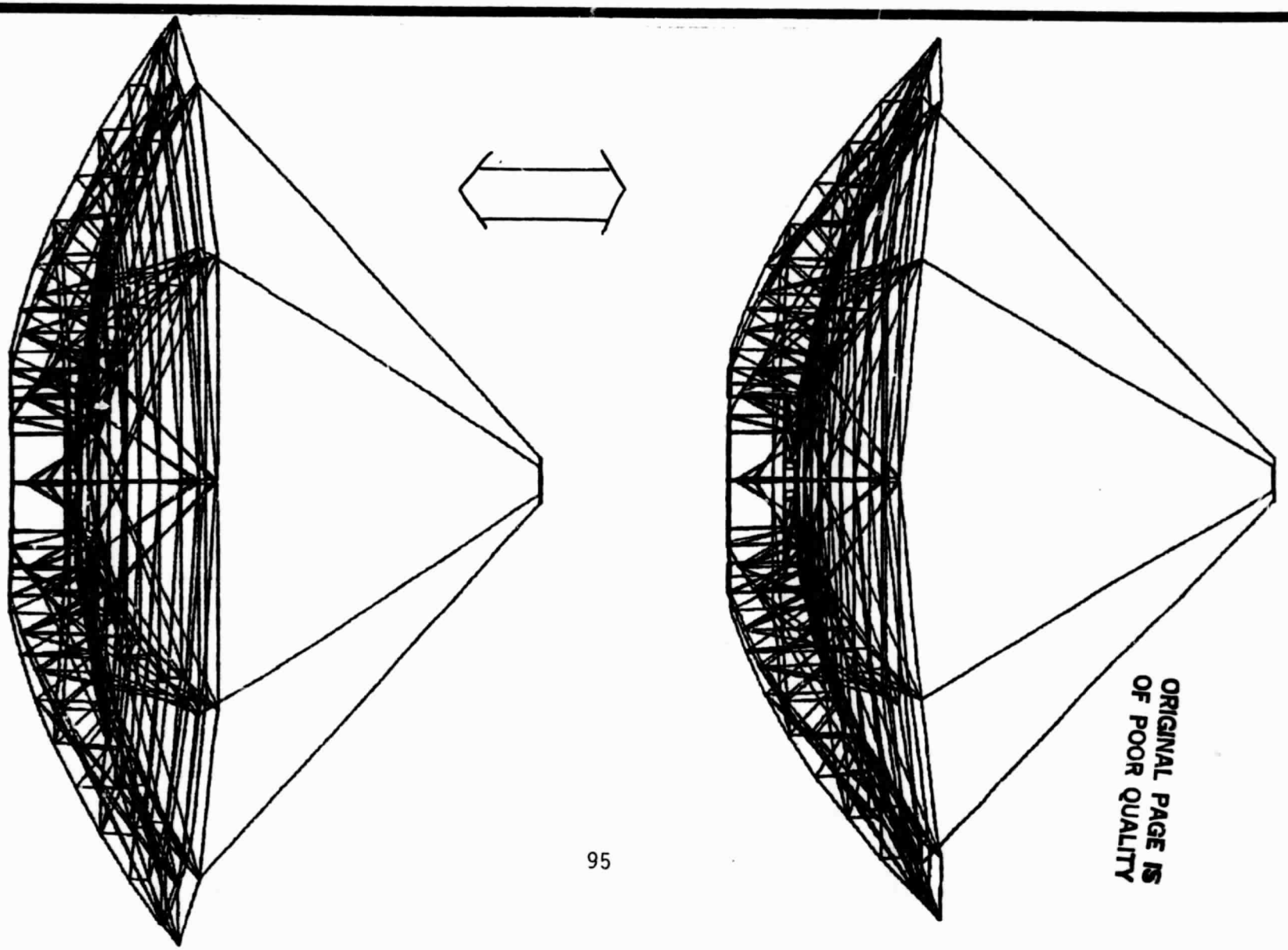

The front view of the LDR backup structure shows 12 radial ribs. Nine points were selected on each rib (total of 108) to compute the RMS surface error during and after slewing of the LDR (discussed later on). The same points were used to define the optical axis of the mirror in terms of the average normal to the surface to compute the LOS error (during and after slewing).

STRAWMAN STRUCTURAL MODEL

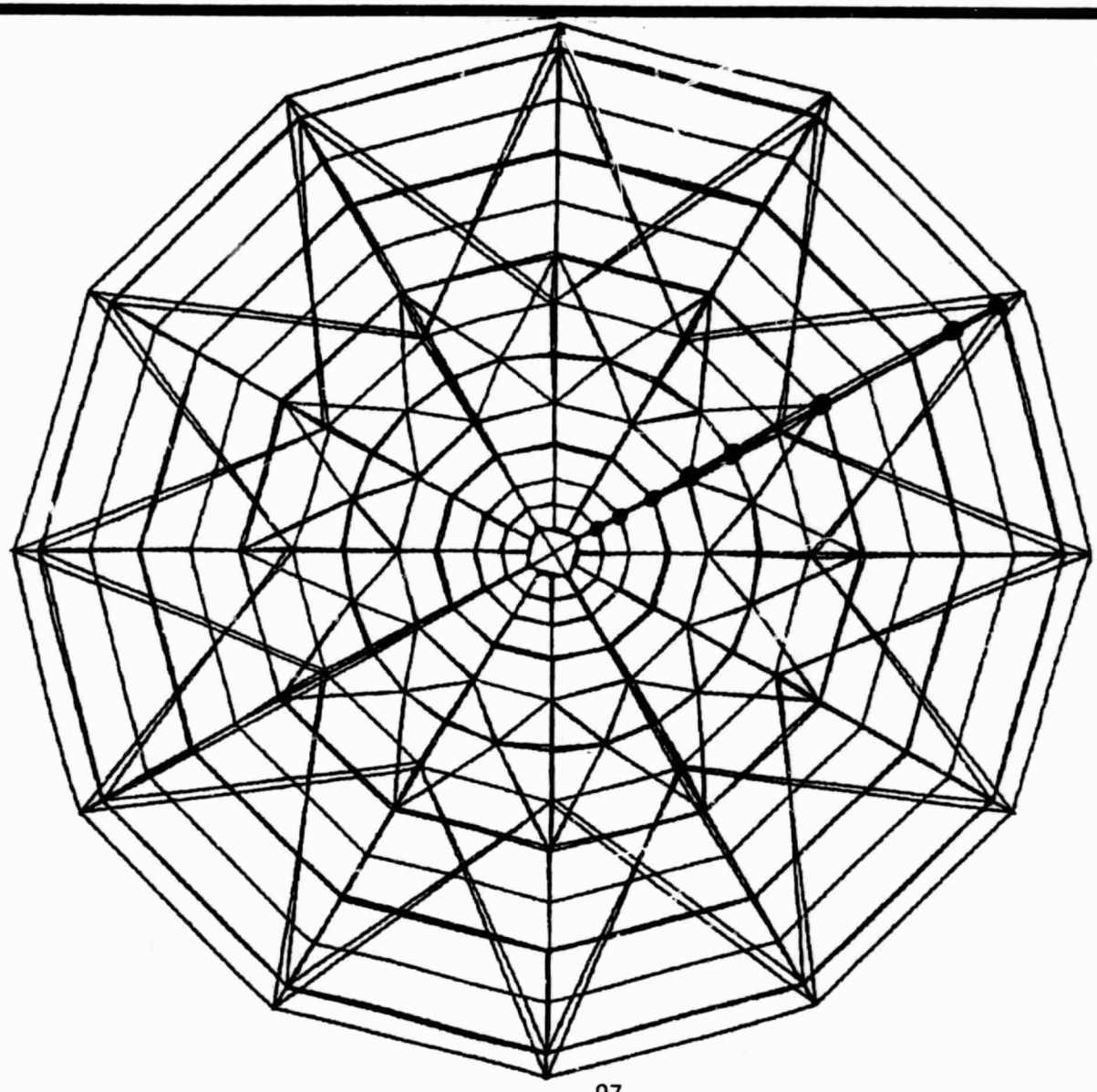

The state space model, which is the starting point for the control design, is derived from the structural model shown earlier. This state space model may be further simplified for the control synthesis. An evaluation model is necessary to study the effects such as nonlinearities and loss of accuracy due to model reduction.

CONTROL DESIGN METHODOLOGY

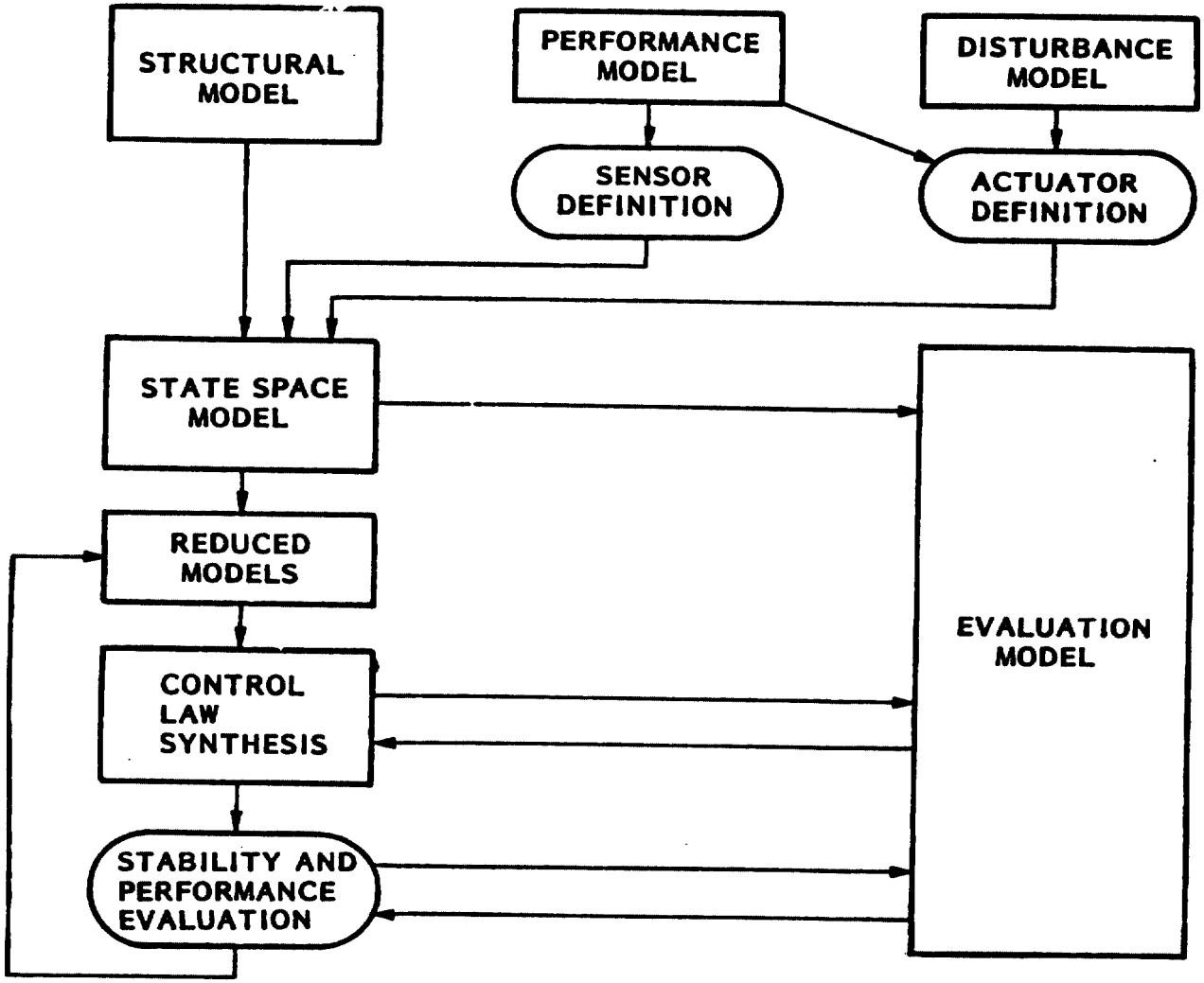

The classical modal representation of the structure is shown here. ω_n represents the natural frequencies of the structure including the rigid body modes; f represents the forces applied at the nodes. In practice, forces are applied only at a few nodal points of the structure and there is a linear relation between u and f.

LDR CONTROL MODEL

- THE FIRST STEP IN THE DESIGN OF A PVCS SYSTEM FOR LDR IS THE DERIVATION OF A CONTROL MODEL FROM THE DATA PROVIDED BY FINITE-ELEMENT STRUCTURAL PROGRAMS

- CLASSICAL MODAL EQUATION

  δ - VECTOR OF DISPLACEMENTS AT ALL NODES
  q - VECTOR OF MODAL AMPLITUDES
  f - VECTOR OF CONTROL FORCES AT THE NODES
  u - CONTROL VECTOR

$$\delta = \phi q$$

$$\ddot{q} + \left[\omega_n^2\right] q = \phi^T f$$

$$f = Au$$

The dynamic equations for the LDR can be written in the state space form as shown here. The open loop poles are eigenvalues of the matirx F. F has complex eigenvalues and eigenvectors. The computation of matrices F, G, and H from structural data and actuator/sensor definitions usually requires a direct handling and processing of data by computer - hand calculations become prohibitive for large systems like the LDR.

STATE SPACE MODEL

- **STATE VECTOR**

$$x \triangleq \begin{bmatrix} \dot{q} \\ q \end{bmatrix}$$

- **SYSTEM EQUATION**

$$\dot{x} = F x + G u$$
$$y = H x$$

$$F \triangleq \left[\begin{array}{c|c} -2\zeta_n\omega_n & -\omega_n^2 \\ \hline I & O \end{array}\right], \quad G \triangleq \begin{bmatrix} \Phi^T A \\ \hline O \end{bmatrix} \text{ and } H = R \begin{bmatrix} \Phi \\ \hline \Phi \end{bmatrix}$$

- **MATRIX A DEPENDS ON THE ACTUATOR LOCATIONS AND R DEPENDS ON THE SENSOR LOCATIONS**

- **DIAGONAL ELEMENTS $-2\zeta_n\omega_n$ REPRESENT THE NATURAL DAMPING (ABOUT 1/2%)**

- **IN THE LDR SIMULATION F IS 40 x 40, G IS 40 x 3 AND H IS 6 x 40**

The control integration combines the advantages of LAC and HAC while minimizing their disadvantages. This results in a structure which has very high performance yet is very stable.

HIGH AND LOW-AUTHORITY CONTROL INTEGRATION

HAC EFFECTS

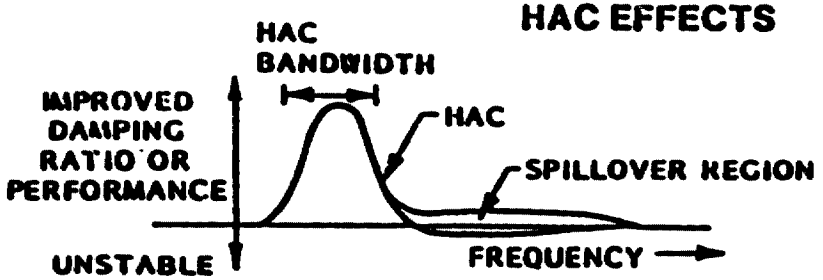

HIGH AUTHORITY

- LARGE DAMPING RATIO CHANGES
- EIGENVECTOR CHANGES
- LQG SYNTHESIS WITH FREQUENCY SHAPING
- ENHANCED CONVENTIONAL LQG ROBUSTNESS

LAC EFFECTS

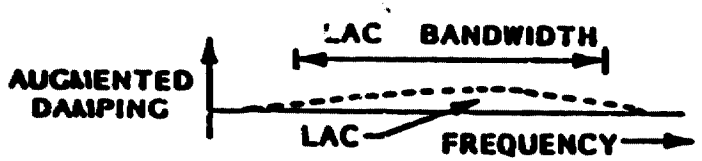

LOW AUTHORITY

- BROADBAND DAMPING AUGMENTATION
- ROBUST AGAINST MODELING ERROR
- SIMPLIFIED SYNTHESIS (LEAST SQUARES, JACOBI'S PERTURBATION)

INTEGRATED HAC/LAC

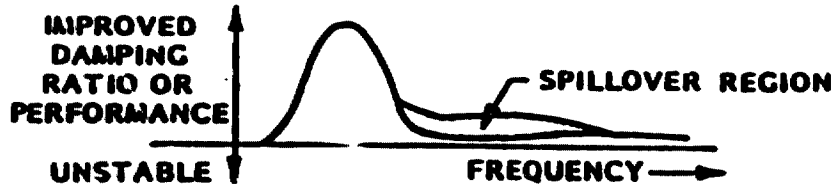

AGENDA

	INTRODUCTION AND SUMMARY	W. ALFF
	MIRROR SEGMENTS	L. BANDERMANN
	SUNSHADE	L. BANDERMANN
	STRUCTURE MODEL (INTRODUCTION)	L. BANDERMANN
	STRUCTURE AND CONTROL OVERVIEW	J. AUBRUN
▷	SECONDARY MIRROR CHOPPING	K. LORELL
	CONTROL SYSTEM PERFORMANCE	B. SRIDHAR

Space chopping is a technique used by astronomers to improve the signal-to-noise ratio (SNR) of weak sources. By rapidly switching the telescope field-of-view andsubtracting the two signals, weak sources can be detected in a region of comparable background IR radiation.

SPACE CHOPPING

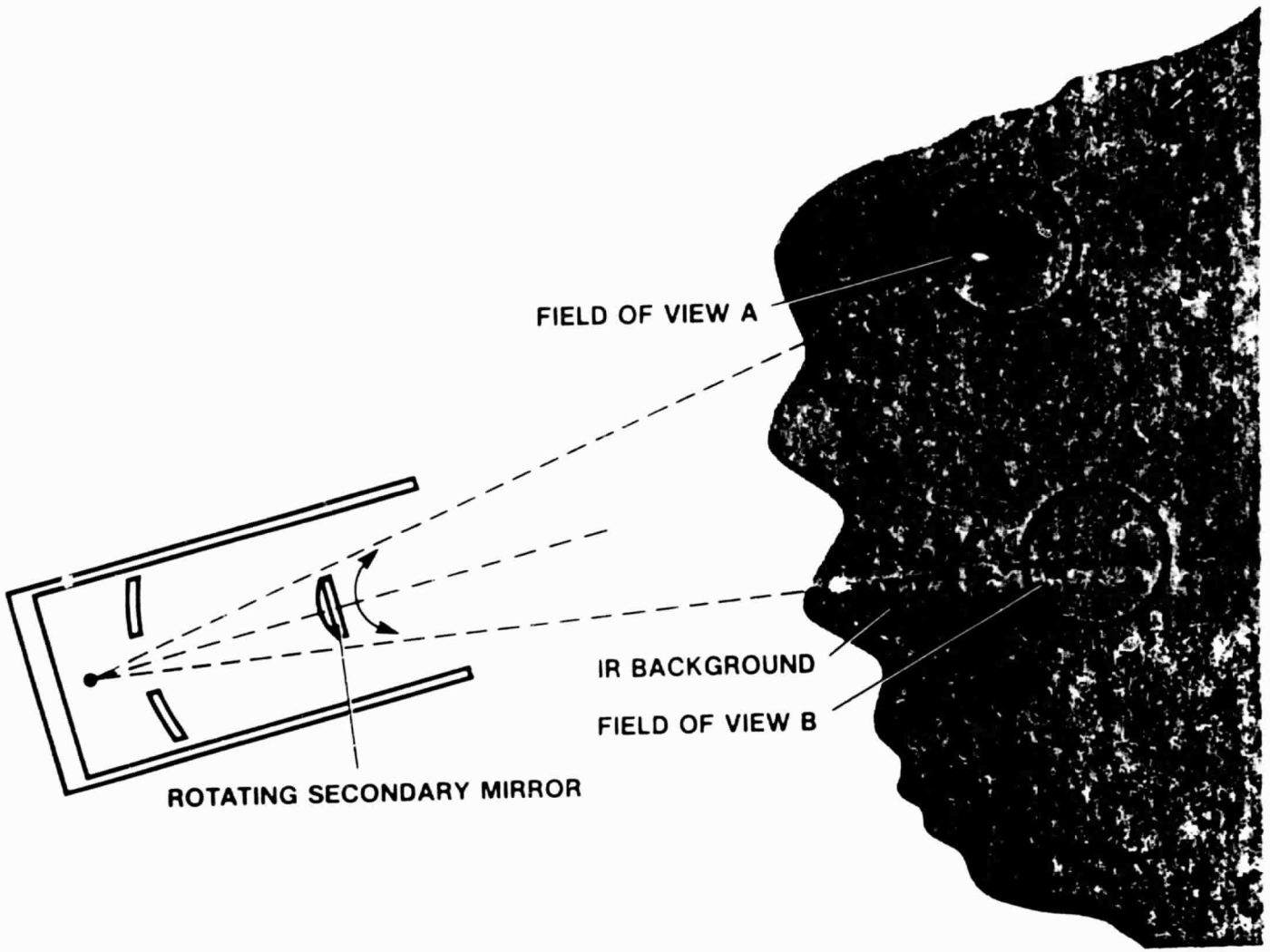

This chart shows the design optimization procedure.

Two types of actuators to be used in driving the secondary mirror are shown, electromagnetic and elctrodynamic. The electromagnetic actuator uses a permanent magnet an a moving coil to generate force. The electrodynamice actuator has two powerd pole pieces and is analogous to a series wound d.c. motor. It has the advantage of using a very narrow gap to generate strong magnetic interactions.

ELECTROMAGNETIC AND ELECTRODYNAMIC ACTUATORS

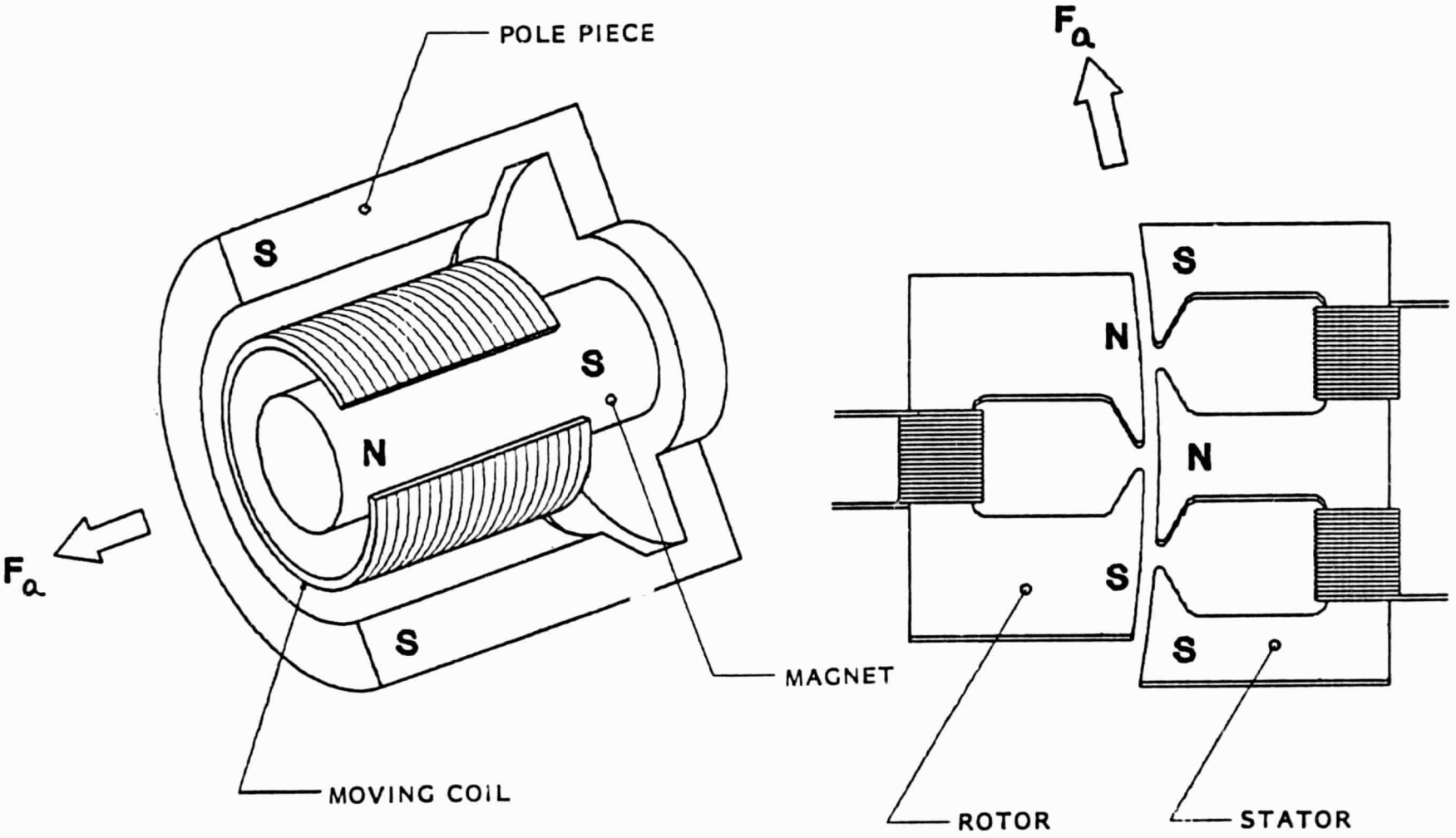

This chart shows a typical mirror actuator configuration with principle geometric quantities. The technique for using actuator motion to cancel reaction forces is illustrated.

TYPICAL MIRROR/ACTUATOR CONFIGURATION

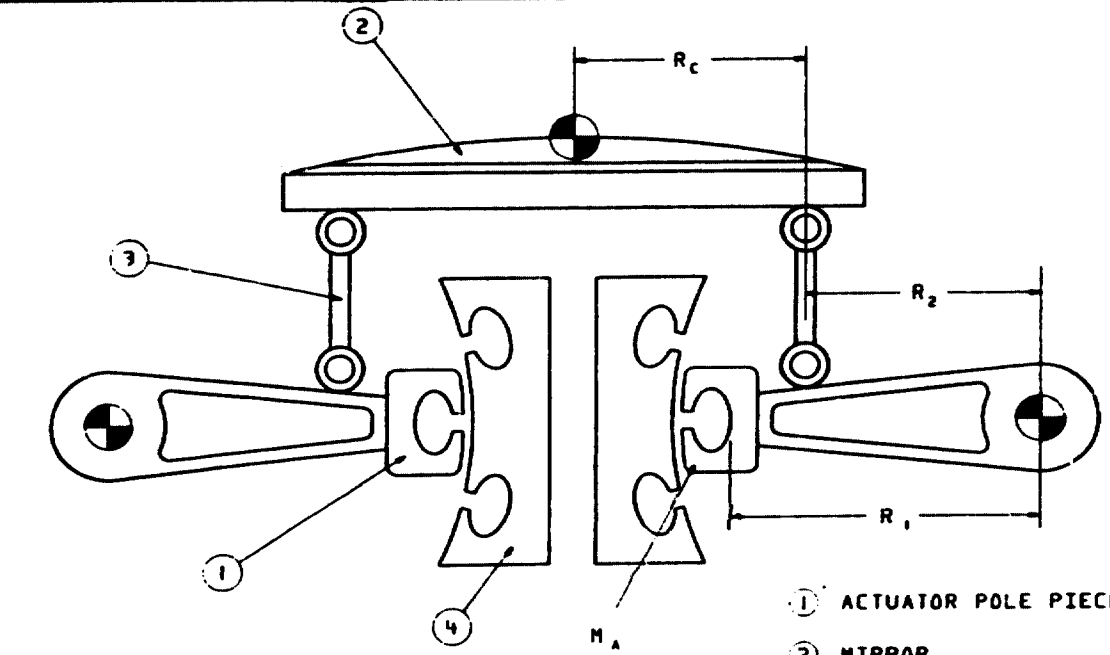

1. ACTUATOR POLE PIECE (ROTOR)
2. MIRROR
3. LINKAGE
4. ACTUATOR POLE PIECE (STATOR)

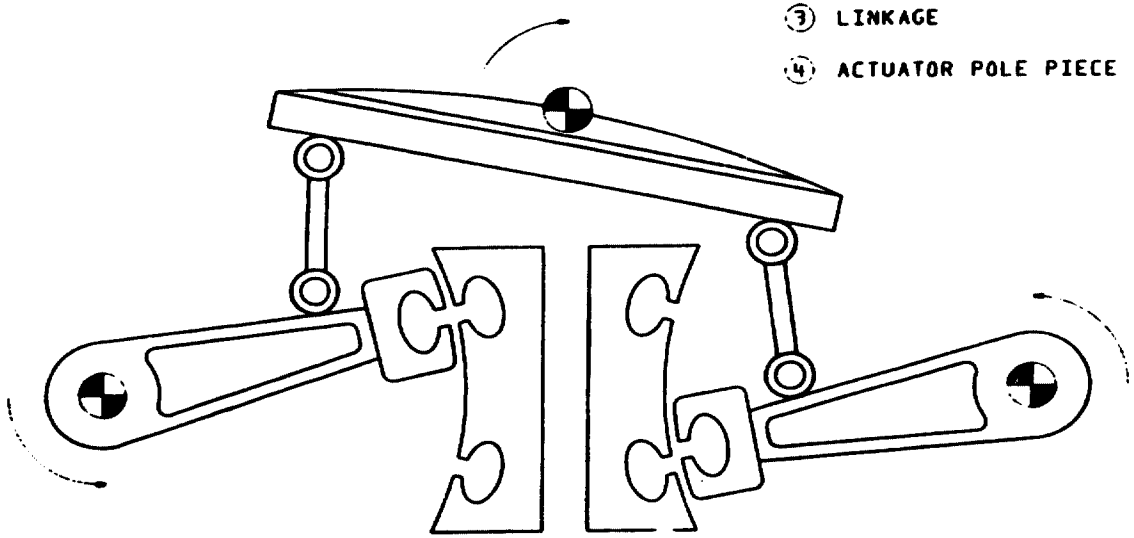

Typical position versus time traces are shown here for a 20 secondary mirror chopping. Note the increase in the time available to move the mirror between the two endpoints when the duty cycle, is decreased from 90% to 80%.

EFFECT OF DUTY CYCLE VARIATION

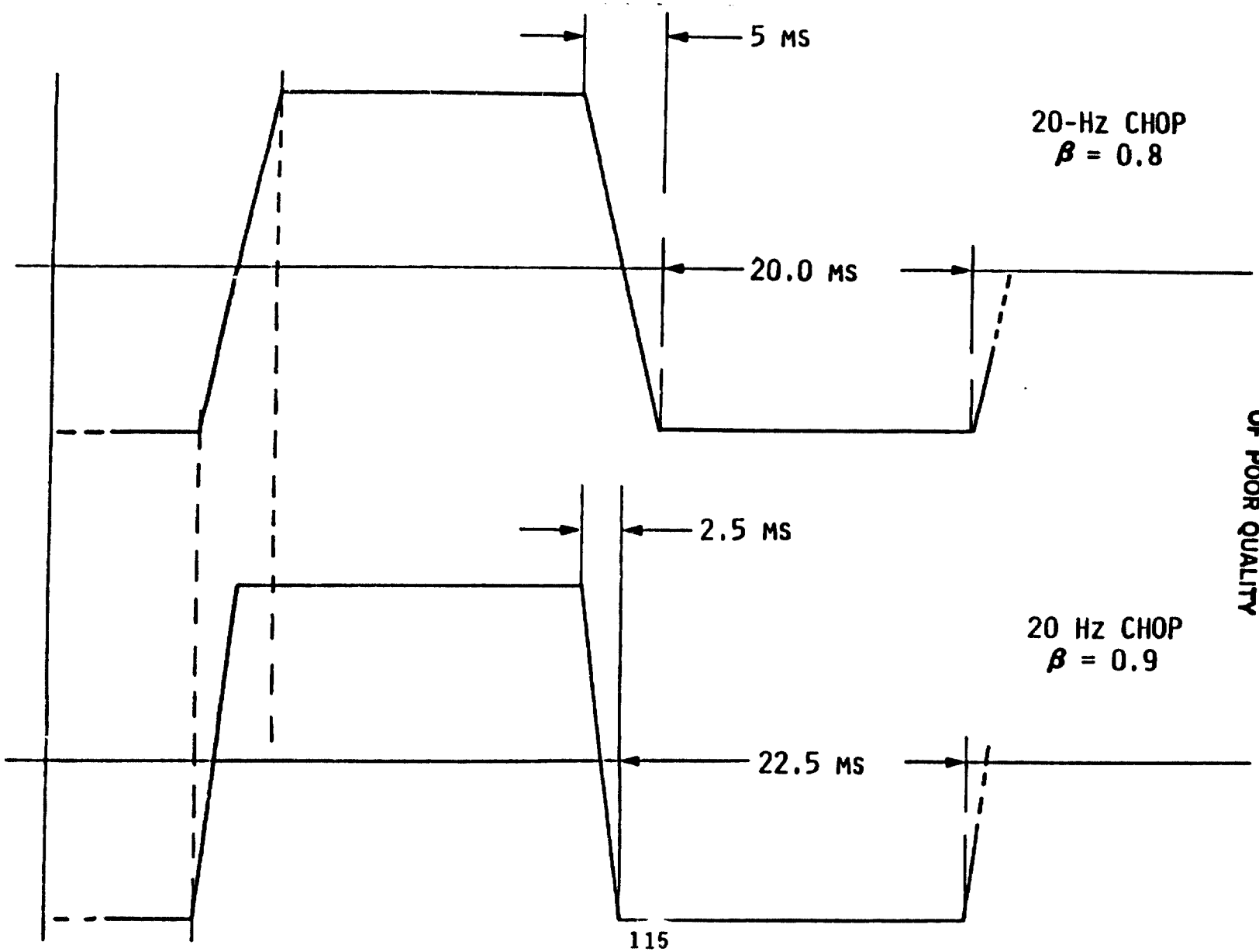

This schematic diagram shows the transition periods of acceleration, coasting, and deceleration. A minimum amount of energy is dissipated when $\alpha = 0.33 = 1/3$

TRANSITION PERIOD DETAIL

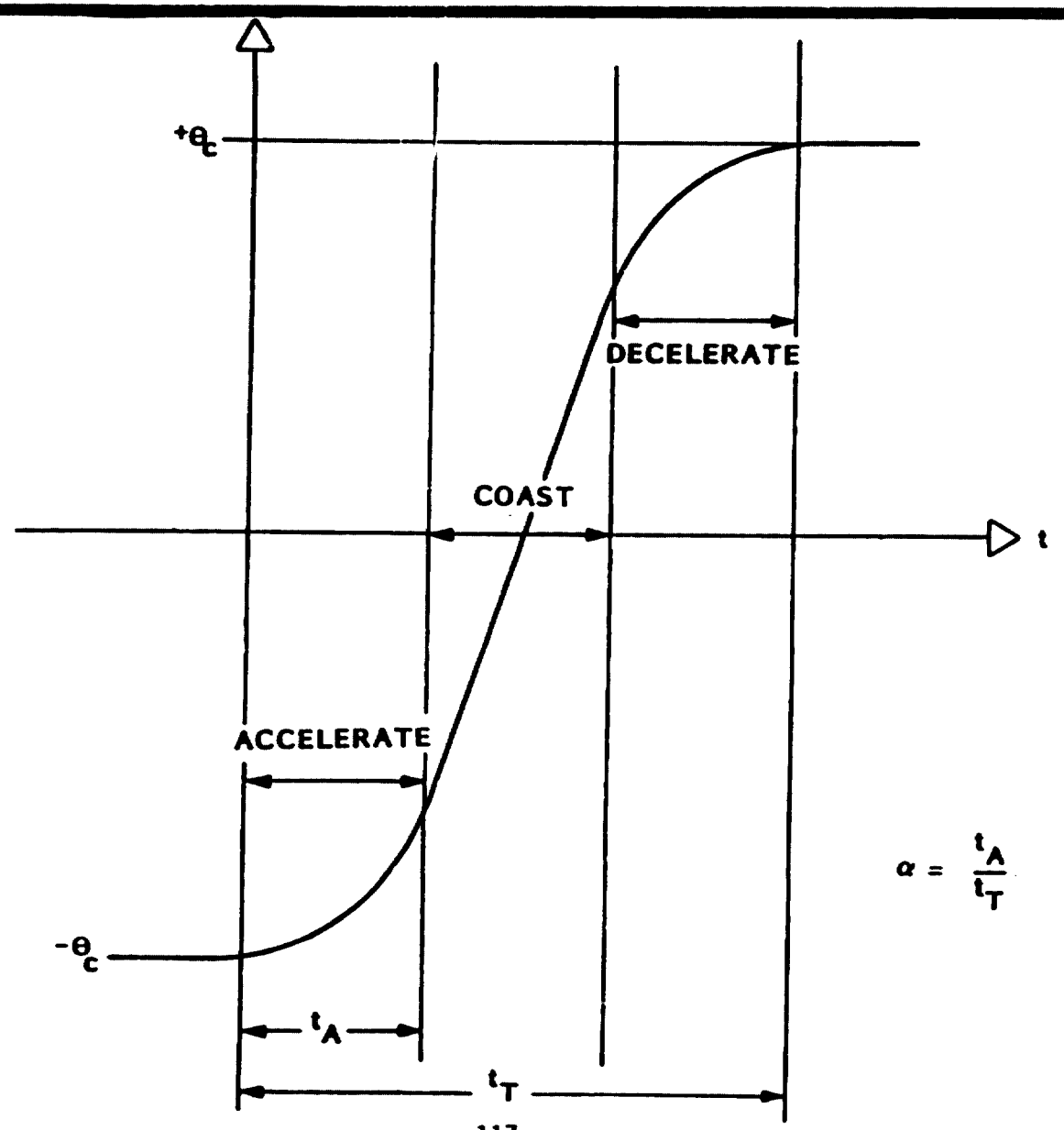

$$\alpha = \frac{t_A}{t_T}$$

The design equations used to optimize a mirror/actuator system with respect to minimum electrical dissipation are shown here. This design is for a fully reaction-cancelling system.

DESIGN OPTIMIZATION – RELEVANT EQUATIONS

1 BALANCING CONDITION (NO NET ANGULAR MOMENTUM)

$$\gamma(I_a + m_a R_1^2) = I_m$$

2 REQUIRED FORCE (FOR A GIVEN α, β, υ, θ_c)

$$f_r = (I_m + I_a + m_a R_1^2)\, C_\theta / R_1$$

$$C_\theta \triangleq 4\upsilon^2 \theta_c / \alpha(1-\alpha)(1-\beta)^2$$

3 FORCE AVAILABLE (FOR A GIVEN ACTUATOR SIZE AND EFFICIENCY)

$$f_a = (K_a/\delta_a) m_a$$

4 POWER DISSIPATED (ENERGY LOST PER UNIT TIME)

$$P_E = \frac{4}{3} R' m_a i_{max}^2 \alpha(1-\beta)$$

DESIGN OPTIMIZATION SEQUENCE

- CALCULATE REQUIRED FORCE AND AVAILABLE FORCE
- DETERMINE IF AVAILABLE FORCE ≥ REQUIRED FORCE
- CHOOSE ACTUATOR RADIUS THAT MINIMIZES REQUIRED FORCE
- CALCULATE ACTUATOR SIZE TO PRODUCE DESIRED FORCE
- CALCULATE OPTIMUM GEAR RATIO BASED ON BALANCING CONDITION
- CALCULATE ENERGY DISSIPATION

The required actuator force and power are shown as a function of the figure of merit for the particular example of the 10 cm diameter SIRTF mirror and a 20 Hz chop.

REQUIRED FORCE AND POWER DISSIPATION VERSUS K_a/δ_a

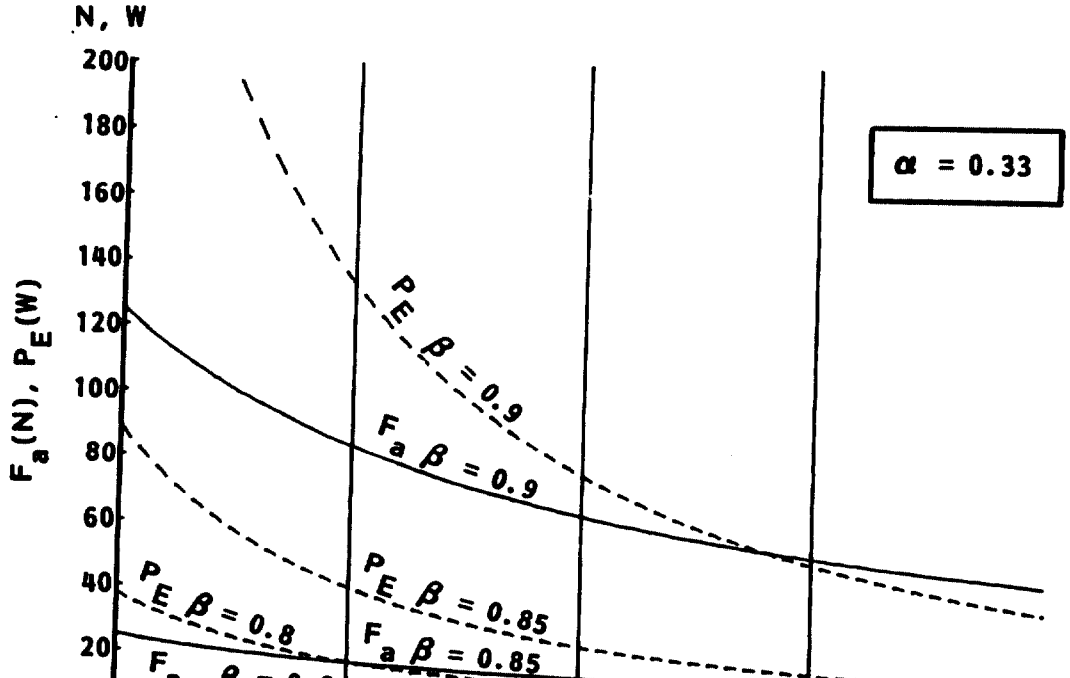

This diagram shows the actuator moving pole mass and the actuator arm length as a function of the figure of merit (κ_a/ζ_a), for the same example as previously shown.

ACTUATOR MASS AND RADIUS VERSUS K_a/δ_a

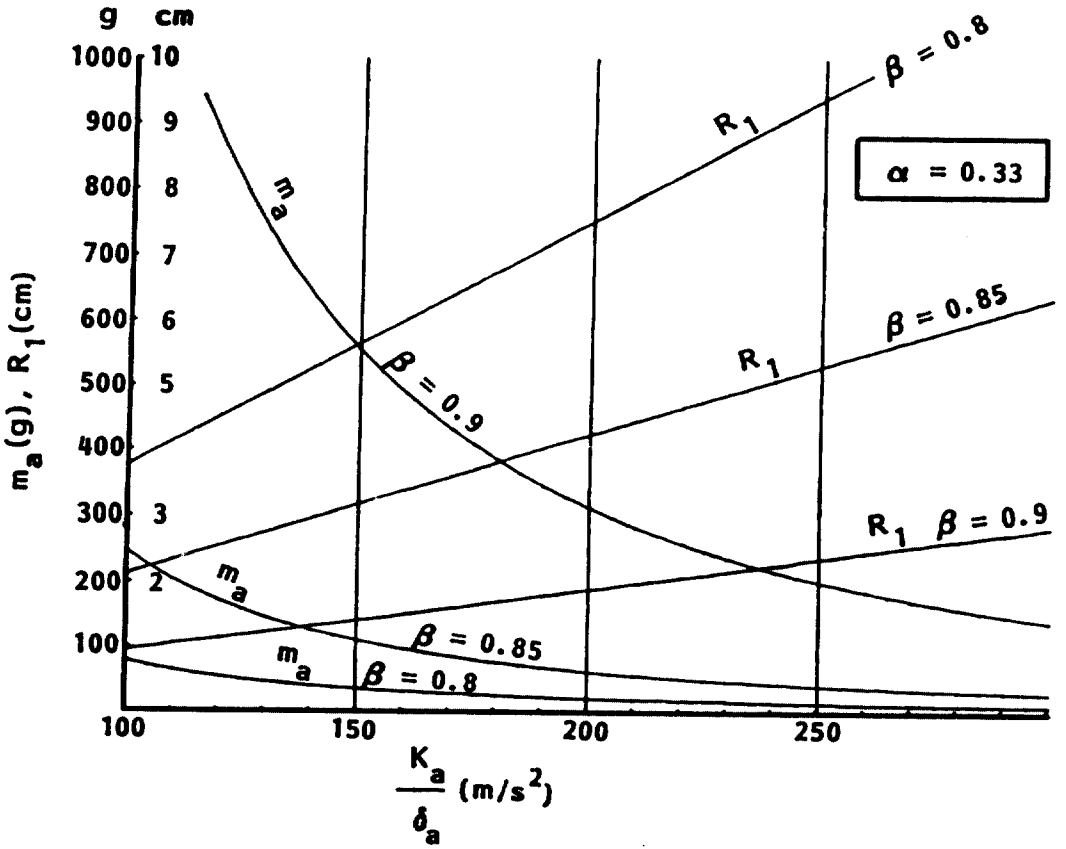

The foild shows the basic secondary mirror chopping requirements.

SECONDARY MIRROR CHOPPING

- **REQUIREMENTS**
  - FREQUENCY (ν) 10 Hz
  - SCAN ANGLE (β) FOV ($\Delta\alpha$)
  - DUTY CYCLE (ρ) 80%

SCAN ANGLE (β)

$$\beta = 3.2\sqrt{D/F \cdot \Delta\alpha}$$

$$\Delta\alpha = \text{MAX}\ \{150\,\mu\text{rad},\ 10 \times 2.44\ \lambda/D\}$$

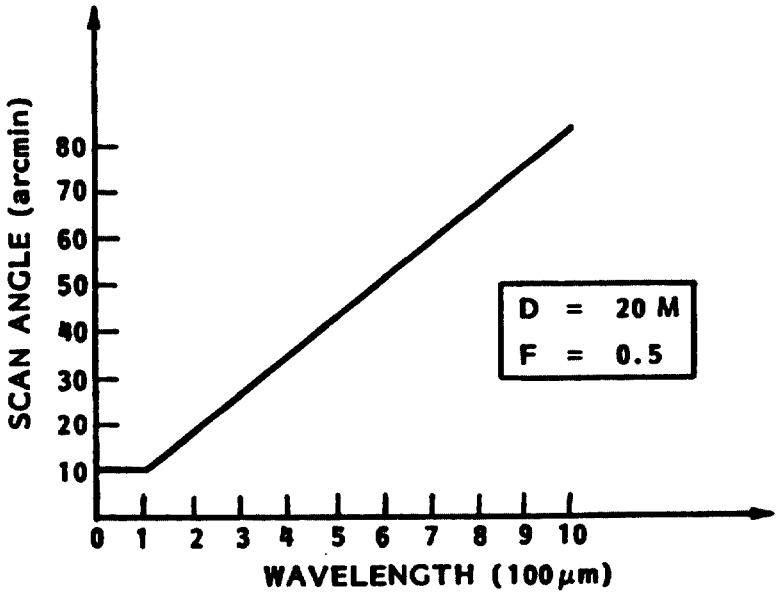

This foil shows the dependence of actuator force and dissipated power on various system parameters and chopping requirements.

ACTUATOR FORCE AND POWER DISSIPATION

- ACTUATOR FORCE IS PROPORTIONAL TO:
  - (SECONDARY DIAMTER)^5
  - (CHOPPING FREQUENCY)^4
  - (SCAN ANGLE)^2

- POWER DISSIPATED BY THE ACTUATOR IS PROPORTIONAL TO:
  - (SECONDARY DIAMETER)^5
  - (CHOPPING FREQUENCY)^4
  - (SCAN ANGLE)^2
  - MAXIMUM CURRENT)^2
  - (1 - DUTY CYCLE)

This chart summarizes the results for LDR secondary mirror chopping at various rates. Note the rapid increase in actuator force, power dissipated and transmitted disturbing force with chopping frequency.

ACTUATOR FORCE AND POWER DISSIPATION

SECONDARY DIAMETER = 0.5 m
SCAN ANGLE = 83.33 arcmin
MAXIMUM CURRENT = 10 amp
WAVELENGTH = 1 mm

FREQUENCY (cycles/s)	ACTUATOR FORCE (N-M)	HEAT DISSIPATION (W)	FORCE TRANSMITTED TO THE STRUCTURE (N-M)
1	0.65	1.40	0.0065
2	10.47	22.34	0.0147
4	167.52	357.40	1.6752
5	409.00	872.00	4.0900
10	6,540.00	13,961.00	65.40

Here are several LDR secondary mirror chopping actuator designs for an optimized 2 HZ chop as well as modified designs when the actuator arm R_1 isshortened tc a realistic length (10 cm). Note that the penalty for this shortening lies in increased power dissipation.

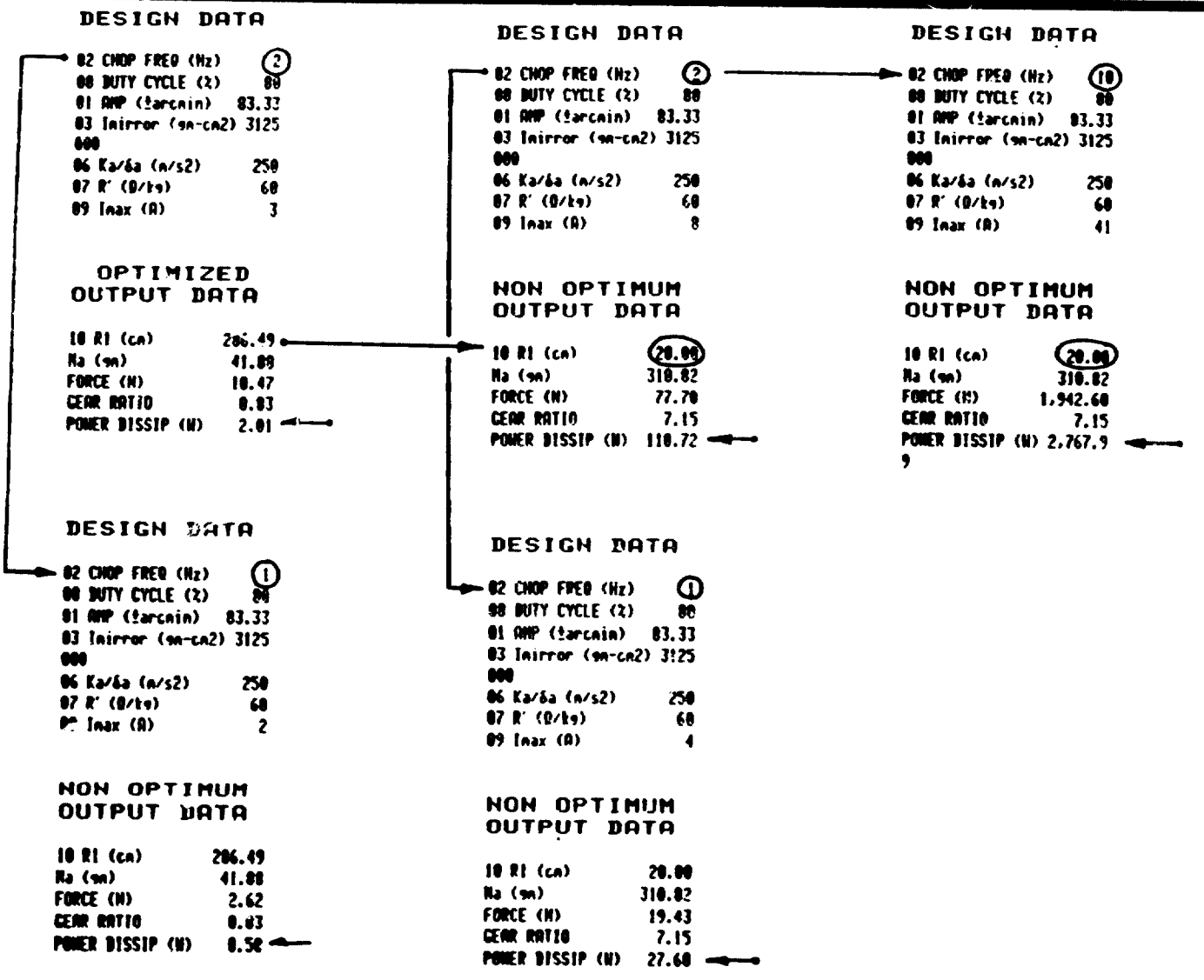

ELECTRODYNAMIC ACTUATORS

- SPACE CHOPPING IMPOSES STRINGENT REQUIREMENTS ON THE SECONDARY MIRROR ACTUATION SYSTEM
- NEED COMPACT ACTUATORS CAPABLE OF GENERATING FORCES ON THE ORDER OF 50 TO 100 N IN A SHORT TIME

  OPTIMALLY DESIGNED HIGH-PERFORMANCE REACTIONLESS ELECTRODYNAMIC ACTUATORS CAN MEET THESE REQUIREMENTS
- LOCKHEED HAS BUILD AND TESTED SUCH ACTUATORS

AGENDA

INTRODUCTION AND SUMMARY	W. ALFF
MIRROR SEGMENTS	L. BANDERMANN
SUNSHADE	L. BANDERMANN
STRUCTURE MODEL (INTRODUCTION)	L. BANDERMANN
STRUCTURE AND CONTROL OVERVIEW	J. AUBRUN
SECONDARY MIRROR CHOPPING	K. LORELL
▷ CONTROL SYSTEM PERFORMANCE	B. SRIDHAR

POINTING AND VIBRATION CONTROL SYSTEM (PVCS)

- REQUIREMENTS
- VIBRATION SOURCES
- POINTING AND VIBRATION CONTROL CONCEPT
- CONTROL SYSTEM SIMULATION
- CONCLUSIONS

PVCS REQUIREMENTS

- PURPOSE AND FUNCTION
  - TO SLEW THE SYSTEM FROM ONE ATTITUDE TO ANOTHER WHILE MEETING THE REQUIREMENTS ON JITTER
  - TO MAINTAIN POINTING STABILITY IN THE PRESENCE OF DISTURBANCES

- PERFORMANCE SPECIFICATION

SLEW	120 deg IN 10 MTS
POINTING • ACCURACY • STABILITY	 0.06 arcsec 0.03 arcsec
NODDING	TBD
FIGURE ACCURACY	0.5-μm rms

The PVCS block diagram shows the important elements in the control of the LDR. The presence and the complexity of a particular block depends on the structure and the performance requirements. The elements on the right of the dotted line have to do with the figure control/alignment system, which may be totally independent of the pointing/vibration controller if vibrations can be reduece to a low enough level. This system may use a capacitive sensing system or an OPS system.

The PVCS uses a single cluster of CMGs for the control of the attitude and of low fre quency modes. Proof-Mass Actuators (PMAs) distributed in strategic locations in the bakup structure may be needed for the control of vibrations at higher frequencies.

PVCS BLOCK DIAGRAM

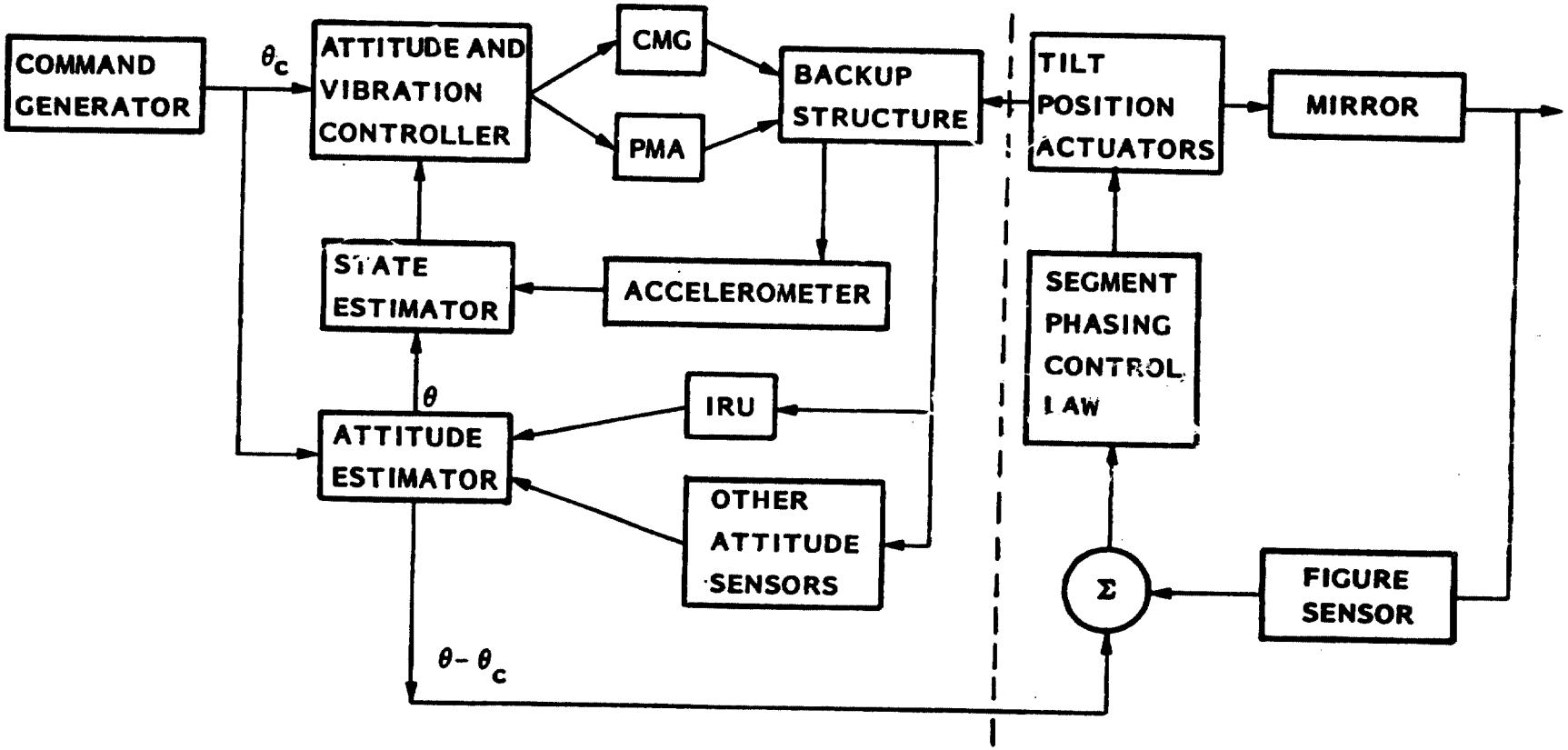

The control approach for the design of a PVCS for the LDR is shown in this Vu-foil.

CONTROL APPROACH

- REDUCE THE AMOUNT OF JITTER AT THE END OF THE SLEW BY JOINT ATTITUDE AND VIBRATION CONTROL
  - OPTIMAL TORQUE PROFILES
  - VIBRATION CONTROL AND IMPROVED PERFORMANCE DUE TO INCREASED DAMPING (ACOSS TECHNOLOGY)
- DECOUPLE THE MIRRORS FROM THE BACKUP STRUCTURE BY USING ELECTROMAGNETIC ACTUATORS
  - VIBRATION ISOLATION
  - FINE POINTING OF THE ATTITUDE

The pointing and stability requirements of the LDR are met by reducing the vibrations at two different levels. The optical system is isolated from the backup structure by the use of force actuators. The vibrations are further reduced by introducing active damping into the backup structure.

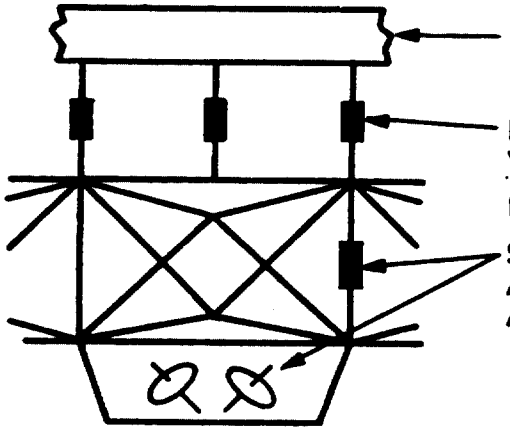

ELEMENT	DESIGN
SEGMENT	FUSED SiO_2
PISTON/TILT ACTUATORS VIBRATION FILTER	MAGNETIC BEARINGS, OTHER
INTEGRATING TRUSS	GRAPHITE/MAGNESIUM
STRUCTURAL AND ATTITUDE CONTROL ACTUATORS	PASSIVE MEMBER DAMPERS ELECTROMECHANICAL/DYNAMICAL ACTUATORS, CMGs, THRUSTERS

The important elements of a technology which has great potential for the pointing and control of large systems, Active Control of Space Structures (ACOSS), are described in this Vu-foil.

ACOSS VIBRATION AND POINTING CONTROL

- OPTIMAL SLEWING AND REDUCED VIBRATION LEVELS MAY BE USED BY USING ACOSS TECHNOLOGY
- LMSC HAS DEMONSTRATED THE VALIDITY OF SUCH AN APPROACH
- OPTIMAL CONTROL TECHNIQUES USED TO REDUCE VIBRATION LEVELS
- COLOCATED RATE FEEDBACK LOOPS USED TO INTRODUCE ACTIVE DAMPING
- METHOD USES HIGH BANDWIDTH PROOF-MASS ACTUATORS, OPTICAL SENSORS, AND ACCELEROMETERS

The LDR control system simulation block diagram is shown here. The command generator gives the attitude and rate commands depending on the nodding and slewing requirements. The LDR control model is derived from the finite element structural model described earlier. The state vector χ contains both rigid body modes and vibration modes. The measurement vector consists of attitude and rate measurements as seen from the CMG locations. An error signal is generated whenever the measurement vector is different from the command vector. The gain matrix C is chosen by a pole-placement method.

SIMULATION BLOCK DIAGRAM

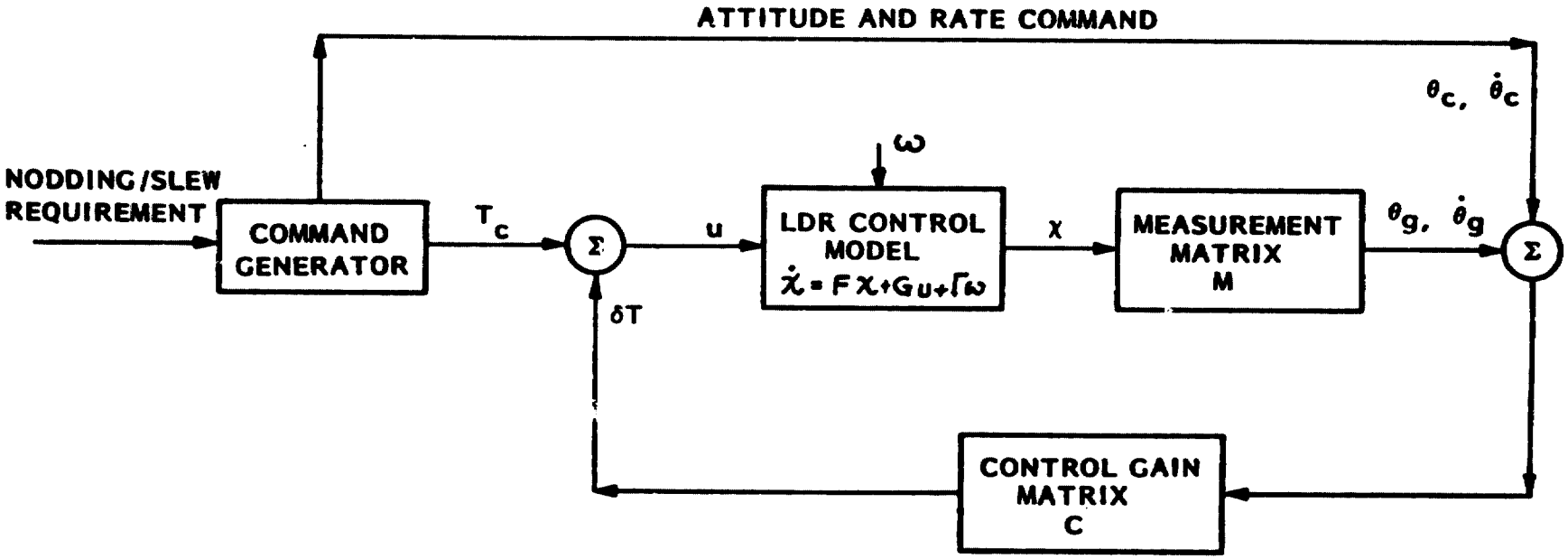

This chart defines the various mathematical symbols used in the analysis discussed on the following foil.

SYMBOLS

χ - STATE VECTOR $[\dot{\theta}_x, \theta_x, \dot{\theta}_y, \theta_y, \theta_z, \dot{\theta}_z, q_1, \dot{q}_1, \ldots \dot{q}_{17}, q_{17}]^T$

u = CONTROL VECTOR $[T_x, T_y, T_z]^T$

y = MEASUREMENT VECTOR $[\dot{\theta}_{g\chi}, \theta_{g\chi}, \dot{\theta}_{gy}, \theta_{gy}, \dot{\theta}_{gz}, \theta_{gz}]^T$

y_d = COMMAND VECTOR $[\dot{\theta}_{xc}\, \theta_{xc}\, \dot{\theta}_{yc}\, \theta_{yc}\, \dot{\theta}_{zc}\, \theta_{zc}]^T$

e = ERROR VECTOR = $y_d - y$

ℓ = L·O·S VECTOR = $[\ell_\chi\, \ell_y\, \ell_z]^T$

ℓ_e = L·O·S ERROR = $[\ell_\chi - \theta_{xc}, \iota_y - \theta_{yc}, \iota_z - \theta_{zc}]^T$

T_c = COMMANDED TORQUE = $[T_{c\chi}\, T_{cy}\, T_{cz}]^T$

ω = DISTURBANCE VECTOR

δ = DISPLACEMENT VECTOR

The system equations are showns here. The Line-Of-Sight (LOS) vector is defined as the perpendicular to a plane passing through 36 points on the primary mirror surface. The matrix Q transforms the states to LOS. The matrix R represents the error in the LOS due to secondary mirror motion. The vector δ is the z displacement, due to vibrations, at points (108 in all) on the mirror. In the simulation F is 40x40, M is 40x1, H is 6x40, Q is 3x40, S is 108x40, and C is 3x6.

SYSTEM MATRICES

$\dot{x}$	=	$Fx + Gu + \Gamma\omega$	DYNAMICS
y	=	Hx	ATTITUDE MEASUREMENTS
ℓ_e	=	$Qx + Rx - \theta_c$	L·O·S ERROR
δ	=	Sx	SURFACE ERROR
u	=	$T_c - C(y_d - Hx)$	CONTROL LAW

Q COMPUTED BY FITTING A PLANE THROUGH PRIMARY MIRROR

R ERROR DUE SECONDARY MIRROR MOTION

This Vu-foil shows the output of the finite element program. The eigenvector matrix ϕ has the dimensions 3000x24.

OUTPUT OF FINITE-ELEMENT PROGRAM

- MODAL FREQUENCIES

$$\omega = [\omega_1\ \omega_2\ \ldots\ \omega_n]$$

- LOCATION, MASS AND M.I OF THE JOINTS

JOINT #	1	2	.....	499	500
ℓ_x					
ℓ_y					
ℓ_z					
M					
I					

- MODE SHAPES (EIGENVECTORS)
  - (x,y,z) MODAL DISPLACEMENT AT A NODE
  - $(\theta_x, \theta_y, \theta_z)$ MODAL ROTATIONS AT A NODE
  - THE EIGENVECTOR MATRIX Φ

$$(500 \times 6) \times 24$$

NO. OF JOINTS — NO. OF D.O.F — NO. OF MODES

The open and closed loop poles of the PVCS are shown here. The poles are symmetric about the real axis, and only the left half top part of the complex 8-plane is shown in the figure. These poles (or roots) represent the characteristic frequencies (and associated damping) of the system. Damping is increased as the poles move to the left of the $j\omega$-axis.

SYSTEM POLES

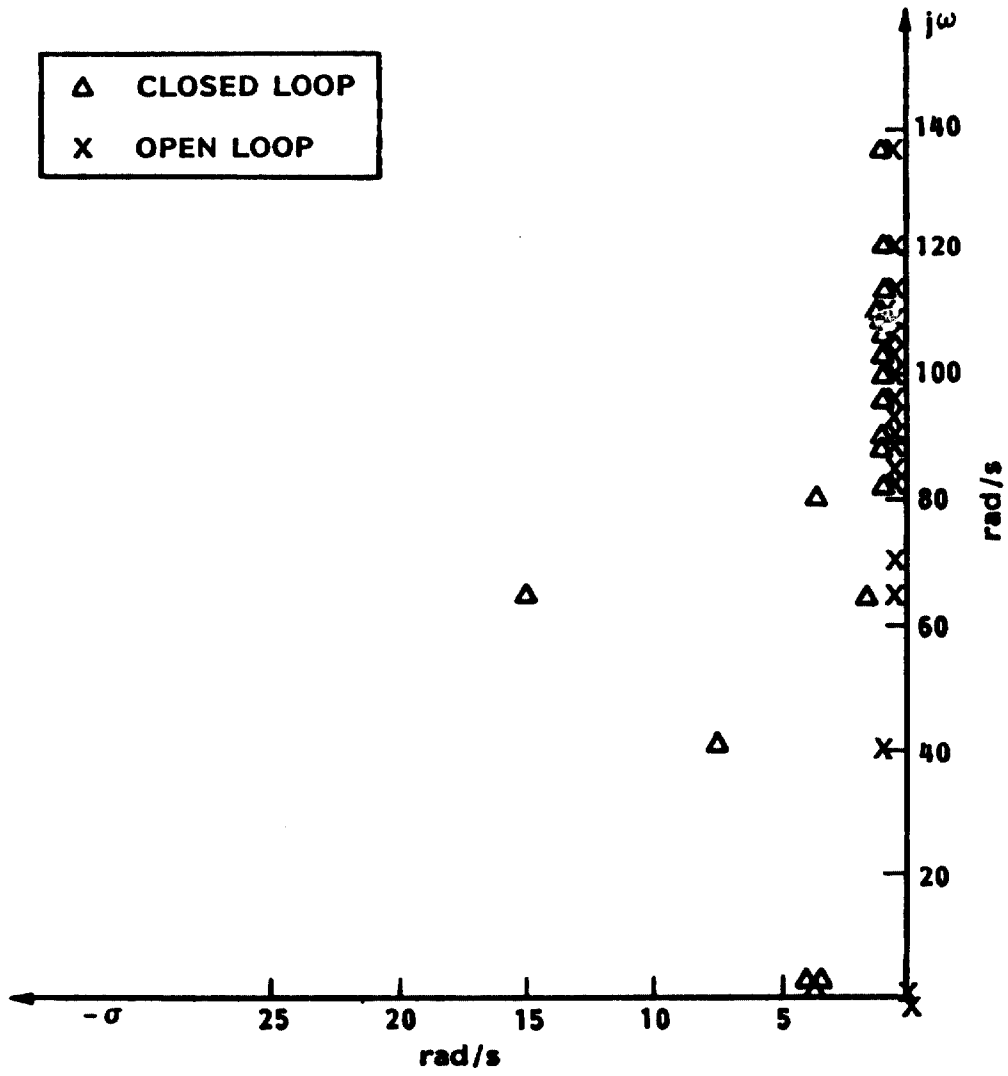

The amount of torque required to slew the LDR varies inversely with the square of the slewing time and directly with the slewing angle. The figure on the right shows the amount of torque required to slew (or nod) the LDR about the x-axis with a bang-bang torque profile. Note that the maximum torque requirement to nod 120 arcsec in 1 sec and to slew 120 degrees in 1 minute is the same and equal to 800 N.m.

MAXIMUM TORQUE REQUIREMENT

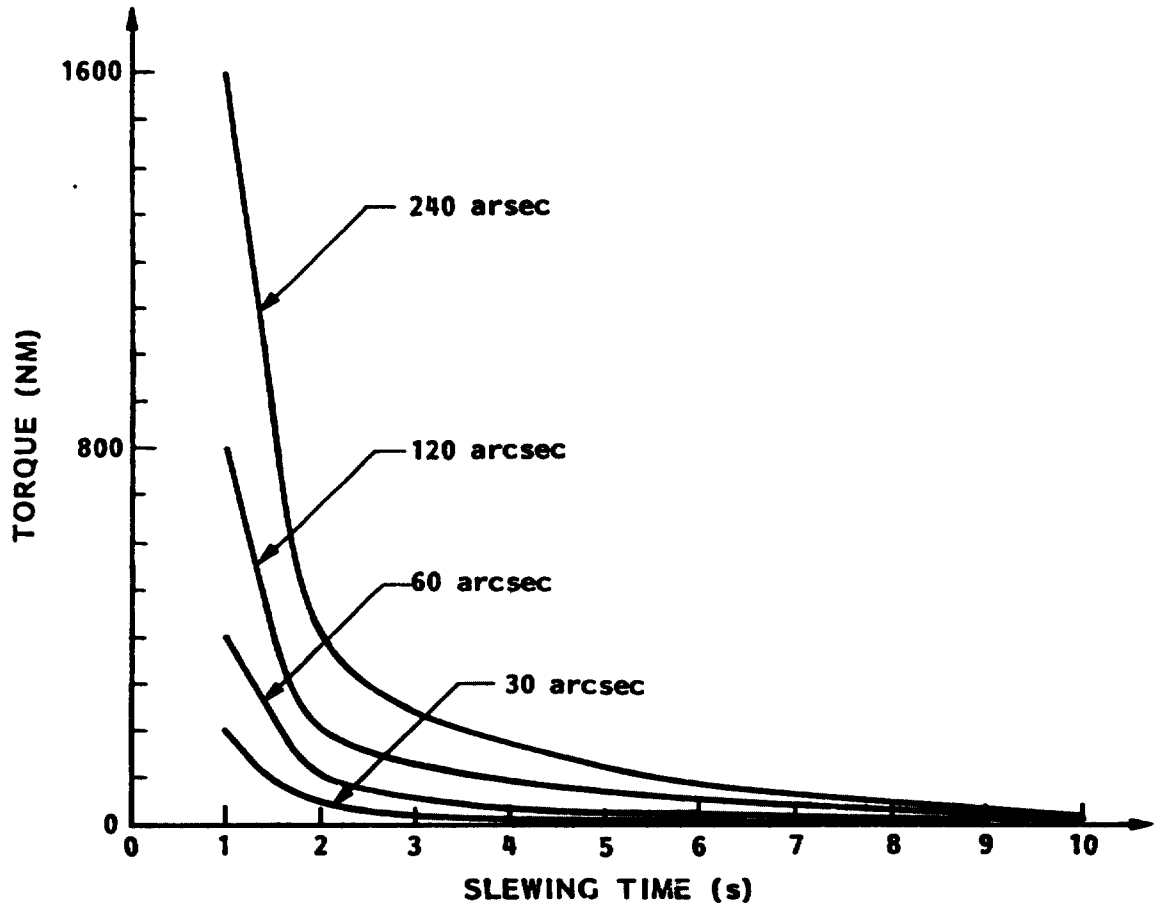

Different torque profiles can be used to slew the LDR. The bang-bang torque requires the minimum maximum torque. To perform the same slew the sine-versine torque profile requires a peak torque which is 2.6 times larger. However, the bang-bang torque produces much higher levels of vibration compared with the other torque profiles shown in the Vu-foil.

TORQUE PROFILES

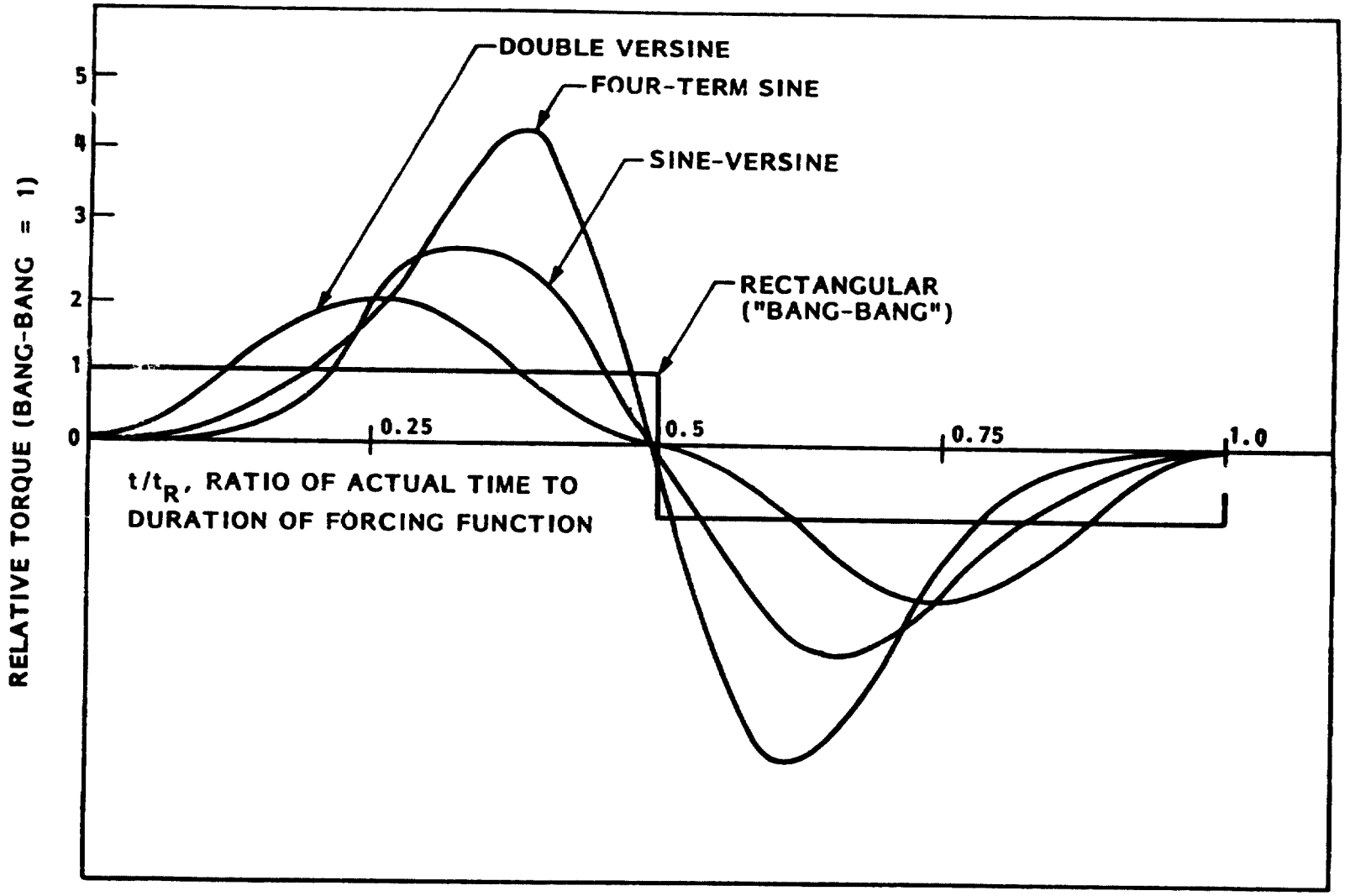

Earlier it was shown that the peak torque requirement for a 120 arcsec nodding in 10 sec is equivalent to slewing by 120 degrees in 1 minute. From the figure and the equations in this Vu-foil it can be seen that for the same torque level, the vibration level varies inversely with the cube of the period (maneuver time). Thus nodding potentially produces much higher levels of vibration than slewing. Since the slewing requirement is 120 degrees in 5 minutes, if we satisfy the requirements during nodding then we satisfy the requirements during slewing.

SINE-VERSINE TORQUE SHAPING

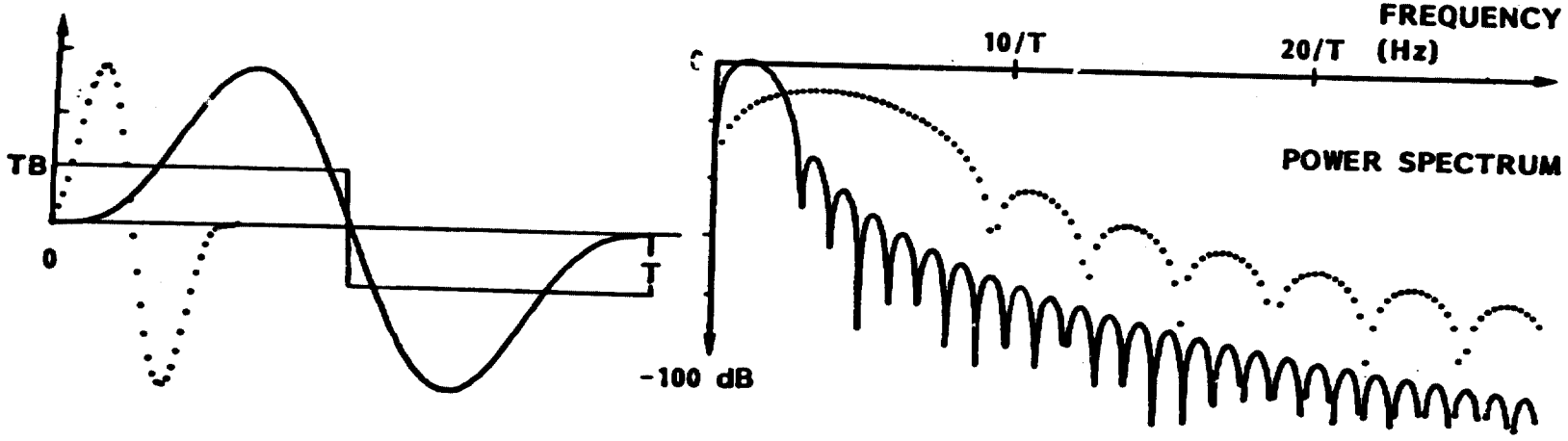

$$f(t) = \frac{2\pi}{3} T_B \sin \dot{\chi} (1 - \cos \chi)$$

$$\chi = \Omega t \; ; \; \Omega = 2\pi/T$$

$$g(\omega) = \frac{(2\pi/\omega)^4 T_B}{(\omega^2 - \Omega^2)(\omega^2 - 4\Omega^2)} \sin(\omega T/2)$$

For $\omega \gg \Omega$ $g(\omega) \sim \frac{(2\pi/\omega)^4}{3T^3} \times \left(\frac{4\theta_{MAX}}{T^2}\right)$

θ_{MAX} ↑ Torque level T_B

The performance of the LDR during a 120 arcsec nodding about the x-axis in 1 sec is shown on the next four Vu-foils. The performance requirements are not met using a bang-bang torque command without feedback (i.e. $\delta T=0$). Notice the high frequency vibrations excited by the bang-bang torque.

BANG-BANG OPEN-LOOP PERFORMANCE

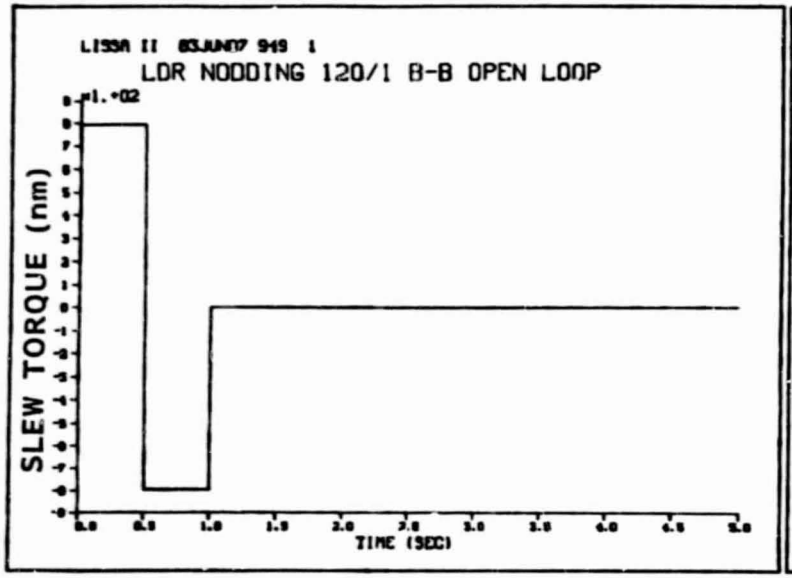

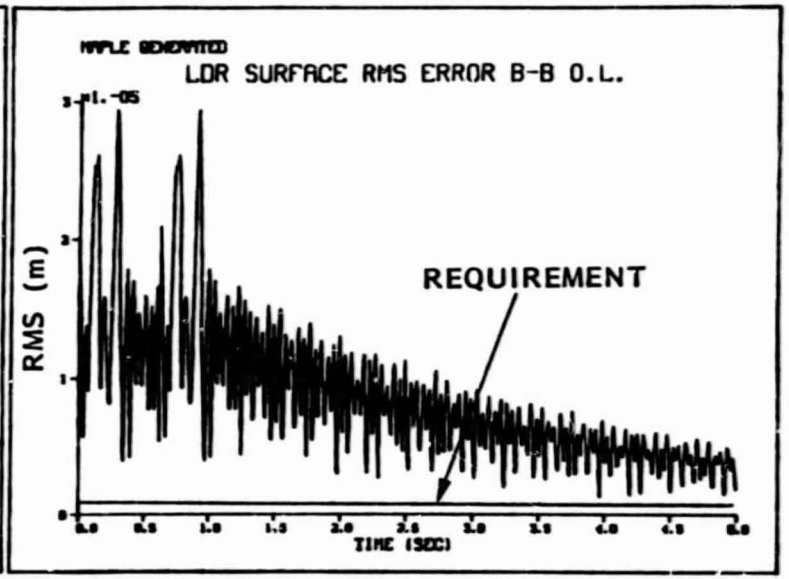

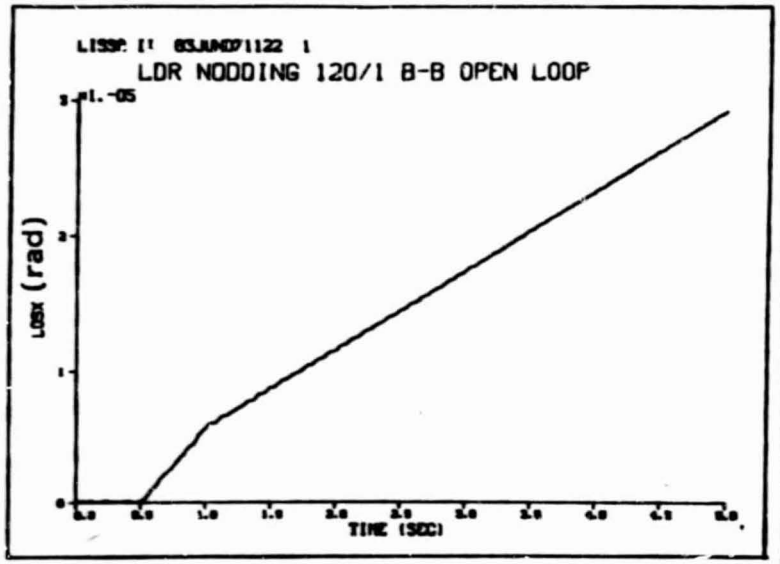

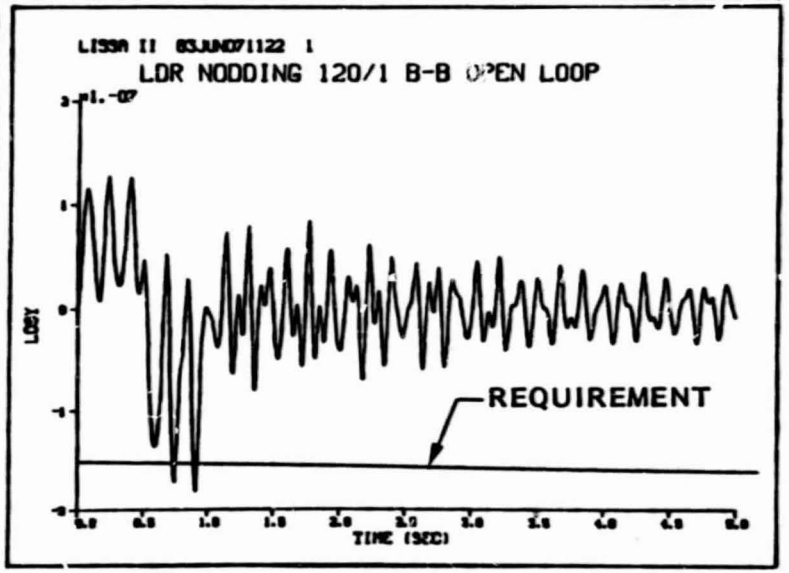

ORIGINAL PAGE IS
OF POOR QUALITY

The control requirements are met using a sine-versine torque profile. Notice the small amount of residual vibrations ater 1 sec.

SINE-VERSINE OPEN-LOOP PERFORMANCE

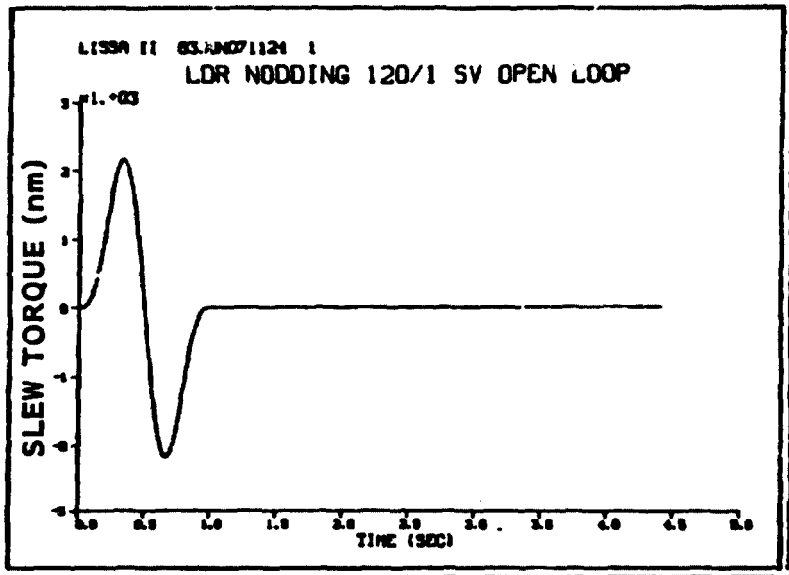

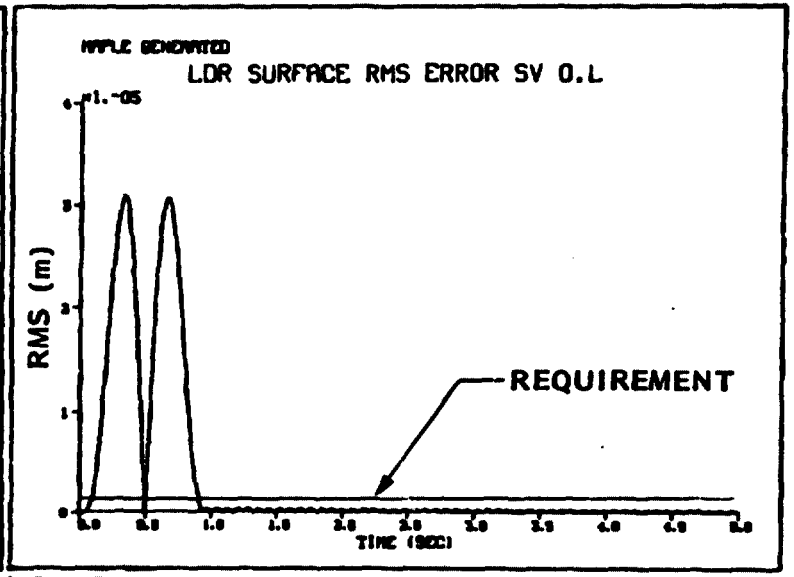

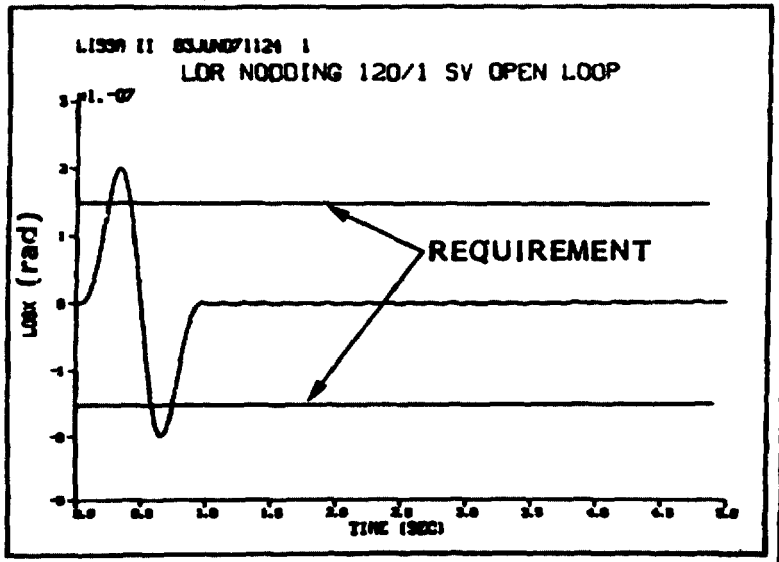

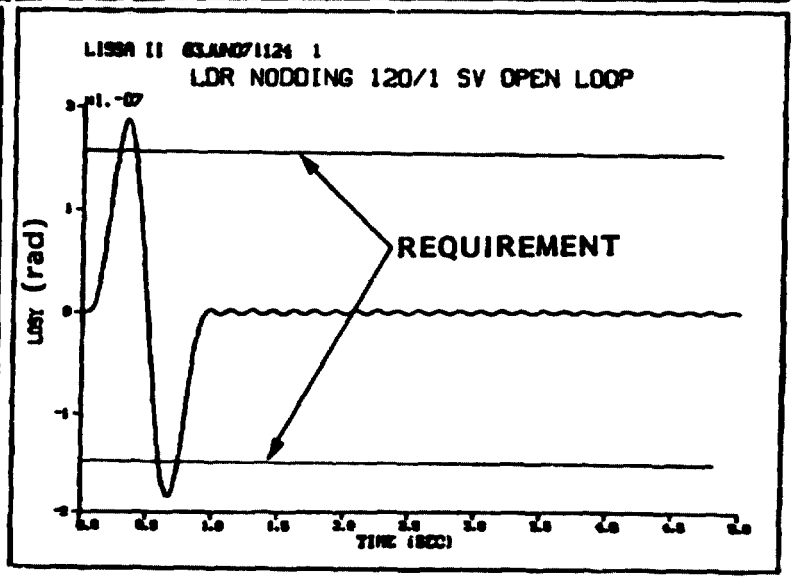

This figure shows the effect of the feedback on the nodding performance using a bang-bang torque. All the control requirements are met. The feedback system superimposes a small amount of control correction torque on the torque command.

BANG-BANG CLOSED-LOOP PERFORMANCE

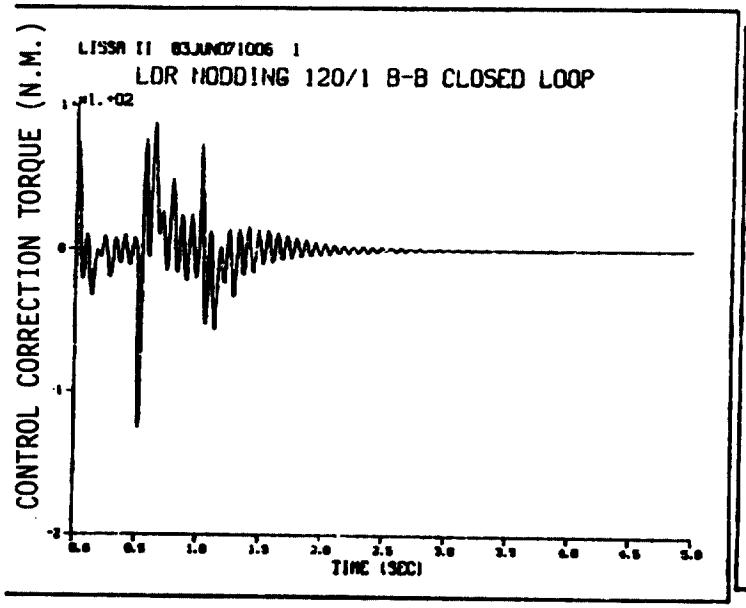

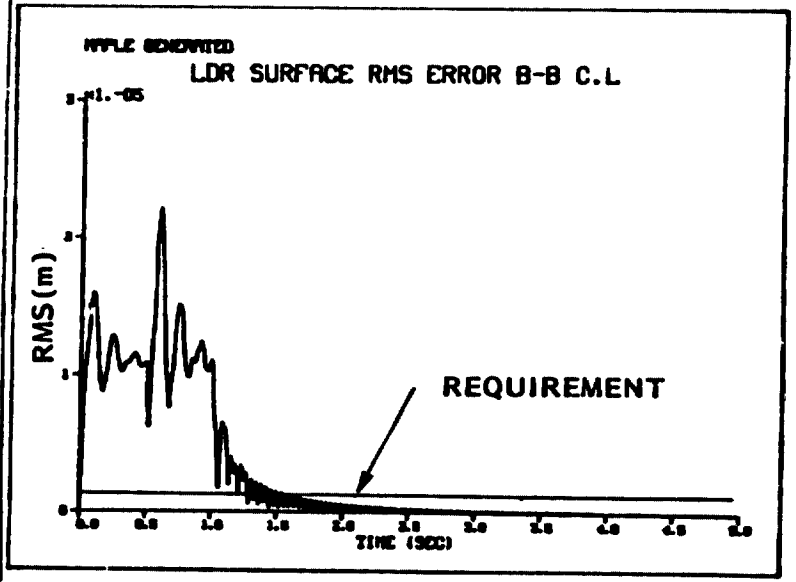

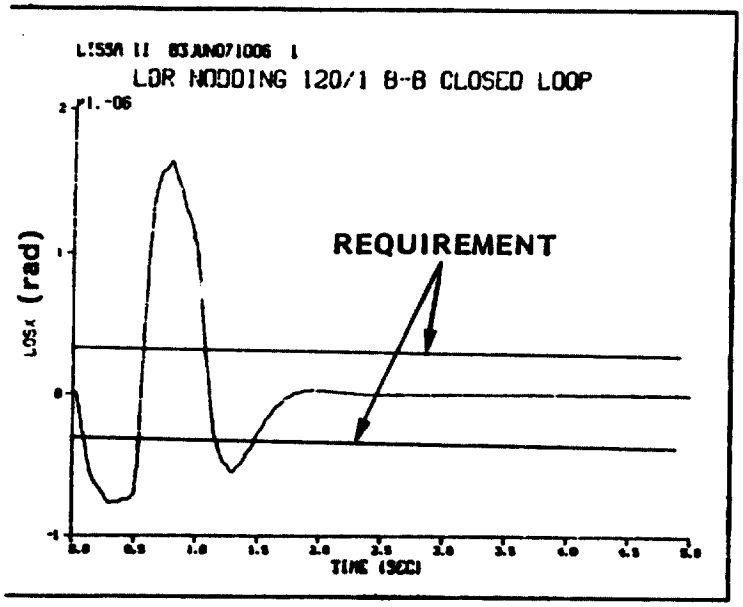

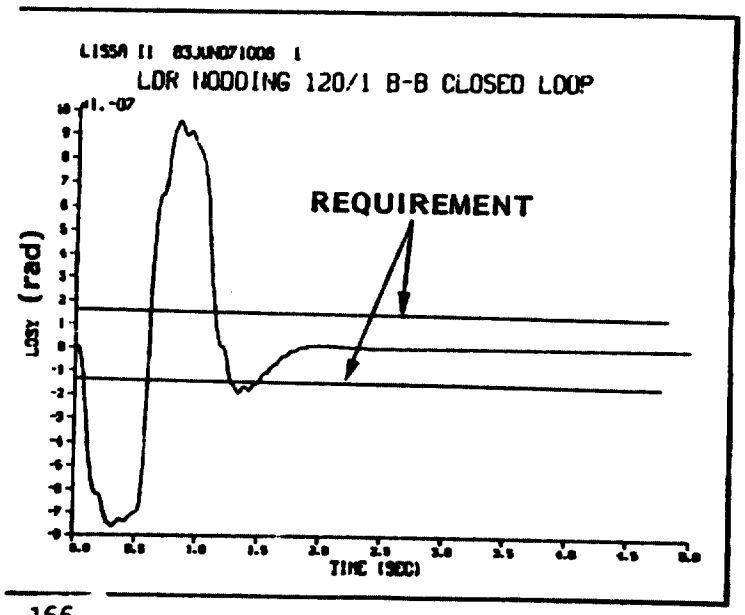

The effect of feedback on the nodding performance of LDR with a sine-versine torque profile is to damp the small residual vibrations; as before, performance requirements are met.

SINE-VERSINE CLOSED-LOOP PERFORMANCE

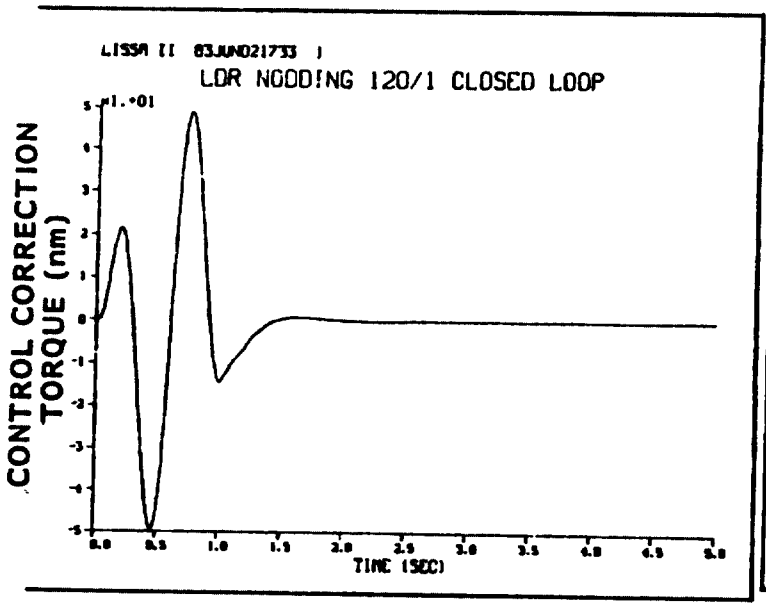

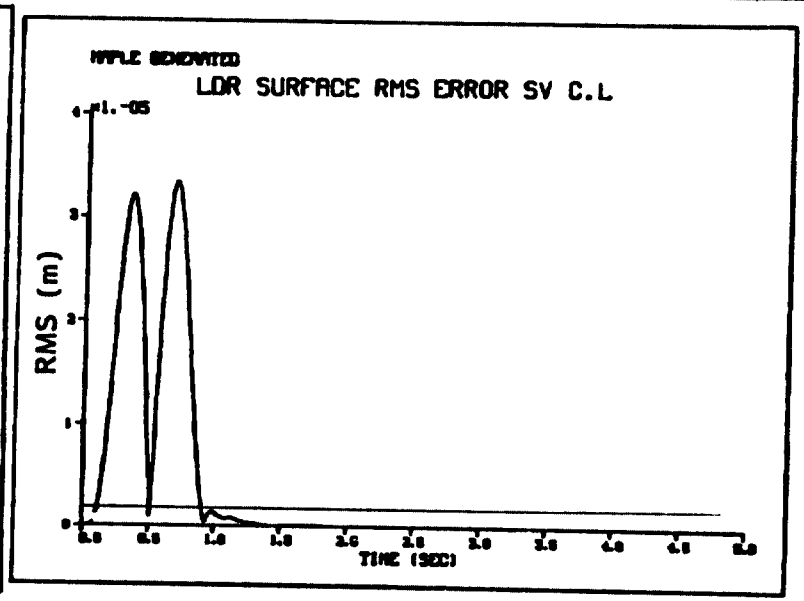

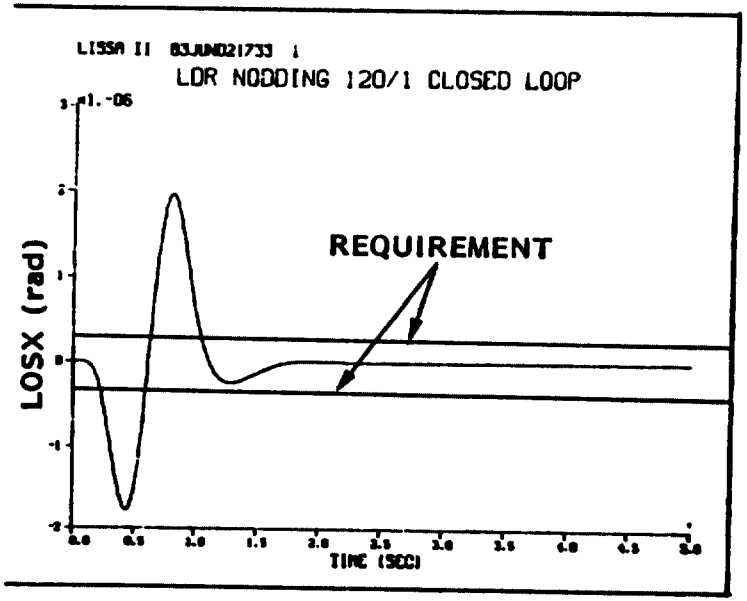

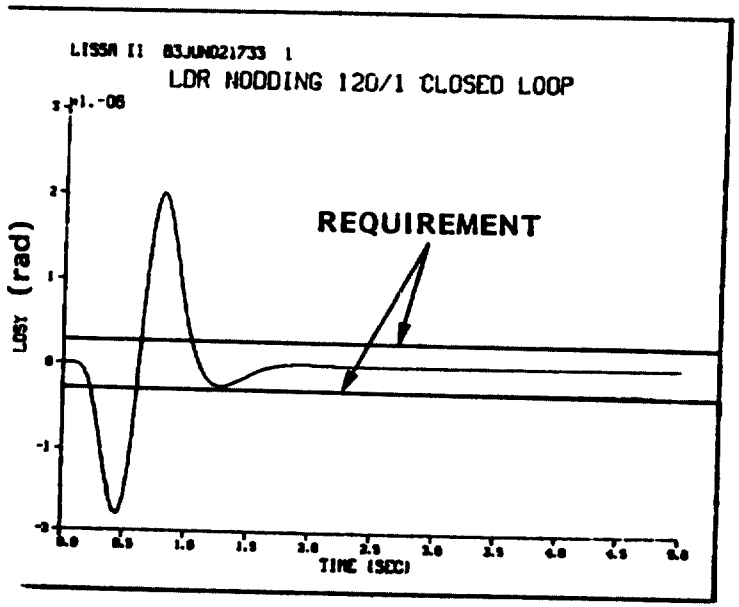

This foil shows the characteristics of a state-of-the-art CMG which can be used to slew or nod the LDR. Note that, since the peak torque required for nodding is only about 2400 N.m., the peak power will be much less than the max peak power indicated on the Vu-foil, i.e. less than 200 W.

SPERRY-RAND MODEL NO. 2400

- PEAK TORQUE 6,500 N-M
- WEIGHT 175 kg
- POWER REQUIREMENTS
  - 1,400 W PEAK
  - 100 W QUIESCENT
  - 30 W STANDBY
- NOISE
  - PEAK AT 130 Hz (WHEEL SPEED)
  - SECONDARY PEAK AT 46 Hz
  - FORCE NOISE 1.3 N (rms)
  - MOMENT NOISE 0.3 Nm (rms)

This foil shows the CMG noise PSD. It has two peaks: one corresponding to the wheel speed and another at about 40% of the wheel speed.

CMG NOISE POWER SPECTRAL DENSITY

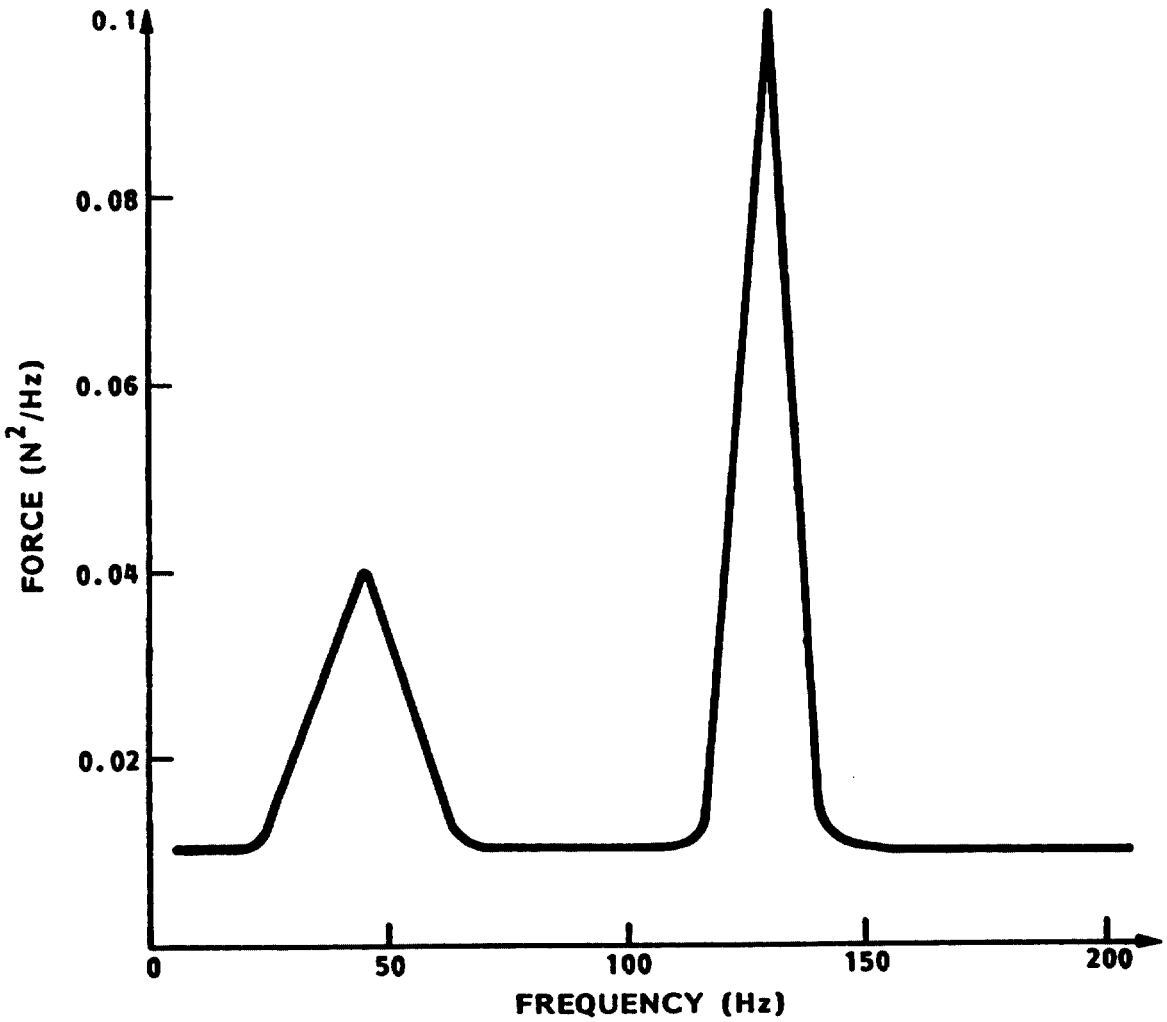

The disturbance due to the cryo-cooler pump is shown here. Compared to the CMG PSD, the cryo-cooler PSD is wide band and the force level is high (ratio 400:1). The cryo-cooler PSD is based on a generic model developed for the ACOSS program by the Riverside Research Institute.

CRYO-COOLER PUMP POWER SPECTRAL DENSITY

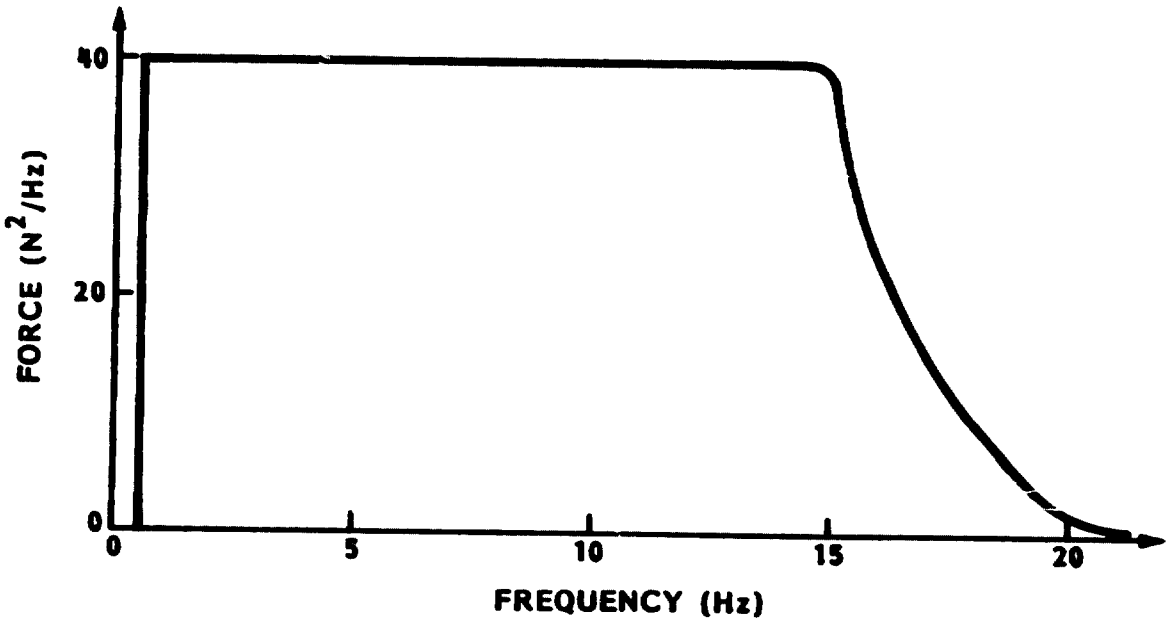

This foil shows the LOSX PSD and integrated PSD due to cryo-cooler vibrations. The closed loop behavior is only slightly better than the open-loop behavior. The control system needs to be designed for better disturbance rejection. But such design is within the state-of-the-art, using optimal control techniques and the integrated HAC/LAC approach.

LOSX PSD

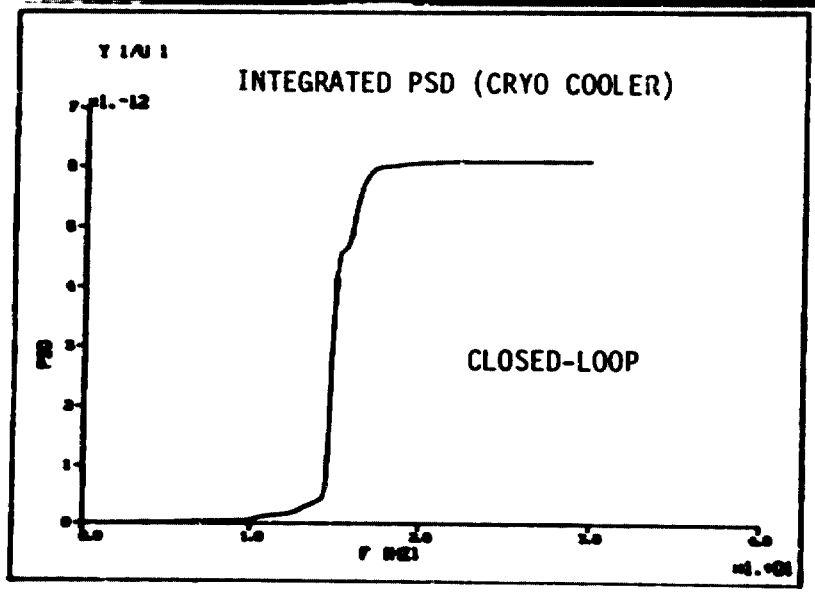

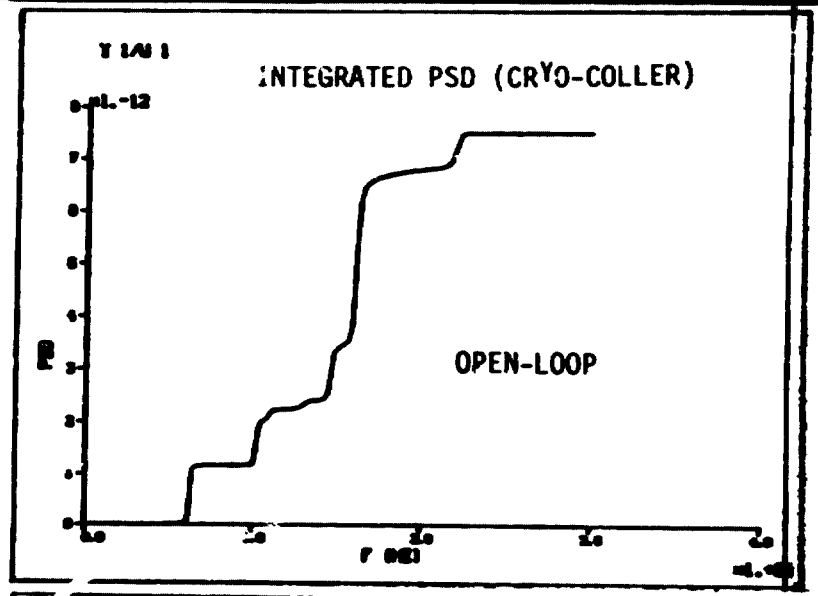

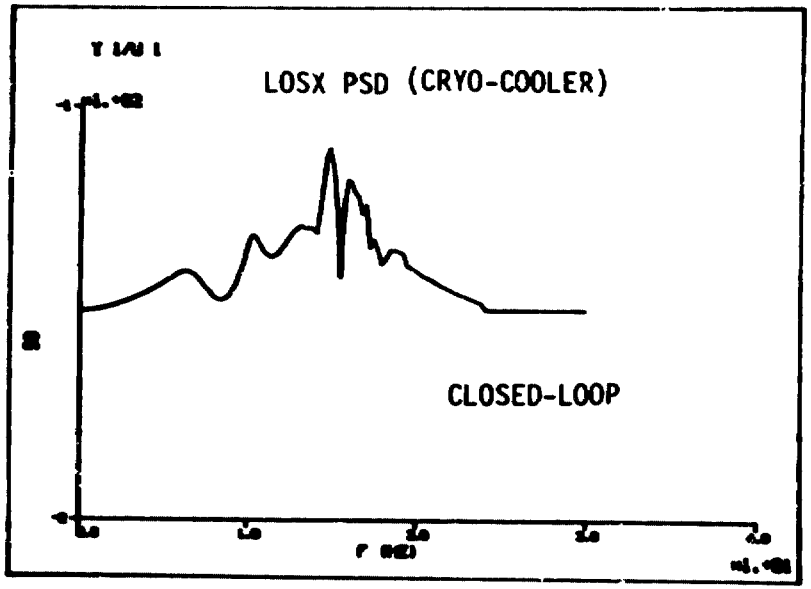

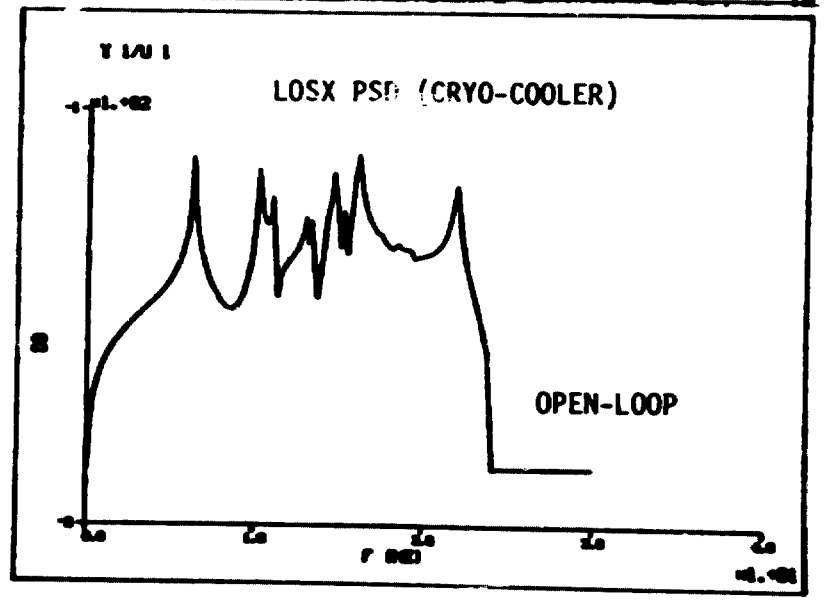

This chart shows the LOSy PSD and integrated PSD for the open loop case.

LOSY PSD AND TRANSFER FUNCTION RATIO

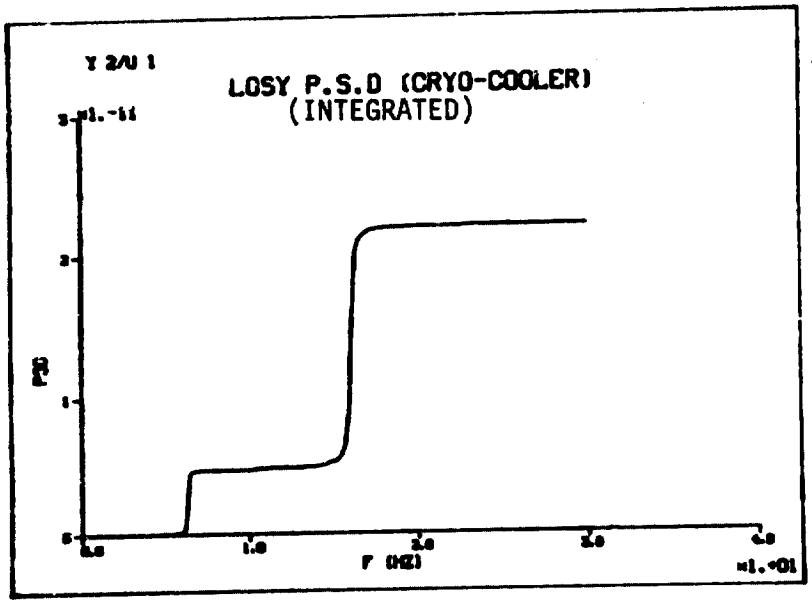

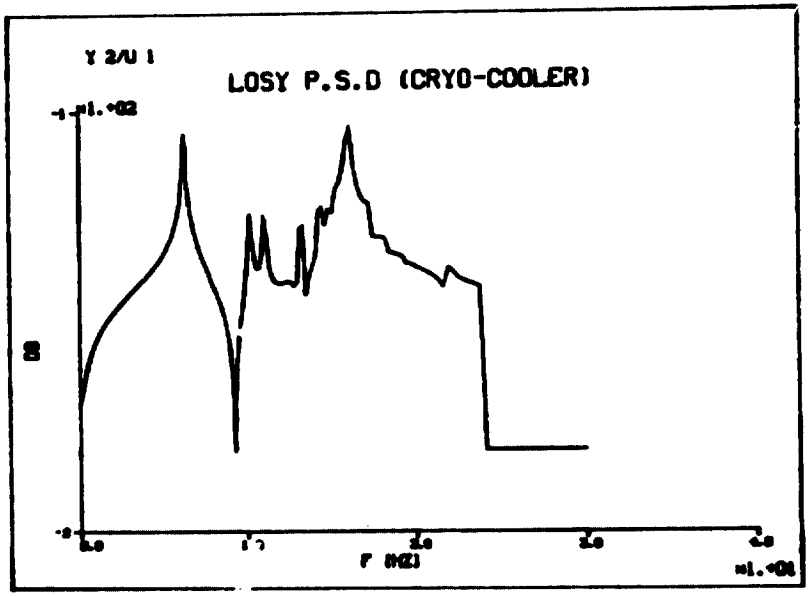

The table on this Vu-foil summarizes the effect of cryo-cooler disturbances on LOS error. The rms error due to cry-coolers is high and does not meed the performance requirements. Two steps should be taken to correct the problem: (i) The control system should be designed to provide better disturbance rejection. This can be done by isolation, use of proof-mass actuators, and high authority control; (ii) since the cryo-cooler can be a major system disturbance source, its vibration characteristics must be defined quite carefully so that the control system can minimize the corresponding LOS errors.

The current study could not evaluate directly the effect of CMG noise on LOS error. The CMG noise power spectrum is above the highest frequency (22 Hz) in the structural model. However, its magnitude is much smaller (1/400) compared to the cryo-cooler.

LOS ERROR DUE TO VIBRATION SOURCES

- CRYO-COOLER

LOSX (OPEN LOOP)	13.2 arcsec (rms)
LOSX (CLOSED LOOP)	11.9 arcsec (rms)
LOSY (OPEN LOOP)	22.6 arcsec (rms)
LOSY (CLOSED LOOP)	12.1 arcsec (rms)

- CMG

  CMG NOISE POWER SPECTRUM IS ABOVE THE HIGHEST FREQUENCY (22 Hz) IN THE STRUCTURAL MODEL AND CANNOT BE EVALUATED DIRECTLY. HOWEVER, ITS MAGNITUDE IS MUCH SMALLER COMPARED TO THE CRYO-COOLER

This chart summarizes our findings and recommendations on the pointing and vibration control of the LDR.

CONCLUSIONS AND RECOMMENDATIONS

- PRELIMINARY ANALYSIS SHOWS THAT THE LDR CAN MEET MOST OF THE REQUIREMENTS WITH A SIMPLE CONTROL SYSTEM

- THE CONTROL SYSTEM ASSUMES ACCURATE STAR TRACKER TO MAINTAIN THE HIGH ACCURACY REQUIREMENTS

- THE LOS ERROR DUE TO CRYO-COOLER DISTURBANCE COULD BE LARGE AND THE CONTROL SYSTEM SHOULD ADDRESS THIS PROBLEM. POSSIBLE SOLUTIONS INCLUDE ISOLATION, USE OF PROOF-MASS ACTUATORS, AND HIGH AUTHORITY CONTROL

- THE STRUCTURAL MODEL SHOULD BE REVISED TO INCLUDE THE SUNSHADE AND HIGHER FREQUENCY MODES

- BETTER KNOWLEDGE OF CRYO-COOLER VIBRATION CHARACTERISTICS IS REQUIRED IN FURTHER STUDIES

APPENDIX

LDR REQUIREMENTS

Mirror diameter	20 m
F No.	0.5
------ On-axis system ------	
Primary emissivity at 100 μm	5%
1 mm	1%
Diffraction limit at	30 μm
Light bucket mode at	2 μm
Field-of-view	1-10 $\widehat{\text{min}}$
Mirror temperature	150-200 K
Mirror surface temperature gradient	TBD
Pointing accuracy	0.06 $\hat{s}$
Pointing stability	0.03 $\hat{s}$
Sun avoidance	60^{o}
Earth limb avoidance	45^{o}
Off-axis rejection $10\mu m < \lambda < 100\mu m$	10^{-16} W/$\sqrt{\text{Hz}}$
$> 100\mu m$	10^{-17} W/$\sqrt{\text{Hz}}$
Slew	120^{o} in 10 min
Orbit inclination	28.5^{o}
Orbit altitude (circular orbit)	700 km
Comet tracking rate	0.4 $\hat{s}$/s
Secondary mirror diameter	TBD
Chopping with secondary,	2 Hz
" , throw	1 $\widehat{\text{min}}$
" , duty cycle	80%
Nodding requirements	TBD